



Universitetet  
i Stavanger

DET TEKNISK-NATURVITENSKAPELIGE FAKULTET

## MASTEROPPGAVE

|   |   |
|---|---|
| Studieprogram/spesialisering:<br>Konstruksjoner og materialer   | Vårsemesteret, 2012   |
| Fordypning:<br>Offshore konstruksjoner  | Åpen  |
| Forfatter:<br>Ole Magnus Stava  | (signatur forfatter)  |
| Veileder:<br>Ph.D. Student Lene Eliassen  |   |
| Tittel på masteroppgaven:<br>Utmatningsanalyse av offshore vindturbin   |   |
| Engelsk tittel:<br>Fatigue analysis of offshore wind turbine  |   |
| Studiepoeng:<br>30  |   |
| Emneord:<br>Offshore wind turbine<br>Wind profiles<br>Turbulence<br>Rainflow counting<br>Bin<br>Damage equivalent load<br>Fatigue | Sidetall: 46<br><br>+ vedlegg/annet: 22<br><br>Stavanger, den 14.juni/2012<br>dato/år |

## **Acknowledgement**

I want to thank Lene Eliassen for supervision through the preparation of this thesis, and for her good and fast feedback.

Thanks to Ingar Stava for proofreading.

## Summary

In this master thesis analyses will be conducted on a 5MW offshore wind turbine, with a jacket foundation. The goal is to investigate how seven different wind profiles affect fatigue in the blade root, the tower top and the tower bottom. The effect of the turbulence level is also investigated. The analyses examine how the fatigue loads differs from one wind profile to the next, which means it is actually the relative fatigue that is being calculated.

There are a total of seven wind profiles investigated, based on the logarithmic wind profile formula. Due to limitations in the software used, power law wind profiles are used in the analysis. The seven wind profiles have different shear, but the differences are small. Calculations have been made to determine which wind profile that is expected to cause the greatest damage. For each wind profiles the turbulence intensity (TI) is changed from 25 % to 11 % to 0 %, to investigate how this will impact. By including turbulence one gets wind fields. The wind fields are simulated by the software application Turbsim.

The wind fields cause different load impact. The loads are calculated by the multi-body software called Fedem Windpower. The loads are then post-processed by Mlife, which is a MatLab application, in order to obtain damage equivalent load (DEL), i.e. relative fatigue.

The DEL's are tabulated in the result chapter for the 18 load conditions analyzed, where the turbulence is reduced from 25 % to 11 % to 0 %. All the DEL's are normalized with respect to the neutral wind profile. Additionally, the result chapter shows graphically the normalized values for selected loads.

DEL caused by the bending moment out of plane (RMy) is considered most significant to investigate which of the wind profiles that are causing the highest DEL. The result chapter shows DEL results caused by RMy that are not as expected when turbulence is included. In the discussion chapter this case is widely discussed. It appears that the reason has to do with the fact that the mean turbulence variation on both sides of one wind profile is larger than the difference between the wind profiles. Since the turbulence simulation is random and the difference between the wind profiles is small, the mean value variation due to random turbulence can be larger than the variation between any of the seven wind profiles. For this reason it is difficult to draw any conclusion when turbulence is included. If however, the turbulence is ignored, the expected results are achieved.

Conclusion:

- No turbulence; the expected results are achieved
- Turbulence included; no clear results

## Table of content:

|  |    |
|--|----|
| Summary .....                                      | 2  |
| 1 Introduction .....                               | 7  |
| 2 Theory .....                                     | 8  |
| 2.1 Wind profiles .....                            | 8  |
| 2.1.1 Logarithmic wind profile .....               | 8  |
| 2.1.2 Atmospheric stability .....                  | 9  |
| 2.1.3 Power law wind profile .....                 | 9  |
| 2.2 Turbulence .....                               | 10 |
| 2.3 Wind field and grid .....                      | 11 |
| 2.4 Turbsim .....                                  | 11 |
| 2.5 Coordinate axes .....                          | 12 |
| 2.6 Sources of loading .....                       | 13 |
| 2.6.1 Gravitational loading .....                  | 13 |
| 2.6.2 Aerodynamic loading .....                    | 13 |
| 2.7 Fedem .....                                    | 19 |
| 2.8 Fatigue .....                                  | 20 |
| 2.8.1 Rainflow counting method .....               | 20 |
| 2.8.2 Scaling of cycles .....                      | 23 |
| 2.8.3 Miners Rule .....                            | 23 |
| 2.8.4 Damage Equivalent Load .....                 | 24 |
| 3 Methodology .....                                | 25 |
| 3.1 NREL offshore 5-MW baseline wind turbine ..... | 25 |
| 3.2 Wind profiles .....                            | 25 |
| 3.3 Turbulence .....                               | 29 |
| 3.4 Wind field and grid .....                      | 29 |
| 3.5 Turbsim .....                                  | 29 |
| 3.6 Fedem .....                                    | 30 |
| 3.7 Rainflow counting .....                        | 31 |
| 3.8 Binning the load range .....                   | 31 |
| 3.9 Calculation of damage equivalent load .....    | 33 |
| 4 Results .....                                    | 34 |
| 5 Discussion .....                                 | 39 |
| 6 Conclusion .....                                 | 44 |
| 7 References .....                                 | 45 |
| 8 Appendix .....                                   | 47 |
| 8.1 Wind profiles .....                            | 47 |
| 8.2 Tables with damage equivalent loads .....      | 55 |

|     |  |    |
|-----|--|----|
| 8.3 | Graphical presentation of damage equivalent loads..... | 59 |
| 8.4 | Bin widths.....  | 65 |
| 8.5 | Turbsim input file .....                               | 66 |
| 8.6 | Mlife text file .....                                  | 68 |

## List of figures:

|             |  |    |
|-------------|--|----|
| Figure 2.1  | Wind field illustration [8].....   | 11 |
| Figure 2.2  | Wind field crossings.....  | 11 |
| Figure 2.3  | a) and b) Coordinate axes [11].....  | 12 |
| Figure 2.4  | Gravitational sinusoidal loading.....  | 13 |
| Figure 2.5  | Control volume.....  | 14 |
| Figure 2.6  | Velocities at the rotor plane [15].....  | 15 |
| Figure 2.7  | Local loads on an aerofoil, [16].....  | 16 |
| Figure 2.8  | Closed cycle.....  | 20 |
| Figure 2.9  | Rainflow counting illustration [21].....   | 22 |
| Figure 3.1  | Curve fitting of VU-logarithmic vs. VU-power law.....  | 27 |
| Figure 3.2  | The seven power law wind profiles.....   | 28 |
| Figure 3.3  | Typical load fluctuation.....  | 31 |
| Figure 3.4  | Binning the load range.....  | 32 |
| Figure 4.1  | RFx – DEL due to force in x-direction at blade root.....   | 36 |
| Figure 4.2  | RM <sub>y</sub> - DEL due to bending moment in y-direction at blade root.....                            | 36 |
| Figure 4.3  | TTFx - DEL due to force in x-direction at tower top.....   | 37 |
| Figure 4.4  | TTM <sub>y</sub> - DEL due to bending moment in y-direction at tower top.....                            | 37 |
| Figure 4.5  | TBFx - DEL due to force in x-direction at tower bottom.....  | 38 |
| Figure 4.6  | TBM <sub>y</sub> - DEL due to bending moment in y-direction at tower bottom.....                         | 38 |
| Figure 5.1  | Load range of the bending moment in y-direction at blade root, BM <sub>y</sub> .....                     | 40 |
| Figure 5.2  | RM <sub>y</sub> - DEL due to bending moment in y-direction at blade root. Not sufficient bins.....       | 41 |
| Figure 5.3  | Development of the ratio RM <sub>x</sub> vs. RM <sub>y</sub> , by reduction of turbulence intensity..... | 42 |
| Figure 8.1  | Very unstable wind profile – $\alpha = 0.105$ .....  | 51 |
| Figure 8.2  | Unstable wind profile – $\alpha = 0.102$ .....   | 51 |
| Figure 8.3  | Near unstable wind profile – $\alpha = 0.100$ .....  | 52 |
| Figure 8.4  | Neutral wind profile – $\alpha = 0.093$ .....  | 52 |
| Figure 8.5  | Near stable wind profile – $\alpha = 0.086$ .....  | 53 |
| Figure 8.6  | Stable wind profile – $\alpha = 0.082$ .....   | 53 |
| Figure 8.7  | Very stable wind profile – $\alpha = 0.059$ .....  | 54 |
| Figure 8.8  | RF <sub>y</sub> – DEL due to force in y-direction at blade root.....                                     | 59 |
| Figure 8.9  | RF <sub>z</sub> – DEL due to force in z-direction at blade root.....                                     | 59 |
| Figure 8.10 | RM <sub>x</sub> – DEL due to bending moment in x-direction at blade root.....                            | 60 |
| Figure 8.11 | RM <sub>z</sub> – DEL due to bending moment in z-direction at blade root.....                            | 60 |
| Figure 8.12 | TTF <sub>y</sub> - DEL due to force in y-direction at tower top.....                                     | 61 |
| Figure 8.13 | TTF <sub>z</sub> - DEL due to force in z-direction at tower top.....                                     | 61 |
| Figure 8.14 | TTM <sub>x</sub> - DEL due to bending moment in x-direction at tower top.....                            | 62 |
| Figure 8.15 | TTM <sub>z</sub> - DEL due to bending moment in z-direction at tower top.....                            | 62 |
| Figure 8.16 | TBF <sub>y</sub> - DEL due to force in y-direction at tower bottom.....                                  | 63 |
| Figure 8.17 | TBF <sub>z</sub> - DEL due to force in z-direction at tower bottom.....                                  | 63 |
| Figure 8.18 | TBM <sub>x</sub> - DEL due to bending moment in x-direction at tower bottom.....                         | 64 |
| Figure 8.19 | TBM <sub>z</sub> - DEL due to bending moment in z-direction at tower bottom.....                         | 64 |

## List of tables:

|            |   |    |
|------------|---|----|
| Table 2.1  | Parameters used to calculate the relative velocity and angles [12].....         | 15 |
| Table 3.1  | Properties for the NREL 5-MW Baseline Wind turbine [22].....                    | 25 |
| Table 3.2  | Names of the wind profiles .....  | 25 |
| Table 3.3  | Monin-Obukhov lengths for the seven wind profiles.....                          | 26 |
| Table 3.4  | Roughness length .....  | 26 |
| Table 3.5  | $\alpha$ – parameters .....   | 27 |
| Table 3.6  | Integrated values of the wind profiles .....                                    | 29 |
| Table 3.7  | Loads extracted from the Fedem simulations.....                                 | 30 |
| Table 3.8  | Changes in DEL for RMy due to varying number of bins .....                      | 32 |
| Table 3.9  | Bin widths found by dividing the smallest load range of the 91 runs by 50 ..... | 33 |
| Table 4.1  | DEL due to 25 % TI.....   | 34 |
| Table 4.2  | DEL normalized with respect to the neutral wind profile for 25 % TI.....        | 34 |
| Table 4.3  | DEL due to 11 % (TI) .....  | 34 |
| Table 4.4  | DEL normalized with respect to the neutral wind profile for 11 % TI.....        | 35 |
| Table 4.5  | DEL due to 0 % TI .....   | 35 |
| Table 4.6  | DEL normalized with respect to the neutral wind profile for 0 % TI.....         | 35 |
| Table 8.1  | Collection of wind profile names, abbreviations, parameters and functions.....  | 47 |
| Table 8.2  | Calculation of the stability parameter, $\psi$ .....                            | 48 |
| Table 8.3  | Calculation of the logarithmic wind profiles.....                               | 49 |
| Table 8.4  | Calculation of the power law wind profiles .....                                | 50 |
| Table 8.5  | DEL due to 25 % TI for VU.....  | 55 |
| Table 8.6  | DEL due to 25 % TI for U.....   | 55 |
| Table 8.7  | DEL due to 25 % TI for NU.....  | 55 |
| Table 8.8  | DEL due to 25 % TI for NEU .....  | 55 |
| Table 8.9  | DEL due to 25 % TI for NS .....   | 56 |
| Table 8.10 | DEL due to 25 % TI for S .....  | 56 |
| Table 8.11 | DEL due to 25 % TI for VS .....   | 56 |
| Table 8.12 | DEL due to 11 % TI for VU.....  | 57 |
| Table 8.13 | DEL due to 11 % TI for U.....   | 57 |
| Table 8.14 | DEL due to 11 % TI for NU.....  | 57 |
| Table 8.15 | DEL due to 11 % TI for NEU .....  | 57 |
| Table 8.16 | DEL due to 11 % TI for NS .....   | 58 |
| Table 8.17 | DEL due to 11 % TI for S .....  | 58 |
| Table 8.18 | DEL due to 11 % TI for VS .....   | 58 |
| Table 8.19 | Bin widths found by dividing the largest neutral load range by 50.....          | 65 |

# 1 Introduction

In recent years there has been an increased interest on renewable energy, by government's organizations and individuals. The motivation for this engagement is due to a number of reasons. One of these reasons is to reduce emissions of greenhouse gases, thereby reducing the impact that this has on the environment. Another motivation is to become independent of foreign oil, because of political instability in oil exporting countries. A third motivation is that the world is hungry for energy, and by meeting this need, an increasing number of people will be lifted out of poverty.

The commitment to renewable energy spans over a wide specter of energy sources. This includes solar energy, wave energy and wind energy etc. Among these, wind energy is an important one. Therefore there has been done a lot of research for the last decades, to improve wind turbines, including offshore wind turbine. This research involves making wind turbines more efficient for electricity production, more cost efficient, to handle more fatigue etc.

Wind turbines in general and offshore wind turbines in particular, have a huge development potential. This is due to large unused regions. This is especially true at offshore locations, in which conflicts are less due to noise and visual esthetics. In addition, offshore wind turbines are exposed to greater wind influences than the case is with land-based wind turbines. This is due to no obstacles, such as mountains and buildings. On the other hand it is more difficult to perform maintenance at offshore locations.

A major research project taking place these days is called OC4. This is a research project taking place across national borders. The abbreviation OC4 stands for Offshore Code Comparison Collaboration Continuation. The goal for OC4 is to develop dynamic computer codes to simulate and assess wind turbines and support structures, and compare these codes to design models. This research project is an ongoing project, and still many questions are unanswered. [1]

This thesis is focusing on the wind turbine model used in the OC4 project; the NREL offshore 5-MW baseline wind turbine. The main goal for the thesis is to provide results for how seven different wind profiles affect the fatigue on the wind turbine.



## 2 Theory

### 2.1 Wind profiles

The wind speed profile is a representation of a mean wind speed that varies with height above the sea surface. In the absence of complex stability and terrain conditions, idealized models are used for this representation. In DNV-RP-C205 (2010) there are three examples of such idealized models. They are the logarithmic wind profile model, the power law wind profile model and the Frøya wind profile model. Of these, the models most widely applied are the logarithmic and power law wind profile. These will be described in the following sections. The Frøya wind profile model will not be dealt with in this thesis. [2]

#### 2.1.1 Logarithmic wind profile

From the reference level the wind speed profile can be calculated at any level by using the logarithmic wind profile based on neutral atmospheric conditions. This can be written as in formula 2.1. [2]

$$U(z) = U(H) \left( \frac{\ln \frac{z}{z_0}}{\ln \frac{H}{z_0}} \right) \quad 2.1$$

Here  $U(H)$  is the reference speed, and  $z$  is a variable which denote the height from still water level. The abbreviation  $z_0$  denotes the roughness length. [2]

The roughness length parameter is in offshore location a parameter that depends on wind speed, upstream distance to land, water depth and wave field. This parameter can be found implicit by formula 2.2. The procedure is to insert a value for  $z_0$ , and continue to do so until both sides are equal. This is called to perform iteration. [2]

$$z_0 = \frac{A_c}{g} \left( \frac{k_a U(z)}{\ln z/z_0} \right)^2 \quad 2.2$$

In formula 2.2  $A_c$  is a constant called Charnock's constant and has a value between 0.011-0.014 in open sea with fully developed waves. However, as one approaches the coast, this value can be 0.018 or more. The abbreviation  $g$  represents the gravity, and  $k_a$  is the Karman's constant with value 0.4. [2]

Finally when this parameter has been found, it is possible to calculate the neutral logarithmic wind profile by formula 2.1. [2]

### 2.1.2 Atmospheric stability

In order to take into consideration the atmospheric stability condition, formula 2.1 has to be modified by a stability correction parameter  $\psi$ . Then the formula will be as follows: [3] [4]

$$U(Z) = U(H) \frac{\ln \frac{Z}{Z_0} - \psi}{\ln \frac{H}{Z_0} - \psi} \quad 2.3$$

As mentioned in the previous section, formula 2.1 is based on an atmospheric stability which is neutral. This neutral stability is the idealized model/shape. In nature however this shape is not always the best fit. One must take into account the differences in atmospheric stability. The atmospheric stability is divided into classes, determined by the Obukhov length  $L_{m0}$ . The Obukhov length represents the relative influence of mechanical and thermal forcing on the turbulence. [3]

The stability correction parameter,  $\psi$ , given in formula 2.3 depends on the ratio  $z/L_{m0}$ , and can be found by the use of formula 2.4 - 2.6. [3]

$$\psi_1 = 2 \ln(1 + x) + \ln(1 + x^2) - 2 \tan^{-1}(x) \text{ for } \frac{z}{L_{m0}} < 0 \quad 2.4$$

$$x = \left(1 - 19,3 \frac{z}{L_{m0}}\right)^{\frac{1}{4}} \quad 2.5$$

$$\psi_2 = -4,8 \frac{z}{L_{m0}} \text{ for } \frac{z}{L_{m0}} \geq 0 \quad 2.6$$

### 2.1.3 Power law wind profile

The power law wind profile is an alternative way to calculate wind speed at different heights, and is calculated by formula 2.7. [2]

$$U(Z) = U(H) \left(\frac{Z}{H}\right)^\alpha \quad 2.7$$

## 2.2 Turbulence

The turbulence intensity can be calculated by using formula 2.8.

$$T = \frac{\sigma_U}{U(H)} \quad 2.8$$

[5]

, where T is turbulence intensity,  $\sigma_U$  is standard deviation, U(H) is mean wind speed at reference height (11.4 m/s). [5]

$$\sigma_U = \frac{U(H)}{\ln\left(\frac{H}{z_0}\right)} + 1.28 \cdot 1.44 \cdot I_{15}, \text{ where } I_{15} = 0.14 \text{ (medium turbulence)} \quad 2.9$$

[6] [7]

## 2.3 Wind field and grid

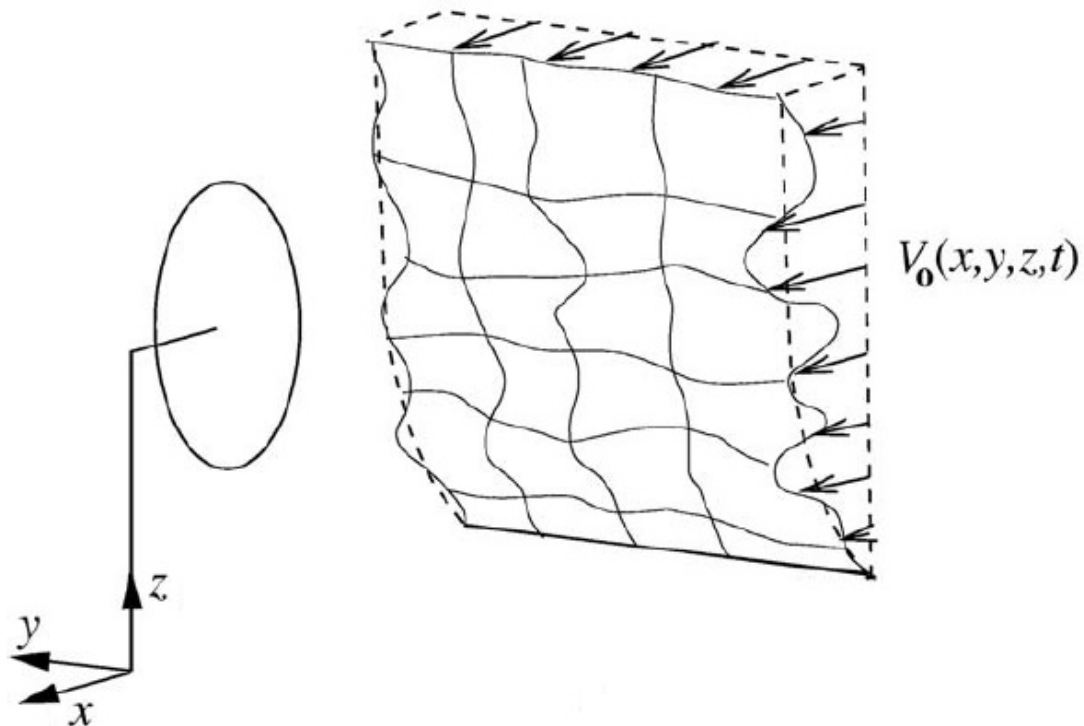


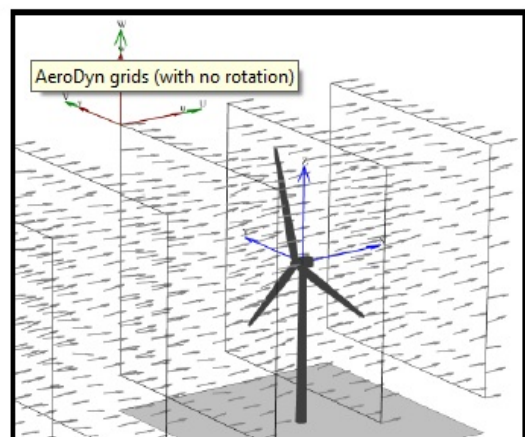
Figure 2.1 Wind field illustration [8]

Figure 2.1 illustrates a wind field. This wind field is bounded by a height and a width, called grid height and grid width. Further, the dashed lines which is bended, represents a wind profile if no turbulence is present. They are constant during the simulation. If one instead takes into account turbulence, the distorted lines represent the wind velocity. These lines represent the velocity at a given time. [8]

## 2.4 Turbsim

Turbsim is a software application used to generate wind fields. A wind field consists of wind profile and turbulence. In turbsim the logarithmic wind profile and the power law wind profile can be selected. [9]

The application uses a statistical model to generate time series of wind fields. An illustration of how wind fields changes with time is given by Figure 2.2. [9]



[10]

Figure 2.2 Wind field crossings

## 2.5 Coordinate axes

In order to describe the forces acting in different on the reference wind turbine, it is necessary to establish coordinate axes. They are illustrated in Figure 2.3 below.

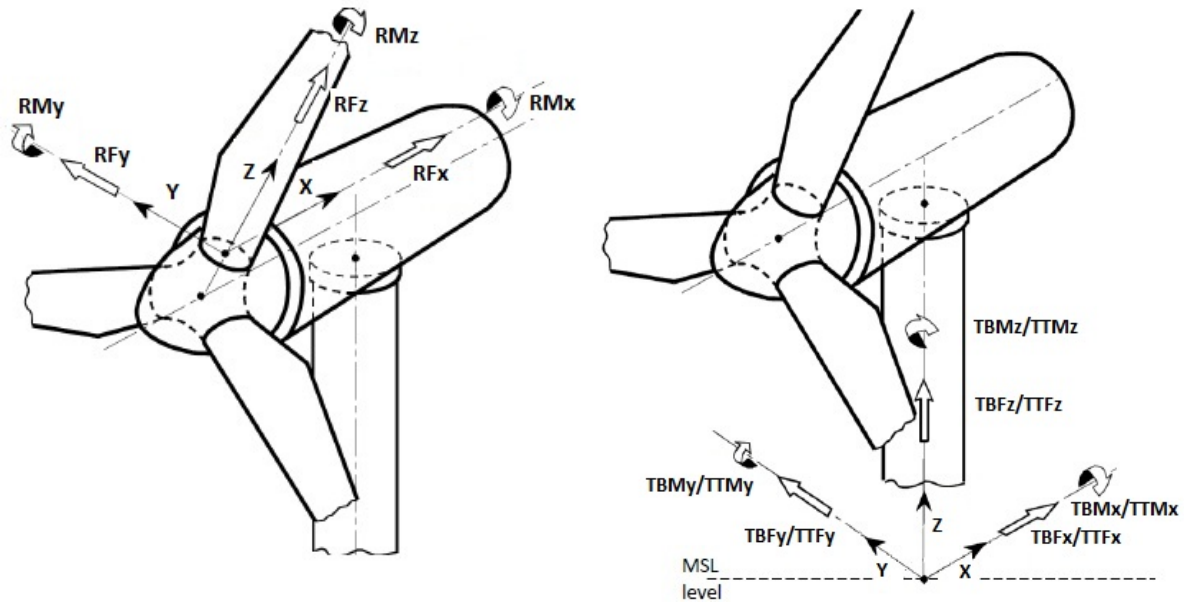


Figure 2.3 a) and b) Coordinate axes

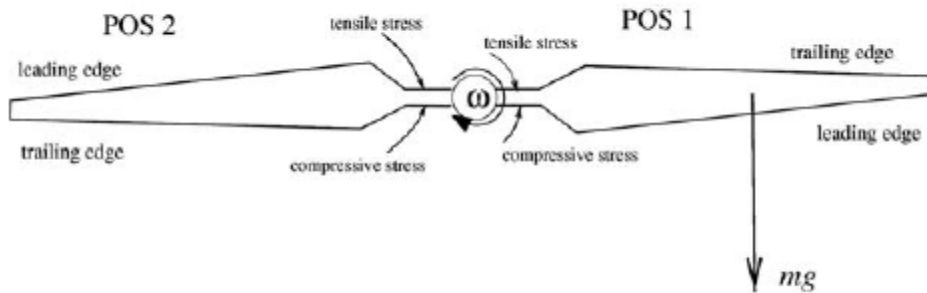
[11]

In the figure, the wind distribution which generates aerodynamic loads comes mainly from the left side. In Figure 2.3 a) the coordinate axes for the blades are illustrated. The x-axis is pointed in the downwind direction, while the z-axis starts at the blade root and ends in the blade tip. Finally the y-axis is given by the right hand Cartesian coordinate system, and pointed left in the rotor plane. The same is true for Figure 2.3 b), but here the z-axis is pointed upward. [11]

## 2.6 Sources of loading

### 2.6.1 Gravitational loading

The gravitational loading of a wind turbine can be illustrated by Figure 2.4



[13]

**Figure 2.4 Gravitational sinusoidal loading**

The positive y-direction in Figure 2.4 is pointed upward. The positive y-direction is illustrated in Figure 2.3. When looking at the leading edge in position 1, the blade root experience compressive stress, when exposed to gravitational load. After the turbine blade has been exposed to a half revolution, the blade root at the leading edge experience tensile stress. By being exposed to an additional half revolution, it returns to the starting point. By doing so it has finish a full cycle. Thus, the blade is exposed to a sinusoidal loading in the rotor plane due to gravity. The gravitational load provides a major contribution of the fatigue due to the large wingspan and weight. It is therefore important to take this into consideration gravitational loading. [12]

### 2.6.2 Aerodynamic loading

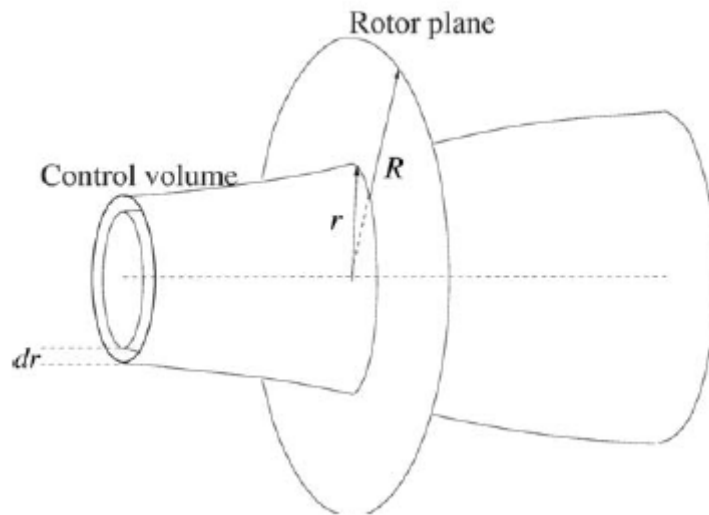
The aerodynamic loading is calculated by use of the the blade element momentum method.

#### 2.6.2.1 The blade element momentum (BEM) method

The blade element momentum method can be described by use of the algorithm described in Sec.2.6.2.5. The algorithm is applied on as many control volume as a wind turbine blade is divided into. A control volume is described in Sec.2.6.2.2. When the algorithm has been performed, the local loads on each node are calculated. The local loads are then used to calculate global loads, such as bending moment and force at the blade root. [12]

### 2.6.2.2 Control volume

In order to use the BEM method, control volumes need to be defined. A control volume consists of an annular element multiplied by the element length,  $dr$ . An illustration of a control volume is given in Figure 2.5 below. [12]



[14]

Figure 2.5 Control volume

Here  $R$  is rotor radius,  $r$  is radius from hub center to the specified node,  $dr$  is element length.

### 2.6.2.3 Calculation of relative velocity

In Figure 2.6 an aerofoil is shown, which is a cross section of a wind turbine blade. It is sliced at a node, to be used as an illustration of the wind speed acting on the wind turbine blade. The dashed line is the rotor plane. This means that the whole wind turbine is turned 90 degree such that the hub is pointed downward. [12]

The wind velocity,  $V_0 (1-a)$ , is acting perpendicular to the rotor plane, while the rotational velocity,  $\omega r (1+a')$ , is acting tangential. These two combined by the use of Pythagoras gives the relative velocity. [12]

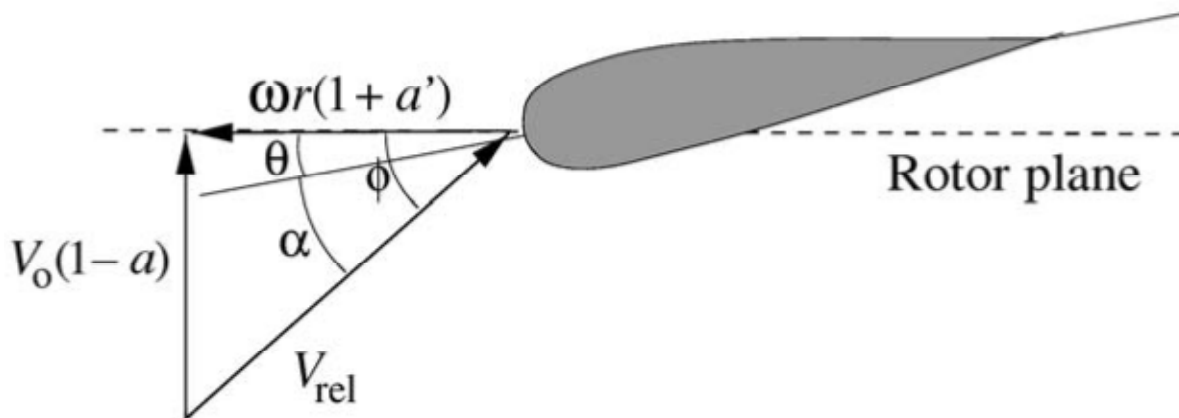


Figure 2.6 Velocities at the rotor plane [15]

Explanation of the parameters used in Figure 2.6 is tabulated in Table 2.1.

|          |  |
|----------|--|
| $V_0$    | Wind speed                                     |
| $\omega$ | Rotational speed                               |
| $r$      | Radius - from hub center to the specified node |
| $a$      | Axial induction factor                         |
| $a'$     | Tangential induction factor                    |
| $\theta$ | Local pitch                                    |
| $\phi$   | Flow angle                                     |
| $\alpha$ | Local angle of attack                          |

Table 2.1 Parameters used to calculate the relative velocity and angles [12]

The formula needed to calculate the relative velocity is: [12]

$$V_{rel} = \sqrt{[V_0(1-a)]^2 + [\omega r(1+a')]^2} \quad 2.10$$

The flow angle is given by formula 2.11. [12]

$$\tan \phi = \frac{V_0(1-a)}{\omega r(1+a')} \quad 2.11$$

The local angle of attack is given by formula 2.12: [12]

$$\alpha = \phi - \theta \quad 2.12$$

The axial and tangential induction parameters are calculated using the BEM method. This is explained below.



### 2.6.2.4 Calculation of local force at nodes

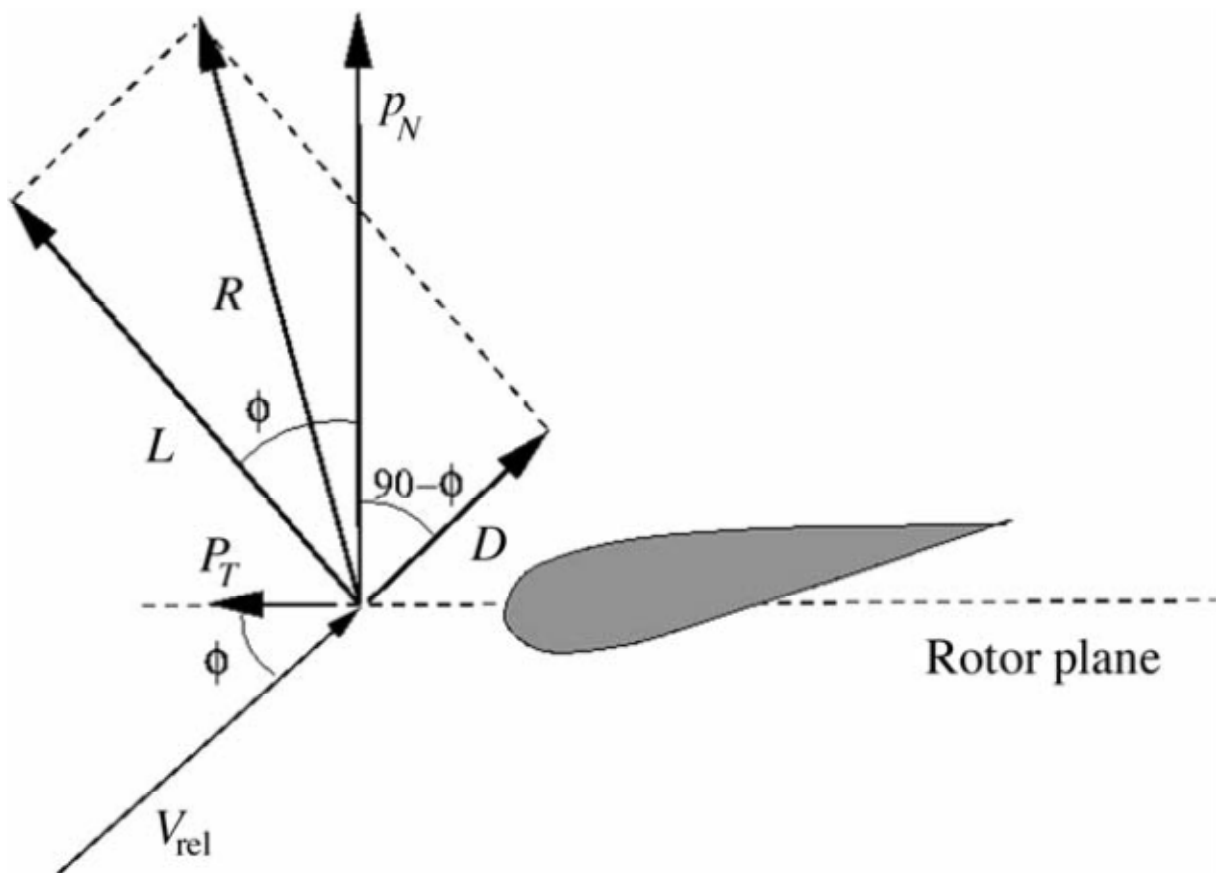


Figure 2.7 Local loads on an aerofoil, [16]

As illustrated in Figure 2.7 the forces acting on the blade element are perpendicular to each other. The force which is parallel to the relative velocity is called drag force,  $D$ , and the force which is perpendicular to the relative velocity is called lifting force,  $L$ . The vector representation in Figure 2.7 illustrate that the drag force component should be minimize in relation to the lifting force component. This is because it is the lifting force component which contributes to the revolution of the wind turbine. In order to keep the lifting force component high, the wind turbine blades is constructed with a twist from the nose of the blade to the trailing edge. To be able to calculate global loads, the local loads drag and lift, have to be projected in normal and tangential direction, relative to the rotor plane. The formulas needed to calculate the local forces at each node are given in formula 2.13 - 2.16. [12]

The lift force,  $L$ , is given by formula 2.13 [12]

$$L = \frac{1}{2} \rho V_{rel}^2 c C_l \quad 2.13$$

Here  $\rho$  is the air density. The letter  $c$  represents the chord length, which is the width of the blade cross section. The lift coefficient is denoted by  $C_l$ , which depends on measured values.

The drag force,  $D$ , is given by formula 2.14. [12]

$$D = \frac{1}{2} \rho V_{rel}^2 c C_d \quad 2.14$$

The drag coefficient is denoted by  $C_d$ , which depends on measured values.

The projected force normal to the rotor plane,  $P_N$ , is given by formula 2.15. [12]

$$P_N = L \cos \phi + D \sin \phi \quad 2.15$$

The projected force tangential to the rotor plane,  $P_T$ , is given by formula 2.16. [12]

$$P_T = L \sin \phi - D \cos \phi \quad 2.16$$

#### **2.6.2.5 BEM algorithm**

To be able to calculate the local loads the BEM algorithm has to be carried out first. This algorithm has the following steps: [12]

1. Set the induction factors,  $a$  and  $a'$ , to be zero initially
2. Calculate the flow angle by use of formula 2.11
3. Calculate the local angle of attack by formula 2.12
4. Use the local angle of attack to find the lift coefficient and the drag coefficient, by curves or tabulated values
5. Use formula 2.17 and 2.18 to find the normal and tangential coefficients, which are a projection of the lift and drag coefficients
6. Calculate  $a$  and  $a'$  by formula 2.19 and 2.20
7. If the initial values given in step 1 do not match the values calculated in step 6, the algorithm must to be performed all over again. If instead the values are approximately the same, the blade element method is completed

The local loads can now be calculated, and by summing the contributions from each node, the loads on the blade root can be found. [12]

The projected coefficient normal to the rotor plane,  $C_n$ , due to drag and lift coefficient, is given by formula 2.17. [12]

$$C_n = C_l \cos \phi + C_d \sin \phi \quad 2.17$$

The projected coefficient tangential to the rotor plane,  $C_t$ , due to drag and lift coefficient, is given by formula 2.18. [12]

$$C_t = C_l \sin \phi - C_d \cos \phi \quad 2.18$$

The axial induction factor is given by formula 2.19. [12]

$$a = \frac{1}{\frac{4 \sin^2 \phi}{\sigma C_n} + 1} \quad 2.19$$

Here  $\sigma$  is the solidity, calculated by formula 2.21. [12]

The tangential induction factor is given by formula 2.20. [12]

$$a' = \frac{1}{\frac{4 \sin \phi \cos \phi}{\sigma C_t} - 1} \quad 2.20$$

The solidity is calculated by formula 2.21. [12]

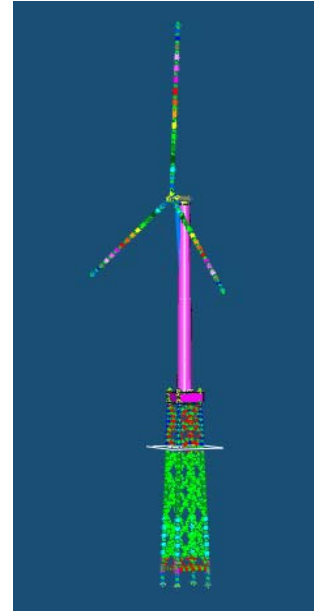
$$\sigma(r) = \frac{c(r)B}{2\pi r} \quad 2.21$$

Here  $\sigma$  represents the fractional part of the annular area covered by blades. B denotes the number of blades. [12]

## 2.7 Fedem

Fedem is a multi-body software, where analysis takes place in a time-domain. The acronym Fedem stands for Finite Element Dynamics in Elastic Mechanisms. The software performs virtual testing of complex mechanical systems. This includes the capability to create, solve and post process data. Fedem is also equipped with solvers which provide fast and numerically stable results. It is possible to observe how the time domain analysis developed with time, through user interface. This means that it is possible to watch animations and curves under development. The Fedem software can be used for load analysis, stress analysis, eigenmode solutions, strain gage solutions and fatigue analysis. However, not all these aspects are fully functional in Fedem windpower, since the software is still under development. For instance fatigue analysis is not verified. [17]

Fedem windpower can be used as a tool to simulate how wind field causes aerodynamic loads on wind turbines. The wind field is generated by another software application. This can for instance be Turbsim, see Section 2.4. By use of the generated wind field, Fedem estimate among other things, loads at specific locations. [17]



Note: The model on the right side is created by Kristian Sætertrø, using Fedem software

## 2.8 Fatigue

Fatigue is a common source to failure in materials. It is a type of failure that occurs over a long period of time. Initially fatigue starts with a tiny crack, which grows non-linearly when subjected to repeating cyclic loads. However, non-linear growth is hard to measure, and to be able to estimate fatigue in a more convenient way, it can be assumed that cracks expands linearly. Palmer-Miner rule is used regarding this issue. See Sec. 2.8.3. [18]

To determine how much cyclic load of different load range, the blades on a wind turbine can withstand without collapsing, there has to be done some experimental tests. The results from these tests are sketched in curves called S-N curves. This is, in other words, the capacity to the material in the blades. [18] [19]

### 2.8.1 Rainflow counting method

The rainflow counting method, developed by the Japanese researchers Matsuishi and Endo, is needed when a material is exposed to irregular loads over a time period. It is needed in order to define fatigue based on Palmer-Miner rule. This rule requires closed cycles, and scaled cycles. The closed cycles are achieved by using the rainflow counting method, and the way to scale cycles are described in section 2.8.2. [18] [20]

The idea behind the rainflow counting method is to pair half-cycles that match each other, in both load mean and range. The half-cycles that match each other are equal in size (or rather equal), but directed in opposite direction. This is illustrated by arrows in Figure 2.9. When they are matched, they form a closed cycle. A closed cycle is illustrated in Figure 2.8. The half-cycles matched must not necessarily be neighbors, i.e. a half cycle at the start of a load history can be paired with a half-cycle at the end. [18] [20]

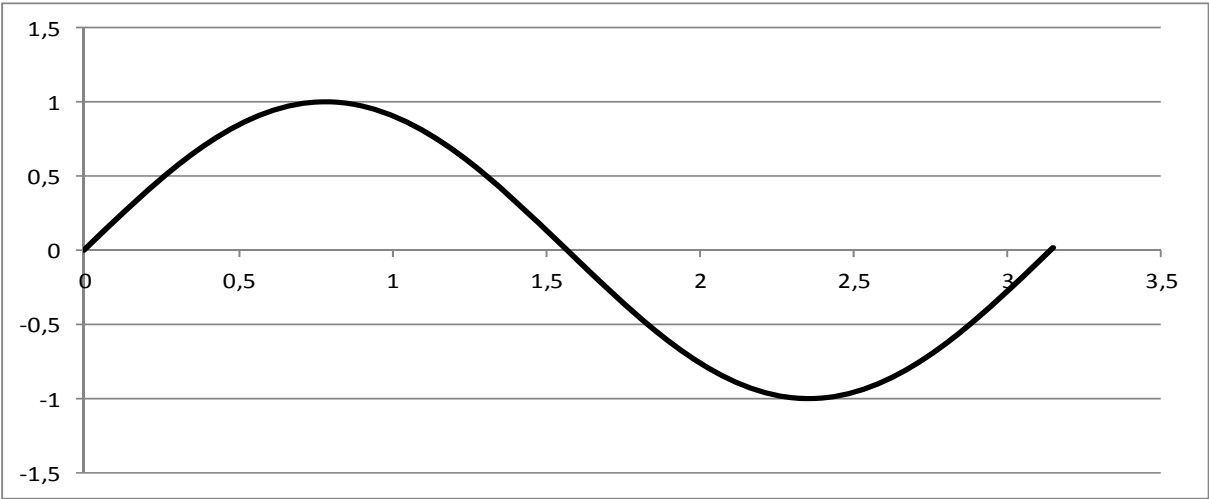


Figure 2.8 Closed cycle

The rainflow counting method may be illustrative described by use of Figure 2.9. First of all there has to be drawn straight lines from the valley to the peak and vice versa, throughout the load spectrum. Afterwards the load spectrum will be turned around 90 degrees clockwise. The result of this revolution is that positive x-axis is on right side, seen from the origin, and the negative x-axis on the opposite side. The sketch in Figure 2.9 has a zigzag pattern. This gave the Japanese researchers, Matsuishi and Endo, associations to a roof construction that exists in Japan, called pagoda roof. Their thoughts were to drop a raindrop on each “roof”. These drop follows “the roof“, and fall to the ground when the following occurs: [20] [21]

- They pass a larger maximum. This occurs when the drop runs from right to left
- They pass a larger minimum. This occurs when the drop runs from left to right
- Hitting another drop when it flows down the “roof”
- Just fall out

[21]

All the drops that fall to ground represent a half-cycle. Those who match each other are coupled. After performing rainflow counting one gets a matrix of closed cycles, where a cycle is defined by its own range and mean. [21]

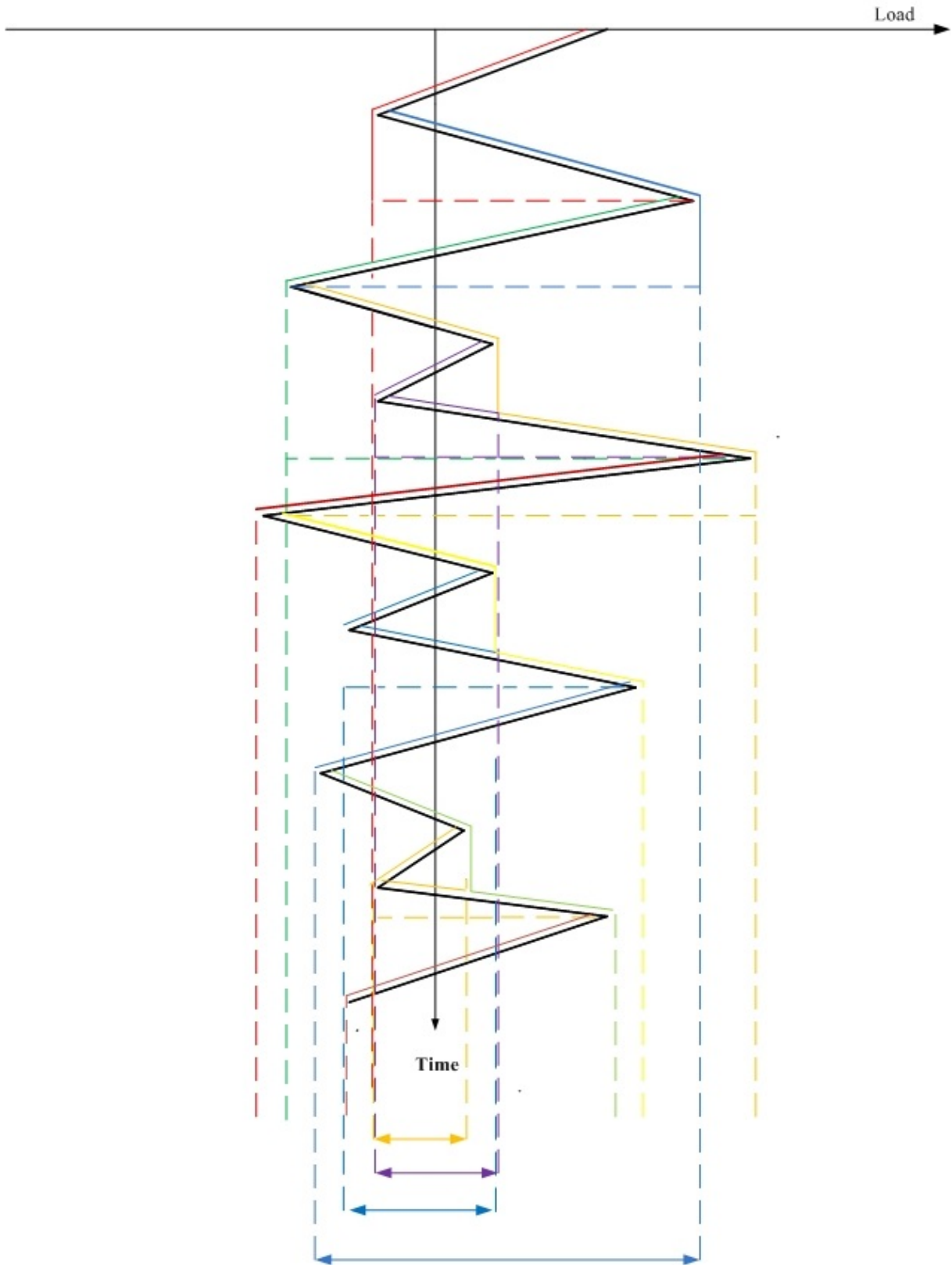


Figure 2.9 Rainflow counting illustration [21]

## 2.8.2 Scaling of cycles

Cycle scaling is necessary if there is a spectrum of mean loads, because the formulas used in the Miner's rule are based on cycle fluctuations around one mean load. The way to achieve one mean load, is to adjust each cycle's load range, by a factor equal or greater than 1, using the following formula: [19]

$$L_k^{RF} = L_k^R \left( \frac{(L^{ult}) - |L^{MF}|}{(L^{ult} - |L_k^M|)} \right) \quad 2.22$$

In formula 2.22,  $L_k^R$ , represents a load range of any cycle in the load spectrum. The corresponding mean load value is represented by,  $L_k^M$ . The abbreviation  $L^{MF}$  represents the fixed mean value, in which the cycles are scaled.  $L^{ult}$  is the ultimate design load of the material being examined. [19]

## 2.8.3 Miners Rule

The Miner's rule, developed by Palmgren and Miner, calculate fatigue in a structure due to cyclic loading. Each cycle contributes with its own fraction sum to the total damage. The contributions are added together, and failure occurs when these reaches unity. In the Miner rule it is assumed that a cycle of a certain size produces the same amount of damage, whether it is located in the beginning or end of the load history. The reality is that this cycle will cause less damage in the beginning than at the end. Despite this assumption, the rule is widely used. The Miner's rule is a simple rule, and can be written as follows: [18] [19]

$$D = \sum_k \frac{n_k}{N_k(L_k^{RF})} \quad 2.23$$

Here is the numerator,  $n_k$ , the number of cycles of a certain range. The denominator,  $N_k(L_k^{RF})$ , is a measured value for how many cycles that are required for the material to fail, given a certain load range of the cycle. In other words,  $N_k$ , is a function of  $L_k^{RF}$ , described in section 2.8.2. That means that each load range has its own number of cycles to failure. To be able to calculate this number, the following formula is used: [19]

$$N_k^F = \left( \frac{L^{ult} - |L^{MF}|}{0.5L_k^{RF}} \right)^m \quad 2.24$$

In the formula,  $L^{ult}$ , means the ultimate design load for the component being analyzed. This is the maximum load that the component can be exposed to, including material factors. Further, the abbreviation inside the absolute value sign,  $L^{MF}$ , represents the fixed mean load. The exponent,  $m$ , is a number obtained by experimental testing. By using one can model an S-N curve. [19]



## 2.8.4 Damage Equivalent Load

The damage equivalent load for any load spectrum has a constant load range, fluctuates around a constant mean load, and has a constant frequency. It is a way to represent the same damage as the variable spectrum loads, calculated by Palmer- Miner rule. [19]

The damage equivalent load (DEL) is used to compare different kinds of load spectrum. To get an accurate basis for comparison, it is required that the frequency is set equal for the load spectra. In addition, the simulation time must have the same length. It also required that the S/N slopes, ( $m$ ), have the same numerical values. When the three parameters mentioned above are set equal for different load spectrum, it is only DEL which varies due to different load spectra. Since only DEL changes, the comparison between the various load histories is easy. It is simply to conduct a relative comparison, i.e. how large the difference is in percent for different load spectra. [19]

The DEL is calculated using formula 2.29. To enable that, one needs formula 2.25 - 2.28. [19]

$$D_j^{ST} = \sum_k \frac{n_{jk}}{N_k} = \frac{n_j^{STeq}}{N_j^{eq}} \quad 2.25$$

In formula 2.25,  $D_j^{ST}$  represent the short-term damage for file j. Further,  $n_{jk}$ , means the count of a certain cycle in file j.  $N_k$  represent the number of cycles to failure at a given size of the cycle.  $n_j^{STeq}$  is the equivalent number of cycles, and  $N_j^{eq}$  is the equivalent number of cycles to failure. [19]

$$n_j^{STeq} = f^{eq} * T_j \quad 2.26$$

In formula 2.26,  $f^{eq}$  represent the chosen frequency, and  $T_j$  the elapsed time. [19]

$$N_j^{eq} = \left( \frac{L^{ult}}{\left(\frac{1}{2} DEL_j^{STF}\right)} \right)^m \quad 2.27$$

In formula 2.27,  $L^{ult}$  is the ultimate design load. The S/N-slopes is represented by  $m$ . [19]

$$L_k^{R0} = L_k^R \left( \frac{L^{ult}}{(L^{ult} - |L_k^M|)} \right) \quad 2.28$$

In formula 2.28 cycles are scaled about a zero mean. The abbreviation is explained below formula 2.22 [19]

$$DEL_j^{ST0} = \left( \frac{\sum_k (n_k (L_k^{R0})^m)}{n_j^{STeq}} \right)^{\frac{1}{m}} \quad 2.29$$

Formula 2.29 calculate the damage equivalent load. [19]

### 3 Methodology

The main goal for the thesis is to investigate the effect that seven different wind profiles have on the fatigue of the reference wind turbine. This chapter gives a step by step description of the methodology applied. At selected locations on the wind turbine fatigue analysis will be performed using the different wind profiles. These locations are blade root, tower top and tower bottom. In addition, a description of the wind turbine analyzed, will be given. To be able to perform the fatigue analysis the following software's have been used: Turbsim, Fedem, Mlife (Matlab application) and Microsoft Excel.

#### 3.1 NREL offshore 5-MW baseline wind turbine

The 5-MW NREL wind turbine is used in the OC4-project. This is a wind turbine which originally was developed by the National Renewable Energy Laboratory in the United States (NREL). It is used as a mal for large, megawatt offshore wind turbines. Some properties for this wind turbine are listed in Table 3.1. [22]

| Rating                                   | 5 MW                    |
|--|-------------------------|
| <b>Rotor orientation, Configuration</b>  | Upwind, 3 blades        |
| <b>Rotor, Hub diameter</b>               | 126 m, 3 m              |
| <b>Hub height</b>                        | 90.55 m                 |
| <b>Cut-In, Rated, Cut-Out wind speed</b> | 3 m/s, 11.4 m/s, 25 m/s |
| <b>Cut-In, Rated Rotor speed</b>         | 6.9 rpm, 12.1 rpm       |
| <b>Rotor Mass</b>                        | 110 000 kg              |
| <b>Nacelle Mass</b>                      | 240 000 kg              |
| <b>Tower Mass</b>                        | 347 460 kg              |

Table 3.1 Properties for the NREL 5-MW Baseline Wind turbine [22]

#### 3.2 Wind profiles

The names of the wind profiles used the analysis are given in Table 3.2:

| Wind profiles        | Abbreviations |
|----------------------|---------------|
| <b>Very unstable</b> | VU            |
| <b>Unstable</b>      | U             |
| <b>Near unstable</b> | NU            |
| <b>Neutral</b>       | NEU           |
| <b>Near stable</b>   | NS            |
| <b>Stable</b>        | S             |
| <b>Very stable</b>   | VS            |

Table 3.2 Names of the wind profiles

In the analysis there are two different formulas that describe the wind profiles; the logarithmic wind profile and the power law wind profile. The formulas are 2.3 and 2.7 respectively, given in the theory chapter.

The logarithmic wind profile for the analysis includes among other things, the Obukhov lengths given in Table 3.3.

| Wind profiles | Monin-Obukhov lengths, $L_{m0}$ , [m] |
|---------------|---------------------------------------|
| VU            | -74                                   |
| U             | -142                                  |
| NU            | -314                                  |
| NEU           | 5336                                  |
| NS            | 318                                   |
| S             | 104                                   |
| VS            | 28                                    |

Table 3.3 Monin-Obukhov lengths for the seven wind profiles

Note: The obukhov lengths are given by supervisor Lene Eliassen

It is these lengths that cause different stability correction parameters, which in turn provides seven different logarithmic wind profiles.

In addition to the stability correction parameter, three other parameters are needed in order to obtain the logarithmic wind profile. One of them is the reference height,  $H$ . The reference height for the reference wind turbine is 90.55 m above still sea water level, which is the hub height. The corresponding wind speed is the reference speed,  $U(H)$ , chosen to be 11.4 m/s. This wind speed represents the mean wind speed at hub height.

The last parameter needed is the roughness length  $z_0$ , which is calculated by formula 2.2. In the analysis the  $z_0$ -value is chosen to be 0.001. In order to obtain that the  $A_c$  constant is given the value 0.0615. An overview of the parameters used to calculate the roughness length is given in Table 3.4.

| Parameter names                      | Abbreviations           | Values       | Entities            |
|--------------------------------------|-------------------------|--------------|---------------------|
| Charnock's constant                  | $A_c$                   | 0.0615       | [-]                 |
| Karman's constant                    | $\kappa_a$              | 0.4          | [-]                 |
| Gravity                              | $g$                     | 9.81         | [m/s <sup>2</sup> ] |
| Reference wind speed                 | $U(H)$                  | 11.4         | [m/s]               |
| Reference height                     | $H$                     | 90.55        | [m]                 |
| <b>Roughness length (calculated)</b> | <b><math>z_0</math></b> | <b>0.001</b> | <b>[m]</b>          |

Table 3.4 Roughness length

By using the information given so far, it is possible to calculate the seven logarithmic wind profiles. The calculated values are tabulated in Table 8.2 and Table 8.3 in Appendix.

However in this analysis, power law wind profiles are used instead. This is done because of limitation in the analysis application Turbsim, which is used to generate wind fields. The limitation implies that Turbsim only makes it possible to analyze the neutral atmosphere, in which stability is not taken into account. However the analysis requires that the stability correction parameters,  $\psi$ , are taken into account, because these create the seven wind profiles.

Therefore a method called curve fitting is used, in which the power law wind profile is adjusted until it fits the corresponding logarithmic wind profile, such that the stability correction parameter is included in the analysis. This implies to use formula 2.3 and 2.7, in which the  $\alpha$ -exponent represent the adjustment. The adjustment is done by Excel spread sheet,

and it is used a log-log scale to better see the best fit. Illustration of curve fitting is given in Figure 3.1, as well as Figure 8.1- Figure 8.7 in Appendix.

As can be seen in the figures, not all adjustments are equally accurate. This appears particularly in Figure 8.7, and also to some extent in Figure 8.6. For this reason the expected results for these two power law wind profiles, will not match the corresponding logarithmic wind profiles, which is the basis for the seven wind profiles analyzed. Due to this, inaccuracies will occur.

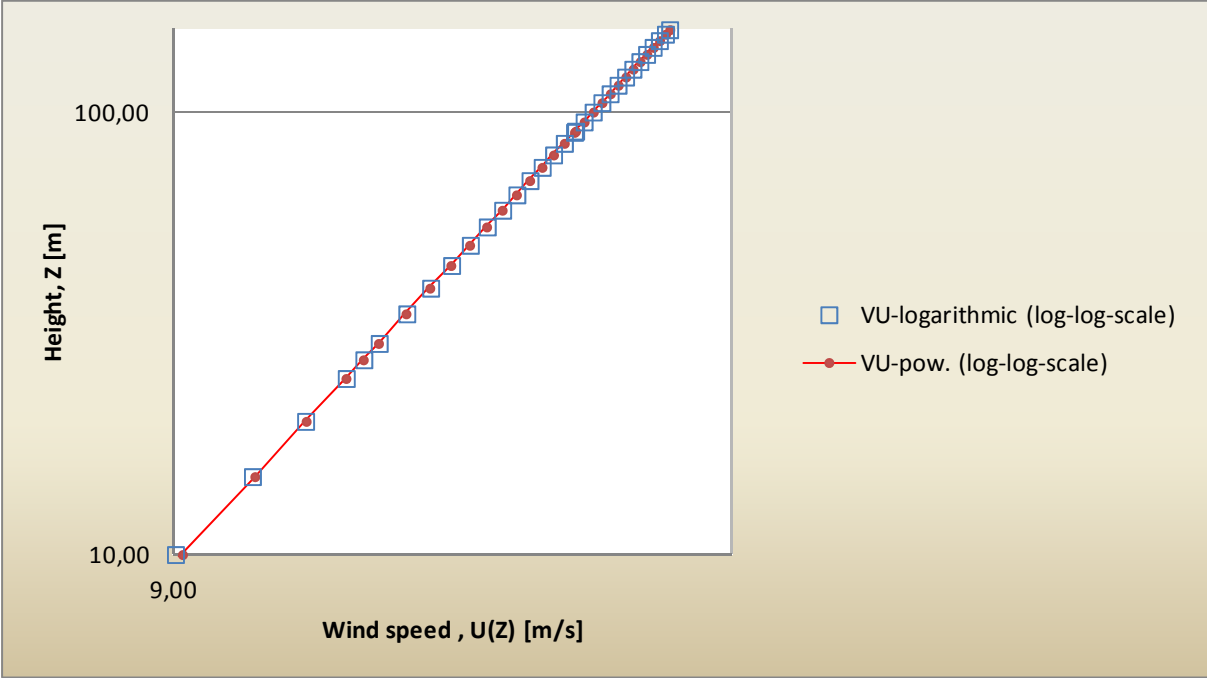


**Figure 3.1** Curve fitting of VU-logarithmic vs. VU-power law

Curve fitting is done for all seven wind profiles, and the alpha parameters obtained are tabulated in Table 3.5 below.

| Wind profiles | $\alpha$ - parameters |
|---------------|-----------------------|
| VU            | 0.105                 |
| U             | 0.102                 |
| NU            | 0.100                 |
| NEU           | 0.093                 |
| NS            | 0.086                 |
| S             | 0.082                 |
| VS            | 0.059                 |

**Table 3.5**  $\alpha$  – parameters

Now it is possible to calculate and illustrate the seven power law wind profiles, which is used in the analyses. They are illustrated in Figure 3.2 below, and calculated in Table 8.4 in Appendix.

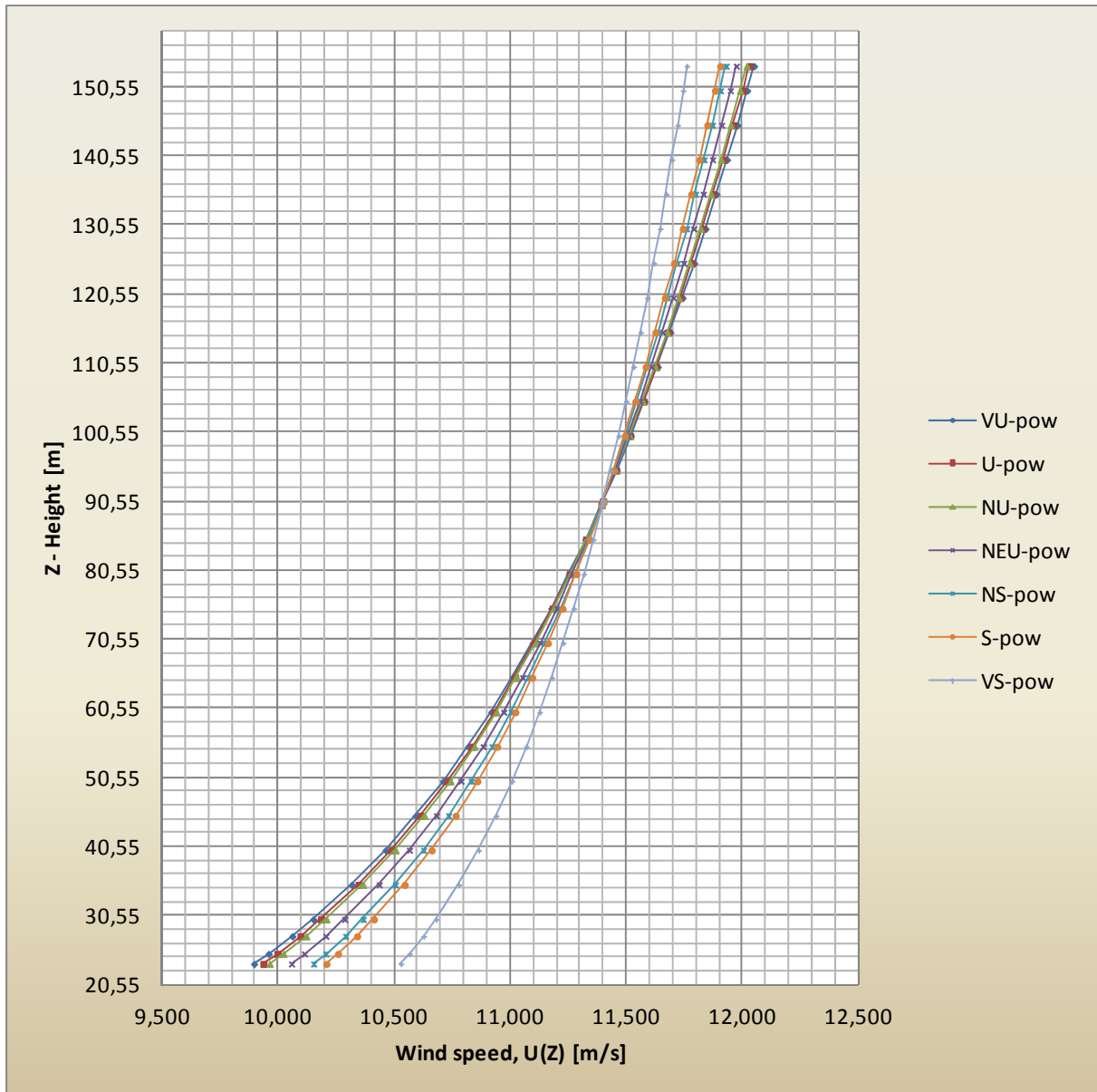


**Figure 3.2 The seven power law wind profiles**

In Figure 3.2 above the seven different power law wind profiles, define by the  $\alpha$ -parameters, are collected. The height on the z-axis, from the bottom value of 23.55 m to the top value of 153.55 m, creates aerodynamic loads which in turn causes fatigue damage on the wind turbine blades. This propagates then to the tower top and bottom.

It can be seen from Figure 3.2 that the seven wind profiles only differs slightly from each other. Due to this, it is not expected such a large difference in fatigue damage at the blade root, for the seven wind profiles. But still there is a difference, and one way to determine the wind profile that has the greatest impact on the wind turbine, is to calculate the areas for the wind profiles in the height interval 23.55 m – 153.55 m. This is done by integration of the formulas tabulated in Table 3.6. The formulas are found by the trend line function in Excel.

| Wind profiles | Formulas integrated in the interval $z = 23.55\text{m}-153.55\text{m}$ | Integrated values (areas) | Normalized with respect to NEU |
|---------------|--|---------------------------|--------------------------------|
| VU            | $1.16\ln(z) + 6.17$  | 1463.6                    | 0.9987 (0.13%)                 |
| U             | $1.13\ln(z) + 6.31$  | 1464.0                    | 0.9990 (0.10%)                 |
| NU            | $1.11\ln(z) + 6.41$  | 1464.4                    | 0.9993 (0.07%)                 |
| NEU           | $1.03\ln(z) + 6.75$  | 1465.4                    | 1.000                          |
| NS            | $0.98\ln(z) + 6.99$  | 1466.3                    | 1.0006 (0.05%)                 |
| S             | $0.91\ln(z) + 7.29$  | 1467.3                    | 1.0012 (0.12%)                 |
| VS            | $0.66\ln(z) + 8.42$  | 1471.1                    | 1.0039 (0.39%)                 |

**Table 3.6 Integrated values of the wind profiles**

### 3.3 Turbulence

In this analysis there have been used three values for the turbulence intensity. The first one has been chosen and set to 25 %. The second has been calculated by use of formula 2.8. In order to do so one has to calculate the standard deviation, which is given by formula 2.9. The result of this calculation gives a turbulence intensity of 11 %. The third value has been set to 0 %.

By reducing the turbulence intensity from 25 % to 11 % to 0%, it is possible to analyze the effects that this has on fatigue.

### 3.4 Wind field and grid

In the methodology chapter so far, the wind profiles and three cases of turbulence have been determined. By combining a wind profile with one of the turbulence intensities, the result is a wind field. An illustration of a wind field is given in Figure 2.1.

In the analyses the grid height and width are set equal to 130 meter. This covers an area of the rotor diameter, plus a little extra (4 m below the rotor and 2 m on each side). The rotor diameter for the reference wind turbine is 126 meter.

### 3.5 Turbsim

In order to analyze how the seven power law wind profile differs in terms of wind speed, it is necessary to generate wind fields. This is done by use of the software application called Turbsim. A total of 91 wind fields are generated.

First of all, the seven wind profiles are generated with a turbulence intensity of 25 %. For each of these wind profiles there have been carried out six runs (recommended by IEC), where the runs are separated by its seed number. This is done to take care of the randomness due to simulation of turbulence. By doing six simulations large deviations from the mean results will be discovered and the confidence in the comparison of the wind profiles is improved. I.e. if one run has a large deviation from the mean speed due to turbulence, this run will not be representative when comparing to other wind profiles. Later on in this document the damage equivalent load (DEL) will be calculated, and the six runs done by Turbsim will then cause six DEL. Of these, there will be calculated an average DEL.

The procedure in the previous section has been repeated for the turbulence intensity of 11%. For the turbulence intensity of 0 %, there has only been performed one run for each wind profile, as deviation from mean values are not an issue for 0 % turbulence.

A text file from Turbsim is also presented in appendix on page 66.

### 3.6 Fedem

In order to perform analyses of the loads that affect the wind turbine, the multi-body software called Fedem can be used. The software uses the wind fields generated by Turbsim. A description of how this software is given in the theory chapter, see Section 2.7.

In the analysis carried out for this thesis, results have been exported from Fedem for three specific locations. The specific locations are at blade root, tower top and tower bottom. For each of these locations the total load picture is given by six loads; forces in x, y and z-direction and bending moment in x, y and z direction. The loads extracted from Fedem simulations are given in Table 3.7. They are exported from Fedem together with the corresponding wind speed in x, y, and z-direction, as well as time. The time is divided into time steps at an interval of 0.05 second. At this time steps information are calculated and stored. For each simulation performed, the total simulation time is 650 seconds. The fifty first of these is neglected due to extremely high vibration at the start of the simulation. The reason that the effect is so large at first is that the wind turbine experiences an airflow that changes from 0 m/s to an air flow of 10-12 m/s, in a fraction of a second. This never happens in real life. What then remains of the simulation is 600 seconds/10 minutes. This is the recommended time for this type of simulations according to IEC 61400-3. [23]

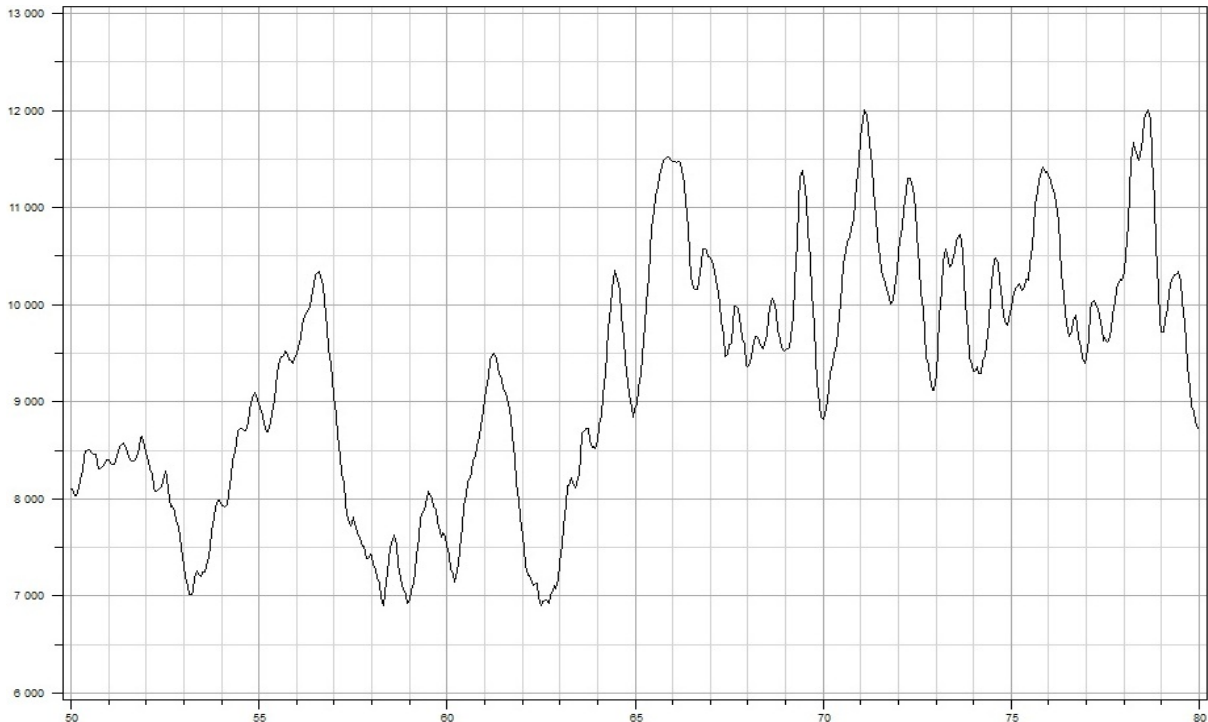
| Loads  | Abbreviation     |
|--|------------------|
| <b>Force in x-direction at blade root</b>            | RFx              |
| <b>Force in y-direction at blade root</b>            | RFy              |
| <b>Force in z-direction at blade root</b>            | RFz              |
| <b>Bending moment in x-direction at blade root</b>   | RMx              |
| <b>Bending moment in y-direction at blade root</b>   | RM <sub>y</sub>  |
| <b>Bending moment in z-direction at blade root</b>   | RM <sub>z</sub>  |
| <b>Force in x-direction at tower top</b>             | TTFx             |
| <b>Force in y-direction at tower top</b>             | TTFy             |
| <b>Force in z-direction at tower top</b>             | TTFz             |
| <b>Bending moment in x-direction at tower top</b>    | TTM <sub>x</sub> |
| <b>Bending moment in y-direction at tower top</b>    | TTM <sub>y</sub> |
| <b>Bending moment in z-direction at tower top</b>    | TTM <sub>z</sub> |
| <b>Force in x-direction at tower bottom</b>          | TBFx             |
| <b>Force in y-direction at tower bottom</b>          | TBFy             |
| <b>Force in z-direction at tower bottom</b>          | TBFz             |
| <b>Bending moment in x-direction at tower bottom</b> | TBM <sub>x</sub> |
| <b>Bending moment in y-direction at tower bottom</b> | TBM <sub>y</sub> |
| <b>Bending moment in z-direction at tower bottom</b> | TBM <sub>z</sub> |

Table 3.7 Loads extracted from the Fedem simulations

The loads extracted from the Fedem simulations are tabulated in Table 3.7, and the coordinate axes are defined in Figure 2.3.

### 3.7 Rainflow counting

The fatigue distribution which affect the wind turbine, create an arbitrarily and complex load spectrum over time. To be used in fatigue computation something has to be done with this complex spectrum. The first method to be used in order to reduce the complexity is the rainflow counting method. The method is described in section 2.8.1. A typical load fluctuation, if turbulence is present, may look like the snap shot given in Figure 3.3. [20]



**Figure 3.3** Typical load fluctuation (extracted from Fedem)

After the rainflow counting is completed, the cycles will be scaled. The description and formula is given in section 2.8.2. In this analysis, the cycles are scaled about zero mean.

### 3.8 Binning the load range

So far in the preparation of the load situation, the cycles are closed and collected at zero mean. This is illustrated in Figure 3.4. This figure also illustrates how the load ranges are binned. By using the first cycle with a range of 130 in the following discussion, one can see the importance of binning the load range. If only three bins are used this range will end up in bin 120-180. Then this cycle will get a range value of 150, i.e.  $(180-120) / 2 = 150$ . If the number of bins is doubled, it will end up in bin 120-150 and get a value of 135. By doubling the number of bins once again the same cycle will end up in the bin 120-135 and get a value of 127.5. The last range is closest to the actual range of 130. This shows that the load range converges alternating towards a certain value. Therefore, in order to achieve a good precision in the result, the number of bins is relevant.



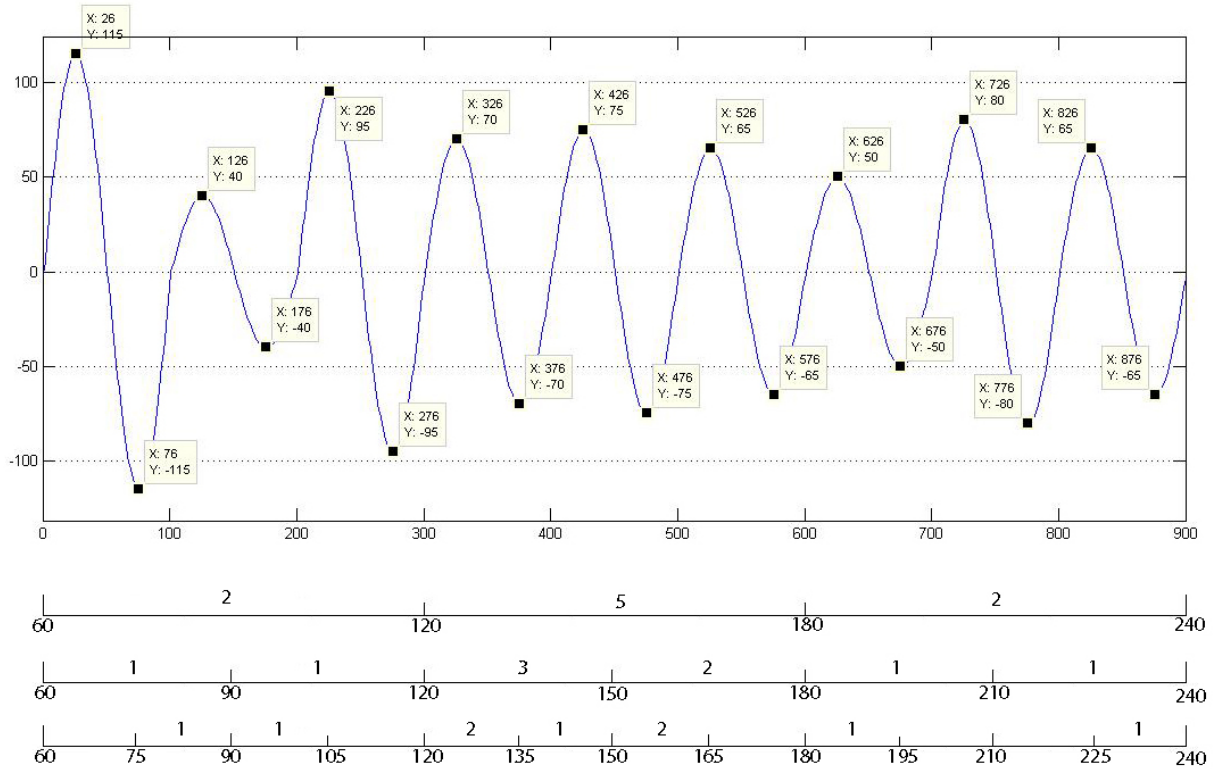


**Figure 3.4 Binning the load range<sup>1</sup>**

In the analysis the number of bins is chosen to be 50, for the run with smallest load range. The reason why 50 bins are used can be explained by the numbers tabulated in Table 3.8. Table 3.8 shows alternating convergence towards certain values, and 50 bins are reasonably accurate.

| RMy  |       |       |       |       |       |       |       |       |       |       |       |       |       |       |       |
|--|-------|-------|-------|-------|-------|-------|-------|-------|-------|-------|-------|-------|-------|-------|-------|
| Bins   | 1     | 2     | 5     | 10    | 20    | 35    | 40    | 45    | 48    | 50    | 52    | 64    | 75    | 76    | 84    |
| <b>Damage equivalent load (DEL)</b>                        |       |       |       |       |       |       |       |       |       |       |       |       |       |       |       |
| VU   | 709   | 948   | 945   | 999   | 1020  | 1020  | 1020  | 1020  | 1020  | 1020  | 1020  | 1020  | 1020  | 1020  | 1020  |
| U  | 723   | 965   | 972   | 1020  | 1040  | 1030  | 1040  | 1040  | 1040  | 1030  | 1030  | 1040  | 1040  | 1040  | 1040  |
| NU   | 735   | 976   | 990   | 1030  | 1050  | 1040  | 1050  | 1050  | 1040  | 1050  | 1040  | 1050  | 1040  | 1040  | 1040  |
| NEU  | 759   | 984   | 1010  | 1050  | 1070  | 1070  | 1070  | 1060  | 1060  | 1070  | 1060  | 1060  | 1070  | 1070  | 1060  |
| NS   | 765   | 965   | 994   | 1050  | 1070  | 1070  | 1070  | 1070  | 1070  | 1070  | 1070  | 1070  | 1070  | 1070  | 1070  |
| S  | 775   | 959   | 1000  | 1060  | 1070  | 1070  | 1070  | 1070  | 1060  | 1070  | 1070  | 1070  | 1070  | 1070  | 1070  |
| VS   | 792   | 859   | 1030  | 1090  | 1090  | 1090  | 1080  | 1080  | 1080  | 1090  | 1090  | 1090  | 1080  | 1080  | 1090  |
| <b>Normalized with respect to the neutral wind profile</b> |       |       |       |       |       |       |       |       |       |       |       |       |       |       |       |
| VU (%)   | 0,934 | 0,963 | 0,936 | 0,951 | 0,953 | 0,953 | 0,953 | 0,962 | 0,962 | 0,953 | 0,962 | 0,962 | 0,953 | 0,953 | 0,962 |
| U (%)  | 0,953 | 0,981 | 0,962 | 0,971 | 0,972 | 0,963 | 0,972 | 0,981 | 0,981 | 0,963 | 0,972 | 0,981 | 0,972 | 0,972 | 0,981 |
| NU (%)   | 0,968 | 0,992 | 0,980 | 0,981 | 0,981 | 0,972 | 0,981 | 0,991 | 0,981 | 0,981 | 0,981 | 0,991 | 0,972 | 0,972 | 0,981 |
| NEU (%)  | 1,000 | 1,000 | 1,000 | 1,000 | 1,000 | 1,000 | 1,000 | 1,000 | 1,000 | 1,000 | 1,000 | 1,000 | 1,000 | 1,000 | 1,000 |
| NS (%)   | 1,008 | 0,981 | 0,984 | 1,000 | 1,000 | 1,000 | 1,000 | 1,009 | 1,009 | 1,000 | 1,009 | 1,009 | 1,000 | 1,000 | 1,009 |
| S (%)  | 1,021 | 0,975 | 0,990 | 1,010 | 1,000 | 1,000 | 1,000 | 1,009 | 1,000 | 1,000 | 1,009 | 1,009 | 1,000 | 1,000 | 1,009 |
| VS (%)   | 1,043 | 0,873 | 1,020 | 1,038 | 1,019 | 1,019 | 1,009 | 1,019 | 1,019 | 1,019 | 1,028 | 1,028 | 1,009 | 1,009 | 1,028 |

**Table 3.8 Changes in DEL for RMy due to varying number of bins**

Note: In Table 3.8 DEL is calculated for the RMy. The numbers are based on the smallest load range for turbulence intensity of 0 %.

<sup>1</sup> The illustration is a collaboration between O.M. Stava and G-M. S. Gudmundsen

Because Table 3.8 shows that 50 bins are sufficient, the smallest load range is divided by 50 for all load cases. This gives the bin widths tabulated in Table 3.9, and is used for each run.

| Loads       | Bin width | Loads | Bin width |
|-------------|-----------|-------|-----------|
| <b>RFx</b>  | 0.7       | TTMx  | 2.6       |
| <b>RFy</b>  | 7.1       | TTMy  | 16.9      |
| <b>RFz</b>  | 7.0       | TTMz  | 10.5      |
| <b>RMx</b>  | 145.5     | TBFx  | 1.6       |
| <b>RMy</b>  | 32.8      | TBFy  | 0.3       |
| <b>RMz</b>  | 2.4       | TBFz  | 0.3       |
| <b>TTFx</b> | 1.6       | TBMx  | 18.8      |
| <b>TTFy</b> | 0.2       | TBMy  | 104.7     |
| <b>TTFz</b> | 0.3       | TBMz  | 10.7      |

**Table 3.9 Bin widths found by dividing the smallest load range of the 91 runs by 50**

### 3.9 Calculation of damage equivalent load

To be able to calculate damage equivalent load (DEL), a MatLab application called Mlife is used. A text file is presented in Appendix on page 68. With this application rainflow counting, cycle scaling and binning of the load range are calculated. In addition, the ultimate load needs to be defined. The ultimate load is not an important parameter in the analyses performed, but it is important that it is much larger than the max load in each run. The parameter *m* in Mlife represents the inverse slope of an S/N curve. This parameter differs from material to material. In the analyses *m* is chosen to be 12 for the blade root and 5 for the tower, same as values used in reference [24].

The important parameters needed are now defined, and by using Mlife the DEL's can be calculated for each load case. The results are tabulated and illustrated in the next chapter.

## 4 Results

In this chapter the results for fatigue is presented. I.e. the relative fatigue calculated by damage equivalent load (DEL). The tables below show DEL for seven wind profiles, where 18 load cases are presented for each wind profile. In addition, three turbulence intensities for each wind profile are presented. In Table 4.2, Table 4.4 and Table 4.6, the DEL's are normalized with respect to the neutral wind profile.

For turbulence intensity (TI) of 25 % and 11 % six runs are conducted for each wind profile, and the mean value for each of the six runs are calculated. For TI of 0 % only one run has been performed for each wind profile. These results are given in Table 8.5 -Table 8.18 in the Appendix.

Some selected graphical presentations of the results are given in this chapter. The remaining results are illustrated in the Appendix.

| Run | RFx | RFy | RFz | RMx  | RMy  | RMz | TTFx | TTFy | TTFz | TTMx | TTMy | TTMz | TBFx | TBFy | TBFz | TBMX | TBMY  | TBMZ |
|-----|-----|-----|-----|------|------|-----|------|------|------|------|------|------|------|------|------|------|-------|------|
| VU  | 178 | 271 | 347 | 5947 | 6857 | 213 | 199  | 58   | 51   | 714  | 3222 | 3507 | 204  | 66   | 54   | 4418 | 13817 | 3543 |
| U   | 186 | 270 | 364 | 5910 | 7247 | 210 | 196  | 57   | 50   | 715  | 3223 | 3408 | 205  | 64   | 53   | 4285 | 13883 | 3445 |
| NU  | 183 | 273 | 336 | 6002 | 7097 | 232 | 200  | 73   | 50   | 718  | 3167 | 3468 | 204  | 86   | 54   | 5650 | 14183 | 3505 |
| NEU | 185 | 272 | 348 | 5952 | 7067 | 183 | 199  | 64   | 50   | 705  | 3188 | 3410 | 203  | 74   | 53   | 4888 | 14050 | 3448 |
| NS  | 183 | 271 | 363 | 5983 | 7025 | 211 | 198  | 73   | 49   | 738  | 3230 | 3380 | 204  | 85   | 52   | 5648 | 13883 | 3418 |
| S   | 182 | 273 | 354 | 5985 | 7008 | 201 | 196  | 62   | 50   | 714  | 3178 | 3482 | 198  | 72   | 54   | 4790 | 13833 | 3518 |
| VS  | 189 | 270 | 360 | 5918 | 7135 | 184 | 197  | 69   | 49   | 718  | 3188 | 3368 | 205  | 80   | 53   | 5307 | 13950 | 3407 |

Table 4.1 DEL due to 25 % TI

| Run | RFx   | RFy   | RFz   | RMx   | RMy   | RMz   | TTFx  | TTFy  | TTFz  | TTMx  | TTMy  | TTMz  | TBFx  | TBFy  | TBFz  | TBMX  | TBMY  | TBMZ  |
|-----|-------|-------|-------|-------|-------|-------|-------|-------|-------|-------|-------|-------|-------|-------|-------|-------|-------|-------|
| VU  | 0,964 | 0,998 | 0,999 | 0,999 | 0,970 | 1,164 | 0,996 | 0,917 | 1,017 | 1,013 | 1,010 | 1,028 | 1,003 | 0,895 | 1,015 | 0,904 | 0,983 | 1,028 |
| U   | 1,006 | 0,993 | 1,048 | 0,993 | 1,025 | 1,146 | 0,981 | 0,895 | 0,991 | 1,014 | 1,011 | 1,000 | 1,008 | 0,871 | 0,991 | 0,877 | 0,988 | 0,999 |
| NU  | 0,991 | 1,005 | 0,967 | 1,008 | 1,004 | 1,265 | 1,003 | 1,148 | 1,007 | 1,019 | 0,993 | 1,017 | 1,007 | 1,161 | 1,004 | 1,156 | 1,009 | 1,016 |
| NEU | 1,000 | 1,000 | 1,000 | 1,000 | 1,000 | 1,000 | 1,000 | 1,000 | 1,000 | 1,000 | 1,000 | 1,000 | 1,000 | 1,000 | 1,000 | 1,000 | 1,000 | 1,000 |
| NS  | 0,992 | 0,999 | 1,043 | 1,005 | 0,994 | 1,152 | 0,994 | 1,152 | 0,978 | 1,046 | 1,013 | 0,991 | 1,005 | 1,153 | 0,976 | 1,155 | 0,988 | 0,991 |
| S   | 0,987 | 1,004 | 1,017 | 1,006 | 0,992 | 1,097 | 0,981 | 0,978 | 1,009 | 1,012 | 0,997 | 1,021 | 0,977 | 0,981 | 1,006 | 0,980 | 0,985 | 1,020 |
| VS  | 1,025 | 0,995 | 1,036 | 0,994 | 1,010 | 1,004 | 0,989 | 1,088 | 0,985 | 1,018 | 1,000 | 0,988 | 1,010 | 1,082 | 0,985 | 1,086 | 0,993 | 0,988 |

Table 4.2 DEL normalized with respect to the neutral wind profile for 25 % TI

| Run | RFx | RFy | RFz | RMx  | RMy  | RMz | TTFx | TTFy | TTFz | TTMx | TTMy | TTMz | TBFx | TBFy | TBFz | TBMX | TBMY | TBMZ |
|-----|-----|-----|-----|------|------|-----|------|------|------|------|------|------|------|------|------|------|------|------|
| VU  | 100 | 262 | 284 | 5512 | 4007 | 122 | 115  | 36   | 26   | 402  | 1605 | 1678 | 117  | 42   | 28   | 2787 | 8178 | 1693 |
| U   | 107 | 261 | 288 | 5478 | 4410 | 120 | 120  | 31   | 25   | 388  | 1563 | 1615 | 120  | 36   | 27   | 2388 | 8488 | 1635 |
| NU  | 105 | 261 | 280 | 5485 | 4198 | 124 | 121  | 36   | 26   | 399  | 1505 | 1630 | 122  | 43   | 28   | 2832 | 8735 | 1650 |
| NEU | 108 | 262 | 284 | 5508 | 4310 | 139 | 120  | 34   | 25   | 398  | 1562 | 1607 | 121  | 40   | 27   | 2665 | 8605 | 1622 |
| NS  | 106 | 261 | 280 | 5488 | 4217 | 135 | 117  | 36   | 25   | 407  | 1610 | 1615 | 118  | 42   | 27   | 2773 | 8372 | 1633 |
| S   | 105 | 261 | 282 | 5505 | 4187 | 119 | 118  | 32   | 26   | 392  | 1547 | 1632 | 118  | 37   | 27   | 2435 | 8383 | 1650 |
| VS  | 104 | 261 | 281 | 5468 | 4047 | 132 | 117  | 35   | 25   | 403  | 1558 | 1587 | 118  | 41   | 27   | 2755 | 8320 | 1607 |

Table 4.3 DEL due to 11 % (TI)

| Run | RFx   | RFy   | RFz   | RMx   | RMy   | RMz   | TTFx  | TTFy  | TTFz  | TTMx  | TTMy  | TTMz  | TBFx  | TBFy  | TBFz  | TBMX  | TBMY  | TBMZ  |
|-----|-------|-------|-------|-------|-------|-------|-------|-------|-------|-------|-------|-------|-------|-------|-------|-------|-------|-------|
| VU  | 0,923 | 1,000 | 1,001 | 1,001 | 0,930 | 0,879 | 0,965 | 1,043 | 1,037 | 1,010 | 1,028 | 1,045 | 0,964 | 1,044 | 1,031 | 1,046 | 0,950 | 1,044 |
| U   | 0,986 | 0,997 | 1,014 | 0,995 | 1,023 | 0,865 | 1,001 | 0,907 | 0,997 | 0,975 | 1,001 | 1,005 | 0,993 | 0,893 | 0,996 | 0,896 | 0,986 | 1,008 |
| NU  | 0,967 | 0,999 | 0,988 | 0,996 | 0,974 | 0,890 | 1,015 | 1,055 | 1,016 | 1,003 | 0,964 | 1,015 | 1,008 | 1,063 | 1,013 | 1,063 | 1,015 | 1,017 |
| NEU | 1,000 | 1,000 | 1,000 | 1,000 | 1,000 | 1,000 | 1,000 | 1,000 | 1,000 | 1,000 | 1,000 | 1,000 | 1,000 | 1,000 | 1,000 | 1,000 | 1,000 | 1,000 |
| NS  | 0,978 | 0,998 | 0,988 | 0,996 | 0,978 | 0,974 | 0,978 | 1,044 | 0,999 | 1,022 | 1,031 | 1,005 | 0,975 | 1,035 | 0,998 | 1,041 | 0,973 | 1,007 |
| S   | 0,968 | 0,999 | 0,992 | 0,999 | 0,971 | 0,853 | 0,986 | 0,918 | 1,003 | 0,985 | 0,990 | 1,016 | 0,971 | 0,912 | 0,999 | 0,914 | 0,974 | 1,017 |
| VS  | 0,957 | 0,997 | 0,989 | 0,993 | 0,939 | 0,951 | 0,979 | 1,032 | 0,973 | 1,012 | 0,998 | 0,988 | 0,977 | 1,029 | 0,973 | 1,034 | 0,967 | 0,991 |

**Table 4.4 DEL normalized with respect to the neutral wind profile for 11 % TI**

| Run | RFx | RFy | RFz | RMx  | RMy  | RMz | TTFx | TTFy | TTFz | TTMx | TTMy | TTMz | TBFx | TBFy | TBFz | TBMX | TBMY | TBMZ |
|-----|-----|-----|-----|------|------|-----|------|------|------|------|------|------|------|------|------|------|------|------|
| VU  | 19  | 255 | 265 | 5310 | 1020 | 81  | 23   | 3    | 6    | 53   | 385  | 289  | 23   | 5    | 6    | 284  | 1600 | 292  |
| U   | 20  | 255 | 265 | 5310 | 1040 | 81  | 25   | 3    | 6    | 53   | 381  | 286  | 25   | 5    | 6    | 276  | 1740 | 289  |
| NU  | 21  | 255 | 265 | 5310 | 1040 | 81  | 25   | 4    | 6    | 54   | 379  | 283  | 25   | 5    | 6    | 288  | 1760 | 287  |
| NEU | 22  | 255 | 265 | 5310 | 1070 | 82  | 28   | 3    | 6    | 54   | 370  | 274  | 28   | 4    | 6    | 255  | 1970 | 278  |
| NS  | 23  | 255 | 265 | 5310 | 1070 | 82  | 30   | 3    | 6    | 55   | 363  | 266  | 30   | 5    | 7    | 271  | 2170 | 269  |
| S   | 23  | 255 | 265 | 5310 | 1070 | 82  | 32   | 4    | 6    | 55   | 360  | 261  | 32   | 5    | 7    | 300  | 2270 | 265  |
| VS  | 27  | 255 | 263 | 5310 | 1090 | 83  | 39   | 4    | 6    | 59   | 338  | 242  | 39   | 5    | 7    | 308  | 2820 | 246  |

**Table 4.5 DEL due to 0 % TI**

| Run | RFx   | RFy   | RFz   | RMx   | RMy   | RMz   | TTFx  | TTFy  | TTFz  | TTMx  | TTMy  | TTMz  | TBFx  | TBFy  | TBFz  | TBMX  | TBMY  | TBMZ  |
|-----|-------|-------|-------|-------|-------|-------|-------|-------|-------|-------|-------|-------|-------|-------|-------|-------|-------|-------|
| VU  | 0,889 | 1,000 | 1,000 | 1,000 | 0,953 | 0,998 | 0,841 | 1,111 | 0,986 | 0,980 | 1,041 | 1,055 | 0,835 | 1,109 | 0,977 | 1,114 | 0,812 | 1,050 |
| U   | 0,926 | 1,000 | 1,000 | 1,000 | 0,972 | 0,998 | 0,895 | 1,088 | 0,984 | 0,985 | 1,030 | 1,044 | 0,899 | 1,085 | 0,975 | 1,082 | 0,883 | 1,040 |
| NU  | 0,949 | 1,000 | 1,000 | 1,000 | 0,972 | 0,999 | 0,910 | 1,144 | 0,990 | 0,993 | 1,024 | 1,033 | 0,903 | 1,111 | 0,983 | 1,129 | 0,893 | 1,032 |
| NEU | 1,000 | 1,000 | 1,000 | 1,000 | 1,000 | 1,000 | 1,000 | 1,000 | 1,000 | 1,000 | 1,000 | 1,000 | 1,000 | 1,000 | 1,000 | 1,000 | 1,000 | 1,000 |
| NS  | 1,060 | 1,000 | 1,000 | 1,000 | 1,000 | 1,001 | 1,097 | 1,072 | 1,010 | 1,015 | 0,981 | 0,971 | 1,083 | 1,053 | 1,012 | 1,063 | 1,102 | 0,968 |
| S   | 1,079 | 1,000 | 1,000 | 1,000 | 1,000 | 1,001 | 1,144 | 1,203 | 1,026 | 1,026 | 0,973 | 0,953 | 1,137 | 1,141 | 1,032 | 1,176 | 1,152 | 0,953 |
| VS  | 1,241 | 1,000 | 0,992 | 1,000 | 1,019 | 1,021 | 1,412 | 1,239 | 1,054 | 1,100 | 0,914 | 0,883 | 1,399 | 1,185 | 1,069 | 1,208 | 1,431 | 0,885 |

**Table 4.6 DEL normalized with respect to the neutral wind profile for 0 % TI**

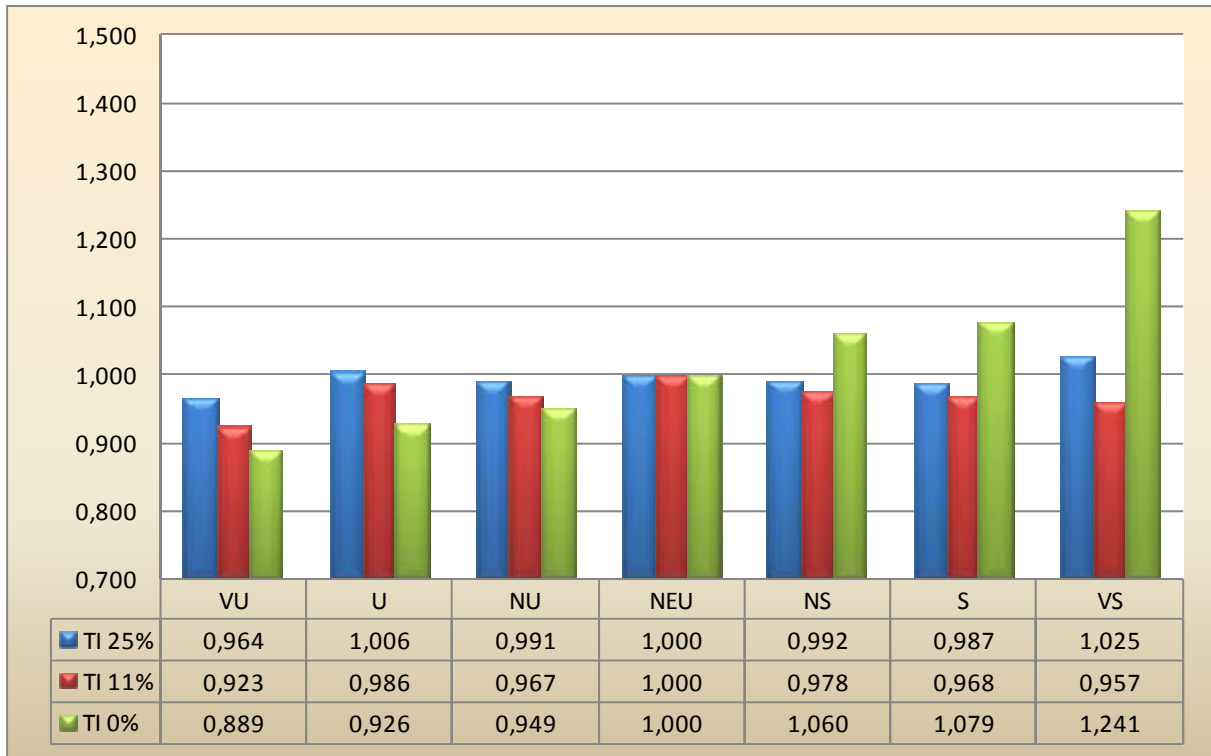


**Figure 4.1 RFX – DEL due to force in x-direction at blade root.**

Note: Seven wind profiles and three different turbulence intensities are illustrated. DEL is normalized with the neutral wind profile.

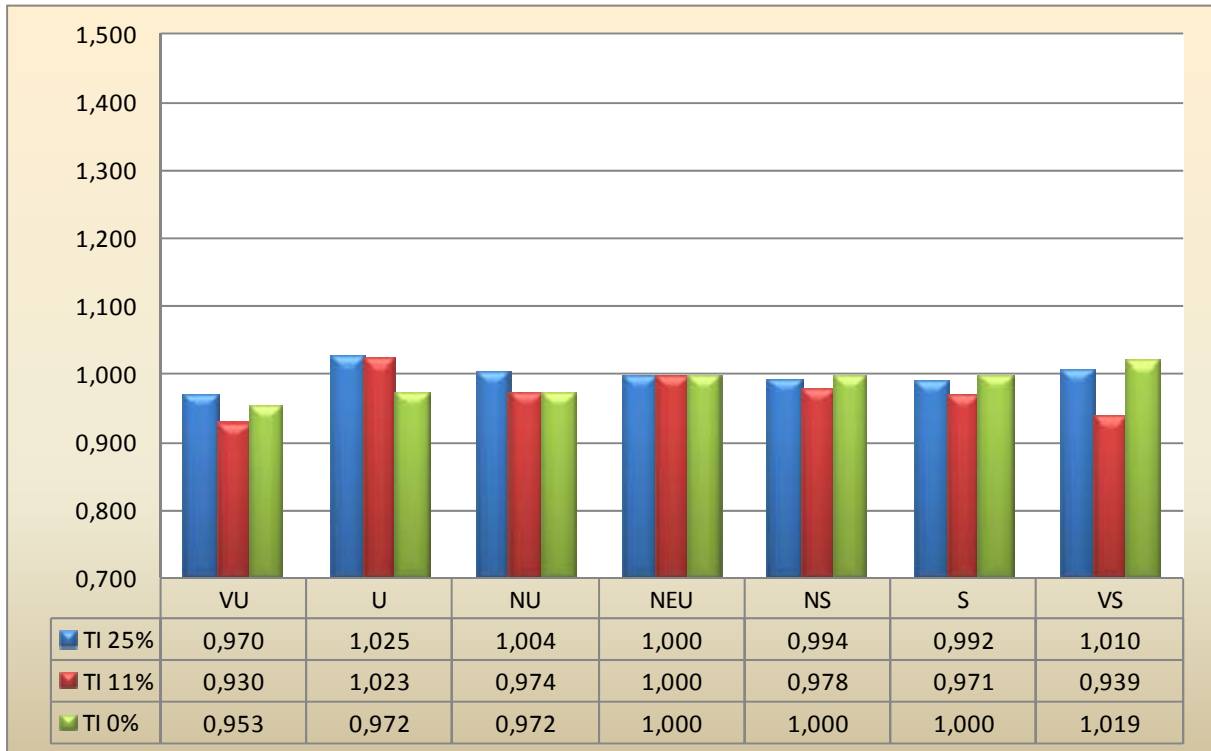


**Figure 4.2 RMy - DEL due to bending moment in y-direction at blade root.**

Note: Seven wind profiles and three different turbulence intensities are illustrated. DEL is normalized with the neutral wind profile.

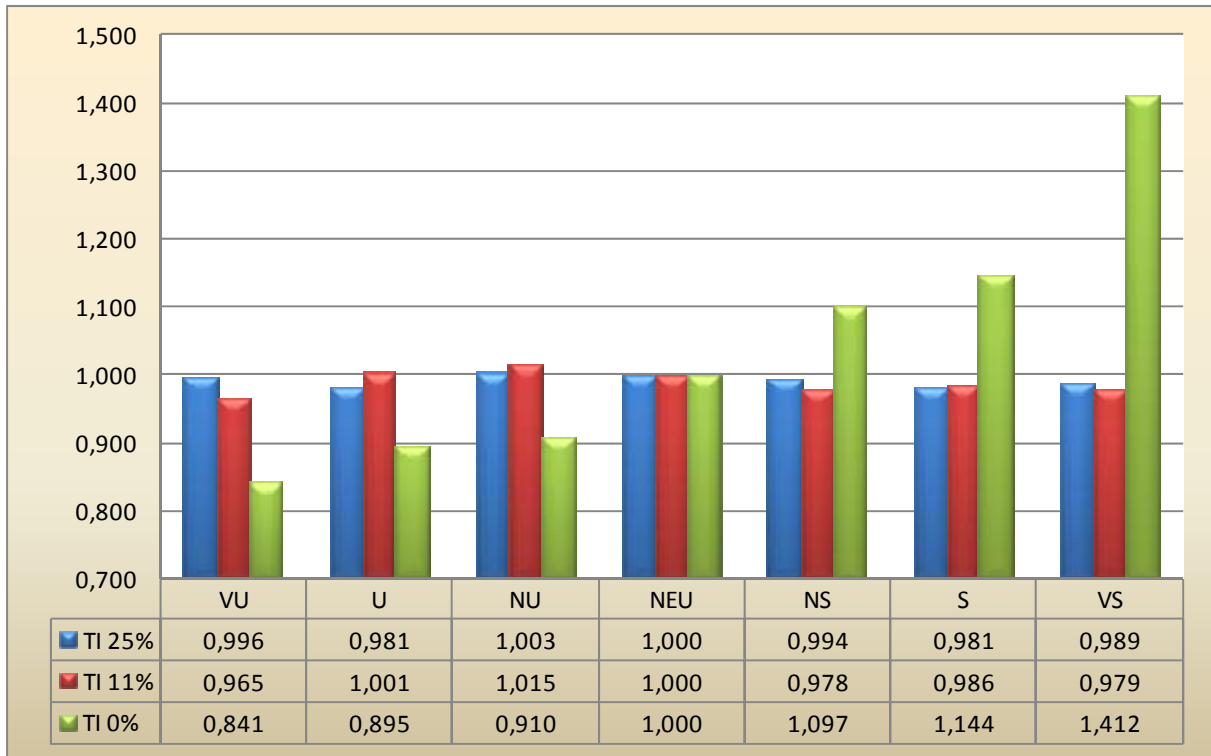


**Figure 4.3 TTFx - DEL due to force in x-direction at tower top.**

Note: Seven wind profiles and three different turbulence intensities are illustrated. DEL is normalized with the neutral wind profile.

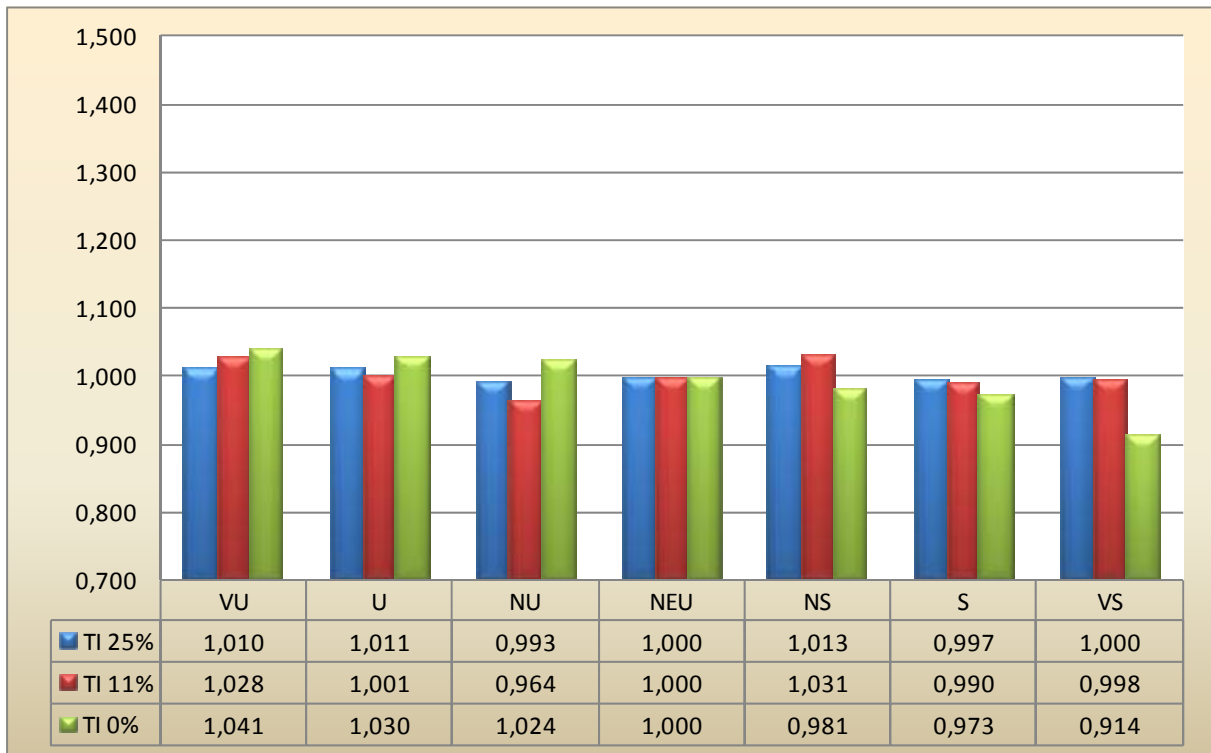


**Figure 4.4 TTM<sub>y</sub> - DEL due to bending moment in y-direction at tower top.**

Note: Seven wind profiles and three different turbulence intensities are illustrated. DEL is normalized with the neutral wind profile.

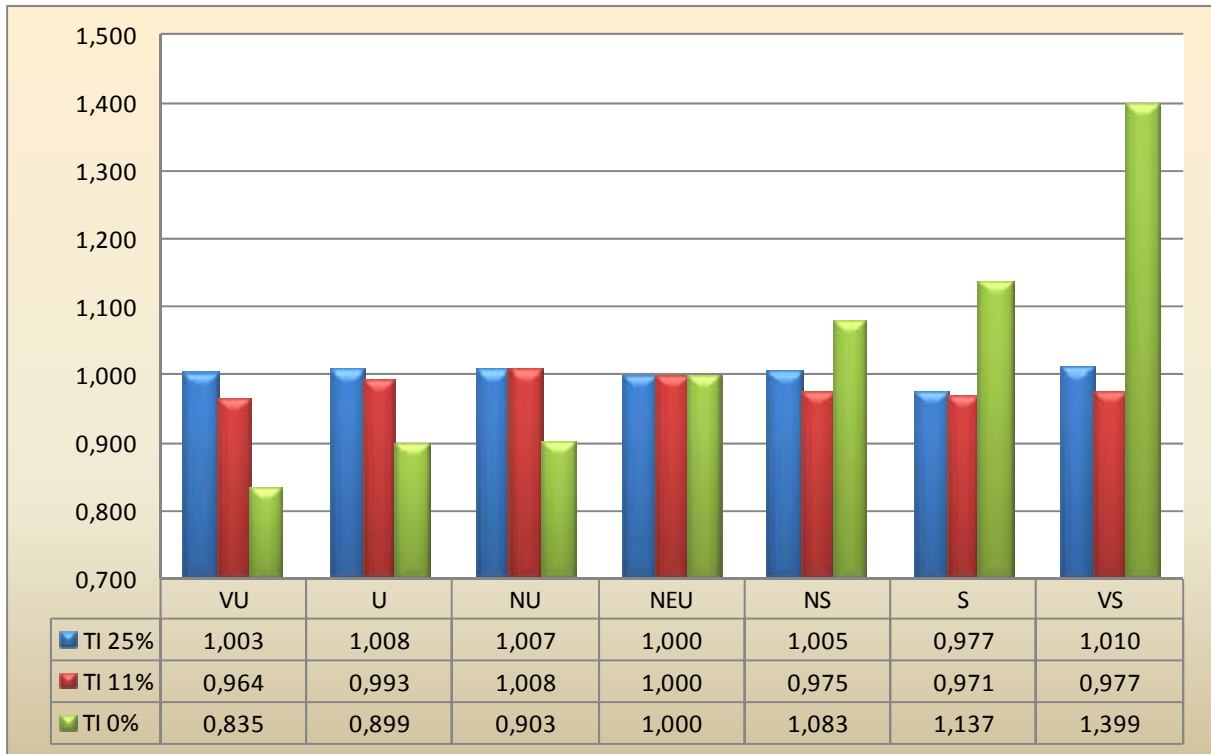


**Figure 4.5 TBFx - DEL due to force in x-direction at tower bottom.**

Note: Seven wind profiles and three different turbulence intensities are illustrated. DEL is normalized with the neutral wind profile.

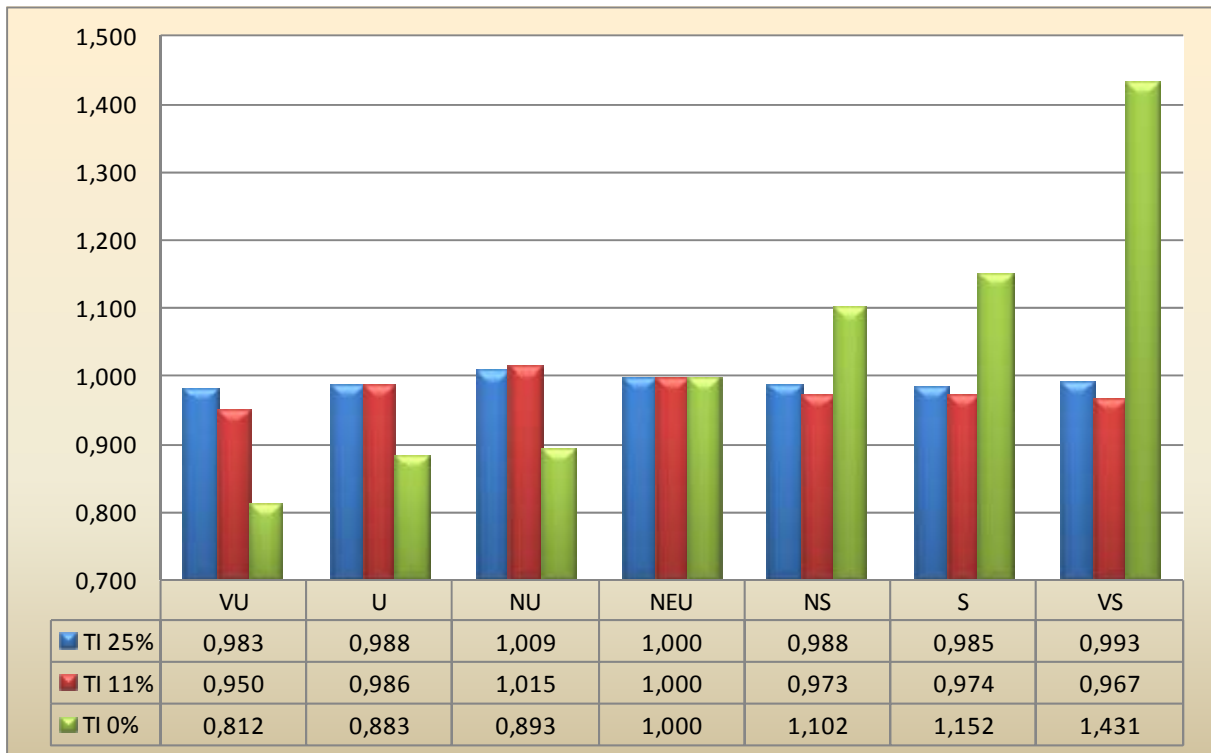


**Figure 4.6 TBM<sub>y</sub> - DEL due to bending moment in y-direction at tower bottom.**

Note: Seven wind profiles and three different turbulence intensities are illustrated. DEL is normalized with the neutral wind profile.

## 5 Discussion

In this chapter the damage equivalent load (DEL) will be discussed, to see which wind profile that creates the greatest fatigue. The locations where DEL is calculated are; the blade root, the tower top and the tower bottom. However, only the results at the blade root will be discussed. The coordinate axes are given in Figure 2.3 a) and b). There are a total of seven wind profiles, each of them influenced by three different turbulence intensities (TI):

- TI of 25 %
- TI of 11 %
- TI of 0 %

The seven power law wind profiles are illustrated in Figure 3.2 and the calculated values are presented in Table 8.4 in the Appendix. The seven wind profiles cause different wind profile area that will act over the width of the rotor. A wind profile area is defined as the wind profile integrated over the grid height defined in Sec. 3.4. The wind profile area values are tabulated in Table 3.6. Initially one would expect that the wind profile with the highest wind profile area to provide the greatest DEL. In Table 3.6 and Table 8.4 TI is 0 %. It is worth noting that the speeds vary little from profile to profile. The tiny variation which appears in Table 3.6 produces a pattern in which the very unstable (VU) wind profile gives the least wind effects on the rotor. From this profile the wind effect increases in a stair pattern up to the wind profile very stable (VS), which give the greatest wind effects on the rotor. The wind profile which is expected to give the greatest DEL is therefore the very stable wind profile, but the differences are expected to be small.

In the blue column in Figure 4.2, the result for the bending moment at blade root,  $RM_y$ , for the seven wind profiles are listed, with 25 % TI included. These results do not match the expected result. It seems as if the distribution is relatively random. This relatively randomness may have been caused by the turbulence intensity, or more precisely the size of the turbulence intensity in percent. When the turbulence intensity is equal to 25 %, it causes a standard deviation of  $0.25 \cdot U_{10}$ . This means that the wind speed can vary  $\pm 25$  % about the mean wind speed on average. For the seven wind profiles this gives a variation due to the turbulence in the interval 2.52 – 2.64 m/s, provided that the z-value is 27.55 m. The corresponding interval without turbulence is 10.56 – 10.06 m/s. The variation for z-value of 153.55 m is 3.01 – 2.95 m/s due to the turbulence. The corresponding interval without turbulence is 12.05 – 11.79 m/s. By these numbers it appears clear that the variation due to turbulence is much larger than the distance between the wind profiles. The result is that wind profiles overlap each other. They flow into each other. For this reason it may be difficult to separate the wind profiles, if only running six runs. Thus based on the above it is not possible to conclude which wind profile that provides the greatest damage.

In an attempt to distinguish the wind profiles, the analyses were re-done, but this time with 11% turbulence intensity only. The results are given in the red column in Figure 4.2. It is seen that the red columns create a certain pattern. It forms a roof pattern. Nor does this correspond with the expected pattern, given the fact that the wind profiles, NS, S and VS are exposed to



greater wind profile areas than wind profile NEU. The greater the wind profile area, the greater is the expected bending moment  $RMy/DEL$ .

There has to be a logical explanation to this roof pattern. The way to explain this may be to distinguish between the expected bending moment  $BMy$  and the  $DEL/RMy$ . The expected  $BMy$  rises from wind profile VU to VS in a stair pattern, in a similar manner as the wind profile area, while the  $RMy$  follow a roof pattern. The reason for the three profiles at the right side of NEU having a smaller  $RMy$ , may be explained by less fluctuation in the loads.

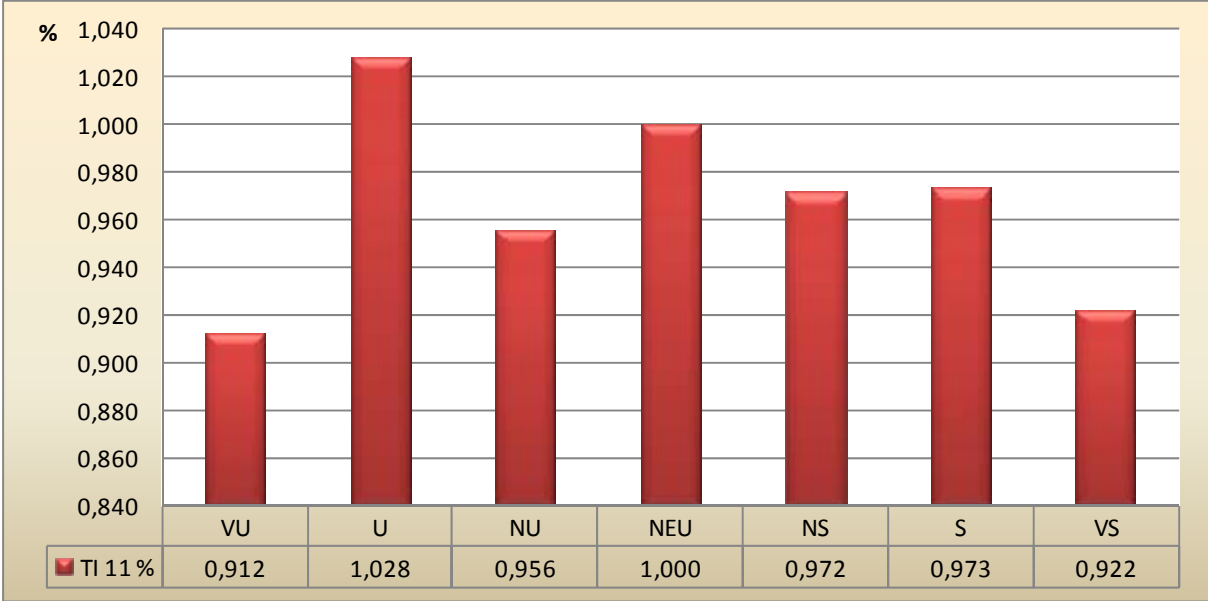


**Figure 5.1** Load range of the bending moment in y-direction at blade root,  $BMy$

In Figure 5.1 the load range is given for seven wind profiles, included TI of 11 %. The range is normalized with the neutral wind profile. The range is found by taking the max and min value from the exported data, which is simulated by Fedem. The first 50 seconds of the simulations are not included due to reasons described in Sec. 3.6.

The figure shows that there is less fluctuation for the wind profiles at the right hand side of the wind profile NEU in Figure 5.1. It also shows, by comparing with Figure 4.2, that the shape and the values are quite similar. The next question to ask is why then the expected  $BMy$  and the given  $DEL RMy$  do not follow the same pattern. The answer may have the same explanation as the case was for  $TI = 25 \%$ . A  $TI$  of 11 % causes, like  $TI$  of 25 %, a large deviation from the mean wind speed, for each of the seven wind profiles. For  $z$ -value of 27.55 m, the deviation varies between 1.11-1.16 m/s, and for  $z$ -value of 153.55 m the variation is between 1.33-1.30 m/s. With the same reasoning as above, the analysis for the seven wind profiles therefore flow into each other, because the distance between the wind profiles is small compared to the turbulence variation.

In order to separate the wind profiles, the turbulence intensity is therefore set to 0 %. The green column in Figure 4.2 represents 0 %  $TI$ .

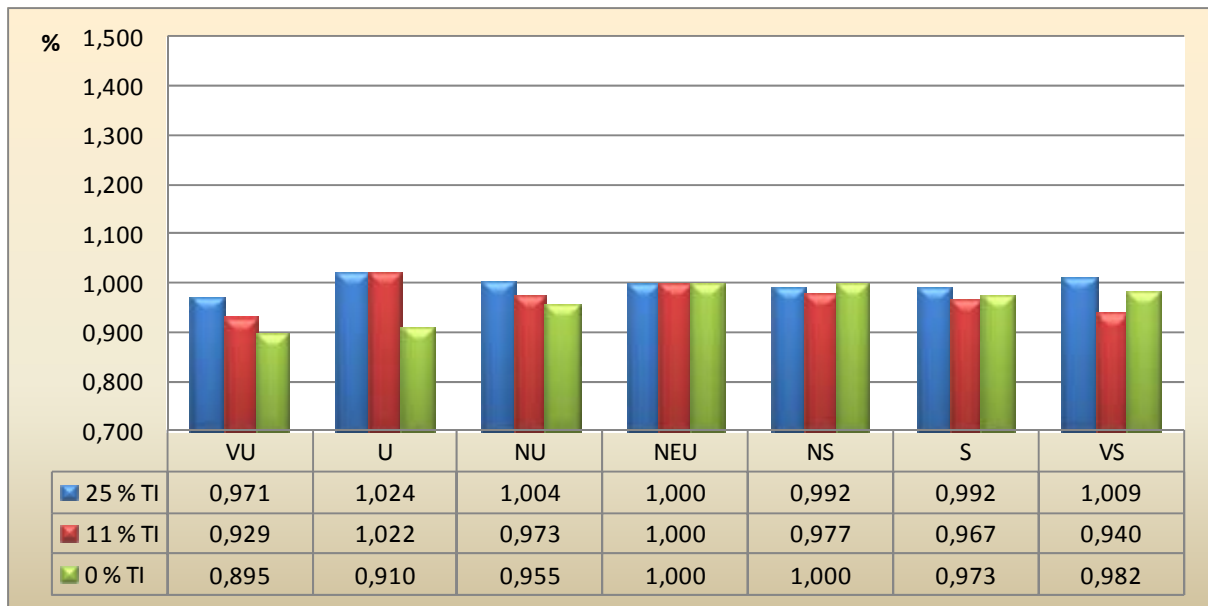


**Figure 5.2 RMy - DEL due to bending moment in y-direction at blade root. Not sufficient bins**

In Figure 5.2 the bin width from Table 8.19 is used. The results do not match Figure 4.2, where the bin width is different. In Figure 5.2 the bending moment in y-direction at the blade root is shown for the seven wind profiles, with turbulence intensities of 25 %, 11 % and 0 %. The bending moment is normalized with the neutral wind profile.

It can be seen from Figure 5.2 that RMy still follows a roof pattern for turbulence intensity of 0 %. There must be an explanation other than turbulence, which explains why the expected result is not achieved. The density of bins has been reviewed to find an explanation. The bins have a say as to the accuracy of the result. The bin widths used are calculated by taking the range of the neutral wind profile with 25 % TI, and dividing this by 50. This means that this wind profile has 50 bins. For the wind profiles with larger load range in Figure 5.2, this lead to inaccurate results when the same bin number is used due to larger bin width.

Therefore the result in Table 8.19 is rejected. It is considered more correct to use a constant bin width instead of constant bin number. The results in Table 3.9 is derived by dividing the smallest load range of the 91 runs by 50, and the bin width obtained is used for the results of all runs presented in Sec. 4 and in the Appendix. The larger load range will then get more than 50 bins, increasing the accuracy.

In the green column in Figure 4.2, the wind profiles follow the expected stair pattern. This is almost consistent with the expected result. For the result to be exactly as expected, the wind profile NS should have been slightly larger than NEU, and S should have been slightly larger than NS. The reason why these three wind profiles are alike seems to have something to do with the number of bins used. As Table 3.8 illustrates, if 50 bins is used, these wind profiles are not possible to separate. However this changes when a different number of bins are used. It seems like the DEL-value experiences an alternating convergence. By increasing the number of bins, the alternating range becomes less and less. At 50 bins, one can say that the DEL shown in Table 3.8 is reasonably accurate.

To summarize, the result in the green column in Figure 4.2, coincides with the expected result. To achieve the expected result, the following is done:

- Turbulence is set to 0 %
- A constant bin width is used for all load cases, found by dividing the smallest load range by 50.

With reference to Figure 4.2, the very stable (VS) wind profile causes the greatest DEL. This corresponds to the expected results. The VS profile causes 2 % greater DEL than NEU. The VS wind profile is therefore the most conservative for RMy. However, reservations must be taken for this result due to inaccuracies for the very stable wind profile.

Another important result worth mentioned is how the ratio RMx vs. RMy develops. As a reminder RMx is the bending moment around the x-axis. The x-axis is perpendicular to the rotor plane. RMy is the bending moment around the y-axis. The y-axis is parallel with the rotor plane. See also Figure 2.3. In Figure 5.3 the ratio between these two values are presented.

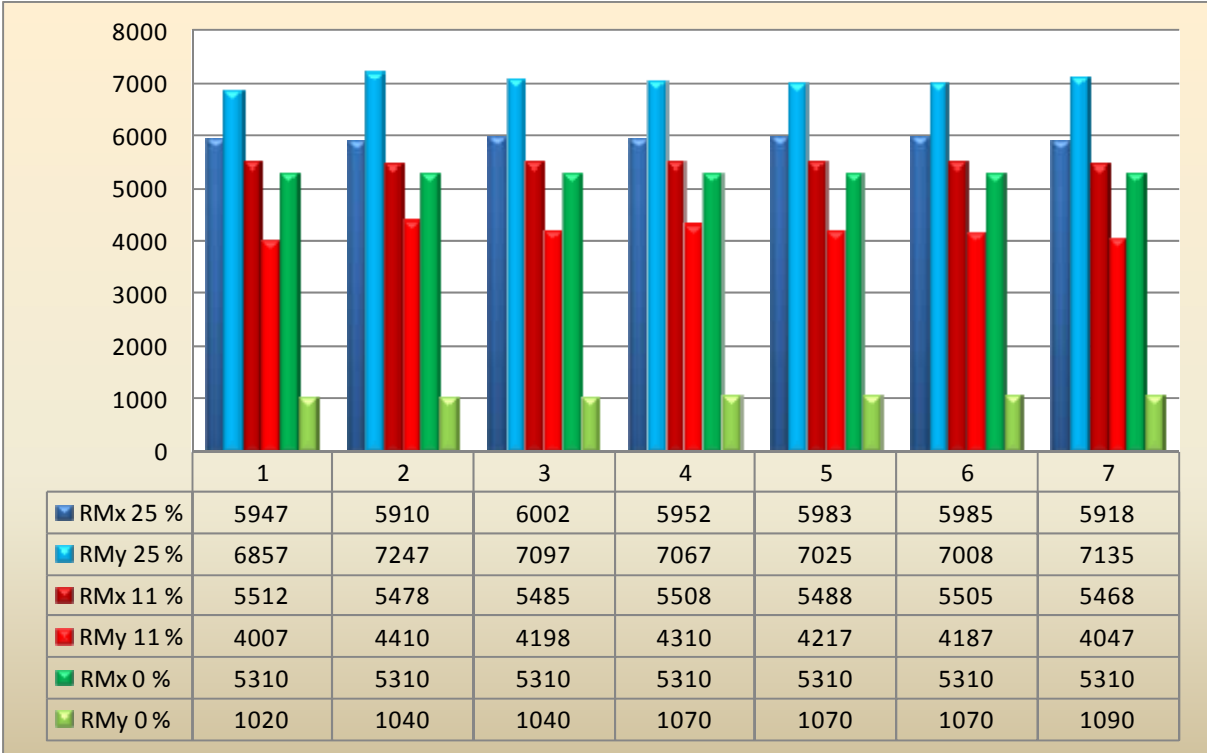


**Figure 5.3 Development of the ratio RMx vs. RMy, by reduction of turbulence intensity**

It appears clear that RMy decreases rapidly compared to RMx as the turbulence intensity decreases. The reason for this may be explained by the oscillating movement in the horizontal direction. The oscillation will decrease as the turbulence decrease, as decreasing turbulence means that the wind speed varies less about its mean value.

Figure 5.3 clearly shows that fatigue damage is larger for RMx than for RMy, when TI is chosen to be zero. The RMx is in this case approximately five times larger than RMy for each of the seven wind profiles. The differences in the values of RMx for the seven different wind

profiles, are however close to zero. Therefore, all the seven wind profiles provide equal fatigue considering  $RM_x$  only. Considering  $RM_y$  instead, the very stable wind profile provides the greatest fatigue.

## 6 Conclusion

In the thesis seven wind profiles, with turbulence included, have been tested on a 5-MW offshore wind turbine. The turbulence has been set to 25 %, 11 % and 0 %, to investigate the effect that the various wind fields have on the DEL's. It seems as if the result is relatively arbitrary when turbulence is included. The reason may be that the number of runs is too few, due to the fact that the values of the seven wind profile do not vary much, compared to the fluctuation provided by turbulence.

The expected result is achieved when turbulence is set to 0 %. For 0% turbulence the results increases in a stair pattern from the very unstable wind profile to the very stable wind profile. The results are consistent with the wind profile areas, i.e. the greater area the greater DEL (see Table 3.6).

A proposal for future work is to perform even more runs/analyses (increase the number of runs significantly), to ensure that the randomness caused by turbulence is not compromising the confidence of the results.

## 7 References

- [1] [http://www.ieawind.org/task\\_30/task30\\_Public.html](http://www.ieawind.org/task_30/task30_Public.html)
- [2] DNV-RP-C205, 2010, chapter 2.3.2, p. 15-16
- [3] DNV-RP-C205, 2010, chapter 2.3.6, p. 22
- [4] Ameya Sathe, Wim Bierboms, 2007, Influence of different wind profiles due to varying atmospheric stability on the fatigue life of wind turbines, DUWIND, Kluyverweg 1, 2629 HS Delft, NL, p. 2
- [5] DNV-RP-C205, 2010, chapter 2.1.2, p. 14
- [6] IEC-61400-3 Wind turbines – Part 3, 2009, Design requirements for offshore wind turbines, p.61
- [7] IEC-61400-1 Wind turbines – Part 1, 2005, Design requirements, p. 22
- [8] Martin O. L. Hansen, 2nd Edition 2008, Aerodynamics of Wind Turbines, Earthscan, chapter 13, Figure 13.4 p. 142
- [9] B.J.Jonkman, 2009, Turbsim User's Guide: Version 1.50, National Renewable Energy Laboratory (NREL)
- [10] B.J.Jonkman, 2009, Turbsim User's Guide: Version 1.50, National Renewable Energy Laboratory (NREL), Figure 6b, p.11
- [11] Fabian Vorpahl, Wojciech Popko, 2011, Description of the Load Cases and Output Sensors to be simulated in the OC4 project under IEA Wind Annex XXX, Fraunhofer Institute for Wind Energy and Energy System Technology (IWES), Figure B1 and Figure B2, p. 12-13
- [12] Martin O. L. Hansen, 2nd Edition 2008, Aerodynamics of Wind Turbines, Earthscan
- [13] Martin O. L. Hansen, 2nd Edition 2008, Aerodynamics of Wind Turbines, Earthscan, Figure 13.1, p.139
- [14] Martin O. L. Hansen, 2nd Edition 2008, Aerodynamics of Wind Turbines, Earthscan, Figure 6.1, p.45
- [15] Martin O. L. Hansen, 2nd Edition 2008, Aerodynamics of Wind Turbines, Earthscan, Figure 6.2, p 47
- [16] Martin O. L. Hansen, 2nd Edition 2008, Aerodynamics of Wind Turbines, Earthscan, Figure 6.3, p.48
- [17] Fedem Technology AS, 2009, FedemR5-0-UsersGuide
- [18] Norman E.Dowling, Engineering for Deformation, Fracture, and Fatigue, 2nd ed., Engineering Science and Mechanics Department, and Materials Science and Engineering Department Virginia Polytechnic Institute and State University, Blacksburg, Virginia
- [19] [http://wind.nrel.gov/designcodes/postprocessors/MLife/MLife\\_Theory.pdf](http://wind.nrel.gov/designcodes/postprocessors/MLife/MLife_Theory.pdf)
- [20] <http://www.sciencedirect.com/science/article/pii/S0142112397000789>
- [21] <http://www.am.chalmers.se/~anek/teaching/fatfract/98-2.pdf>
- [22] J. Jonkman, S. Butterfield, W. Musial, and G. Scott, 2009, Definition of a 5-MW Reference Wind Turbine for Offshore System Development, National Renewable Energy Laboratory
- [23] IEC-61400-3 Wind turbines – Part 3, 2009, Design requirements for offshore wind turbines, Section 7.5.4

- [24] Denis Matha, 2009, Model Development and Loads Analysis of an Offshore Wind Turbine on a Tension Leg Platform, with a Comparison to Other Floating Turbine Concepts, University of Colorado - Boulder

## 8 Appendix

### 8.1 Wind profiles

| Wind profiles  | Monin-Obukhov length ( Lm0 ) | Entity  | $\alpha$ - exponent  | Entity |
|--|------------------------------|---|--|--------|
| Very unstable (VU)   | -74                          | [m]   | 0,105  | [-]    |
| Unstable (U)   | -142                         | [m]   | 0,102  | [-]    |
| Near unstable (NU)   | -314                         | [m]   | 0,100  | [-]    |
| Neutral (NEU)  | 5336                         | [m]   | 0,093  | [-]    |
| Near stable (NS)   | 318                          | [m]   | 0,086  | [-]    |
| Stable (S)   | 104                          | [m]   | 0,082  | [-]    |
| Very stable (VS)   | 28                           | [m]   | 0,059  | [-]    |
| Stability function ( $\psi$ )  |                              |   |  |        |
| $x = \left(1 - 19,3 \frac{z}{L_{m0}}\right)^{\frac{1}{4}}$                         |                              |   | $\psi_2 = -4,8 \frac{z}{L_{m0}}$ for $\frac{z}{L_{m0}} \geq 0$ |        |
| $\psi_1 = 2 \ln(1 + x) + \ln(1 + x^2) - 2 \tan^{-1}(x)$ for $\frac{z}{L_{m0}} < 0$ |                              |   |  |        |
| Wind profile parameters  | Values                       |   | Entities   |        |
| Height above still sea water level (Z)   | Variable                     |   | [m]  |        |
| Roughness length (Z <sub>0</sub> )   | 0,001                        |   | [m]  |        |
| Reference height (H)   | 90,55                        |   | [m]  |        |
| Reference wind speed [U(H)]  | 11,4                         |   | [m/s]  |        |
| Function of logarithmic wind profile   |                              | Function of power law wind profile            |  |        |
| $U(Z) = U(H) \frac{\ln \frac{Z}{Z_0} - \psi}{\ln \frac{H}{Z_0} - \psi}$            |                              | $U(Z) = U(H) \left(\frac{Z}{H}\right)^\alpha$ |  |        |

**Table 8.1** Collection of wind profile names, abbreviations, parameters and functions



| <b>Z</b>      | <b>X [VU]</b> | <b><math>\psi_1</math> [VU]</b> | <b>X [U]</b> | <b><math>\psi_1</math> [U]</b> | <b>X [NU]</b> | <b><math>\psi_1</math> [NU]</b> | <b><math>\psi_2</math> [NEU]</b> | <b><math>\psi_2</math> [NS]</b> | <b><math>\psi_2</math> [S]</b> | <b><math>\psi_2</math> [VS]</b> |
|---------------|---------------|---------------------------------|--------------|--------------------------------|---------------|---------------------------------|----------------------------------|---------------------------------|--------------------------------|---------------------------------|
| [m]           | [-]           | [-]                             | [-]          | [-]                            | [-]           | [-]                             | [-]                              | [-]                             | [-]                            | [-]                             |
| <b>0,1</b>    | 1,006         | 0,515                           | 1,003        | 0,512                          | 1,002         | 0,510                           | 0,000                            | -0,002                          | -0,005                         | -0,017                          |
| <b>5</b>      | 1,232         | 0,751                           | 1,138        | 0,651                          | 1,069         | 0,579                           | -0,004                           | -0,075                          | -0,231                         | -0,857                          |
| <b>10</b>     | 1,378         | 0,911                           | 1,239        | 0,759                          | 1,127         | 0,639                           | -0,009                           | -0,151                          | -0,462                         | -1,714                          |
| <b>15</b>     | 1,489         | 1,033                           | 1,320        | 0,847                          | 1,177         | 0,693                           | -0,013                           | -0,226                          | -0,692                         | -2,571                          |
| <b>20</b>     | 1,579         | 1,133                           | 1,389        | 0,922                          | 1,222         | 0,740                           | -0,018                           | -0,302                          | -0,923                         | -3,429                          |
| <b>25</b>     | 1,656         | 1,218                           | 1,448        | 0,988                          | 1,262         | 0,784                           | -0,022                           | -0,377                          | -1,154                         | -4,286                          |
| <b>27,55</b>  | 1,691         | 1,257                           | 1,476        | 1,019                          | 1,281         | 0,805                           | -0,025                           | -0,416                          | -1,272                         | -4,723                          |
| <b>30</b>     | 1,724         | 1,293                           | 1,501        | 1,047                          | 1,299         | 0,824                           | -0,027                           | -0,453                          | -1,385                         | -5,143                          |
| <b>35</b>     | 1,784         | 1,359                           | 1,549        | 1,100                          | 1,332         | 0,861                           | -0,031                           | -0,528                          | -1,615                         | -6,000                          |
| <b>40</b>     | 1,839         | 1,419                           | 1,593        | 1,148                          | 1,364         | 0,895                           | -0,036                           | -0,604                          | -1,846                         | -6,857                          |
| <b>45</b>     | 1,889         | 1,473                           | 1,633        | 1,193                          | 1,393         | 0,927                           | -0,040                           | -0,679                          | -2,077                         | -7,714                          |
| <b>50</b>     | 1,936         | 1,524                           | 1,671        | 1,235                          | 1,421         | 0,958                           | -0,045                           | -0,755                          | -2,308                         | -8,571                          |
| <b>55</b>     | 1,979         | 1,570                           | 1,706        | 1,274                          | 1,447         | 0,987                           | -0,049                           | -0,830                          | -2,538                         | -9,429                          |
| <b>60</b>     | 2,020         | 1,614                           | 1,739        | 1,310                          | 1,471         | 1,014                           | -0,054                           | -0,906                          | -2,769                         | -10,286                         |
| <b>65</b>     | 2,058         | 1,654                           | 1,771        | 1,345                          | 1,495         | 1,040                           | -0,058                           | -0,981                          | -3,000                         | -11,143                         |
| <b>70</b>     | 2,095         | 1,693                           | 1,801        | 1,377                          | 1,517         | 1,065                           | -0,063                           | -1,057                          | -3,231                         | -12,000                         |
| <b>75</b>     | 2,129         | 1,729                           | 1,829        | 1,408                          | 1,539         | 1,089                           | -0,067                           | -1,132                          | -3,462                         | -12,857                         |
| <b>80</b>     | 2,162         | 1,764                           | 1,856        | 1,438                          | 1,560         | 1,112                           | -0,072                           | -1,208                          | -3,692                         | -13,714                         |
| <b>85</b>     | 2,194         | 1,796                           | 1,882        | 1,466                          | 1,580         | 1,134                           | -0,076                           | -1,283                          | -3,923                         | -14,571                         |
| <b>90</b>     | 2,224         | 1,828                           | 1,907        | 1,493                          | 1,599         | 1,155                           | -0,081                           | -1,358                          | -4,154                         | -15,429                         |
| <b>90,55</b>  | 2,227         | 1,831                           | 1,910        | 1,496                          | 1,601         | 1,157                           | -0,081                           | -1,367                          | -4,179                         | -15,523                         |
| <b>95</b>     | 2,253         | 1,858                           | 1,931        | 1,519                          | 1,617         | 1,175                           | -0,085                           | -1,434                          | -4,385                         | -16,286                         |
| <b>100</b>    | 2,281         | 1,886                           | 1,954        | 1,544                          | 1,635         | 1,195                           | -0,090                           | -1,509                          | -4,615                         | -17,143                         |
| <b>105</b>    | 2,308         | 1,914                           | 1,977        | 1,568                          | 1,652         | 1,214                           | -0,094                           | -1,585                          | -4,846                         | -18,000                         |
| <b>110</b>    | 2,334         | 1,940                           | 1,998        | 1,591                          | 1,669         | 1,233                           | -0,099                           | -1,660                          | -5,077                         | -18,857                         |
| <b>115</b>    | 2,359         | 1,966                           | 2,019        | 1,613                          | 1,685         | 1,251                           | -0,103                           | -1,736                          | -5,308                         | -19,714                         |
| <b>120</b>    | 2,384         | 1,990                           | 2,040        | 1,635                          | 1,701         | 1,268                           | -0,108                           | -1,811                          | -5,538                         | -20,571                         |
| <b>125</b>    | 2,408         | 2,014                           | 2,059        | 1,656                          | 1,717         | 1,285                           | -0,112                           | -1,887                          | -5,769                         | -21,429                         |
| <b>130</b>    | 2,431         | 2,037                           | 2,079        | 1,676                          | 1,732         | 1,301                           | -0,117                           | -1,962                          | -6,000                         | -22,286                         |
| <b>135</b>    | 2,453         | 2,059                           | 2,097        | 1,695                          | 1,746         | 1,318                           | -0,121                           | -2,038                          | -6,231                         | -23,143                         |
| <b>140</b>    | 2,475         | 2,081                           | 2,115        | 1,715                          | 1,760         | 1,333                           | -0,126                           | -2,113                          | -6,462                         | -24,000                         |
| <b>145</b>    | 2,496         | 2,102                           | 2,133        | 1,733                          | 1,774         | 1,348                           | -0,130                           | -2,189                          | -6,692                         | -24,857                         |
| <b>150</b>    | 2,517         | 2,122                           | 2,150        | 1,751                          | 1,788         | 1,363                           | -0,135                           | -2,264                          | -6,923                         | -25,714                         |
| <b>153,55</b> | 2,531         | 2,137                           | 2,163        | 1,764                          | 1,797         | 1,374                           | -0,138                           | -2,318                          | -7,087                         | -26,323                         |

**Table 8.2 Calculation of the stability parameter,  $\psi$**

| <b>Z</b>      | <b>VU</b>    | <b>U</b>     | <b>NU</b>    | <b>NEU</b>   | <b>NS</b>    | <b>S</b>     | <b>VS</b>    |
|---------------|--------------|--------------|--------------|--------------|--------------|--------------|--------------|
| <b>[m]</b>    | <b>[m/s]</b> | <b>[m/s]</b> | <b>[m/s]</b> | <b>[m/s]</b> | <b>[m/s]</b> | <b>[m/s]</b> | <b>[m/s]</b> |
| <b>0,1</b>    | 4,278        | 4,280        | 4,281        | 4,600        | 4,601        | 4,602        | 4,610        |
| <b>5</b>      | 8,303        | 8,332        | 8,352        | 8,508        | 8,526        | 8,564        | 8,709        |
| <b>10</b>     | 9,008        | 9,043        | 9,069        | 9,201        | 9,228        | 9,285        | 9,487        |
| <b>15</b>     | 9,426        | 9,460        | 9,488        | 9,606        | 9,639        | 9,707        | 9,934        |
| <b>20</b>     | 9,725        | 9,759        | 9,787        | 9,894        | 9,931        | 10,004       | 10,240       |
| <b>25</b>     | 9,961        | 9,993        | 10,020       | 10,117       | 10,156       | 10,233       | 10,465       |
| <b>27,55</b>  | 10,064       | 10,095       | 10,121       | 10,214       | 10,253       | 10,331       | 10,559       |
| <b>30</b>     | 10,156       | 10,185       | 10,211       | 10,299       | 10,339       | 10,416       | 10,639       |
| <b>35</b>     | 10,322       | 10,349       | 10,373       | 10,453       | 10,493       | 10,568       | 10,778       |
| <b>40</b>     | 10,468       | 10,493       | 10,515       | 10,587       | 10,625       | 10,698       | 10,890       |
| <b>45</b>     | 10,598       | 10,620       | 10,640       | 10,704       | 10,741       | 10,809       | 10,983       |
| <b>50</b>     | 10,715       | 10,735       | 10,752       | 10,809       | 10,844       | 10,907       | 11,061       |
| <b>55</b>     | 10,823       | 10,839       | 10,855       | 10,904       | 10,936       | 10,993       | 11,127       |
| <b>60</b>     | 10,921       | 10,936       | 10,949       | 10,991       | 11,019       | 11,069       | 11,184       |
| <b>65</b>     | 11,013       | 11,025       | 11,036       | 11,071       | 11,095       | 11,138       | 11,232       |
| <b>70</b>     | 11,098       | 11,108       | 11,116       | 11,144       | 11,165       | 11,200       | 11,275       |
| <b>75</b>     | 11,178       | 11,185       | 11,192       | 11,213       | 11,229       | 11,256       | 11,312       |
| <b>80</b>     | 11,254       | 11,258       | 11,263       | 11,277       | 11,288       | 11,307       | 11,344       |
| <b>85</b>     | 11,325       | 11,328       | 11,330       | 11,337       | 11,343       | 11,353       | 11,372       |
| <b>90</b>     | 11,393       | 11,393       | 11,393       | 11,394       | 11,395       | 11,396       | 11,397       |
| <b>90,55</b>  | 11,400       | 11,400       | 11,400       | 11,400       | 11,400       | 11,400       | 11,400       |
| <b>95</b>     | 11,457       | 11,455       | 11,453       | 11,448       | 11,443       | 11,435       | 11,420       |
| <b>100</b>    | 11,519       | 11,515       | 11,511       | 11,498       | 11,488       | 11,471       | 11,440       |
| <b>105</b>    | 11,578       | 11,571       | 11,565       | 11,547       | 11,530       | 11,504       | 11,457       |
| <b>110</b>    | 11,634       | 11,626       | 11,618       | 11,593       | 11,570       | 11,535       | 11,473       |
| <b>115</b>    | 11,688       | 11,678       | 11,668       | 11,637       | 11,607       | 11,563       | 11,488       |
| <b>120</b>    | 11,741       | 11,728       | 11,716       | 11,679       | 11,643       | 11,589       | 11,500       |
| <b>125</b>    | 11,791       | 11,777       | 11,763       | 11,719       | 11,676       | 11,614       | 11,512       |
| <b>130</b>    | 11,840       | 11,823       | 11,808       | 11,758       | 11,708       | 11,637       | 11,522       |
| <b>135</b>    | 11,887       | 11,868       | 11,851       | 11,795       | 11,738       | 11,658       | 11,532       |
| <b>140</b>    | 11,932       | 11,912       | 11,893       | 11,830       | 11,767       | 11,678       | 11,540       |
| <b>145</b>    | 11,976       | 11,954       | 11,933       | 11,865       | 11,795       | 11,696       | 11,548       |
| <b>150</b>    | 12,019       | 11,995       | 11,973       | 11,898       | 11,821       | 11,714       | 11,555       |
| <b>153,55</b> | 12,049       | 12,024       | 12,000       | 11,921       | 11,838       | 11,725       | 11,560       |

**Table 8.3 Calculation of the logarithmic wind profiles**

| <b>Z</b>      | <b>VU</b>    | <b>U</b>     | <b>NU</b>    | <b>NEU</b>   | <b>NS</b>    | <b>S</b>     | <b>VS</b>    |
|---------------|--------------|--------------|--------------|--------------|--------------|--------------|--------------|
| <b>[m]</b>    | <b>[m/s]</b> | <b>[m/s]</b> | <b>[m/s]</b> | <b>[m/s]</b> | <b>[m/s]</b> | <b>[m/s]</b> | <b>[m/s]</b> |
| <b>0,1</b>    | 5,577        | 5,692        | 5,771        | 6,052        | 6,348        | 6,523        | 7,373        |
| <b>5</b>      | 8,411        | 8,484        | 8,533        | 8,708        | 8,886        | 8,990        | 9,471        |
| <b>10</b>     | 9,045        | 9,105        | 9,146        | 9,288        | 9,432        | 9,516        | 9,901        |
| <b>15</b>     | 9,439        | 9,490        | 9,524        | 9,645        | 9,767        | 9,837        | 10,161       |
| <b>20</b>     | 9,728        | 9,773        | 9,802        | 9,906        | 10,012       | 10,072       | 10,350       |
| <b>25</b>     | 9,959        | 9,998        | 10,023       | 10,114       | 10,206       | 10,258       | 10,499       |
| <b>27,55</b>  | 10,061       | 10,097       | 10,121       | 10,206       | 10,291       | 10,340       | 10,564       |
| <b>30</b>     | 10,151       | 10,185       | 10,208       | 10,287       | 10,367       | 10,413       | 10,622       |
| <b>35</b>     | 10,317       | 10,347       | 10,366       | 10,435       | 10,505       | 10,545       | 10,727       |
| <b>40</b>     | 10,463       | 10,488       | 10,506       | 10,566       | 10,626       | 10,661       | 10,819       |
| <b>45</b>     | 10,593       | 10,615       | 10,630       | 10,682       | 10,735       | 10,765       | 10,901       |
| <b>50</b>     | 10,711       | 10,730       | 10,743       | 10,787       | 10,832       | 10,858       | 10,975       |
| <b>55</b>     | 10,819       | 10,835       | 10,846       | 10,883       | 10,922       | 10,943       | 11,042       |
| <b>60</b>     | 10,918       | 10,931       | 10,940       | 10,972       | 11,004       | 11,022       | 11,104       |
| <b>65</b>     | 11,010       | 11,021       | 11,028       | 11,054       | 11,080       | 11,094       | 11,161       |
| <b>70</b>     | 11,096       | 11,105       | 11,110       | 11,130       | 11,150       | 11,162       | 11,214       |
| <b>75</b>     | 11,177       | 11,183       | 11,187       | 11,202       | 11,217       | 11,225       | 11,263       |
| <b>80</b>     | 11,253       | 11,257       | 11,260       | 11,269       | 11,279       | 11,285       | 11,310       |
| <b>85</b>     | 11,325       | 11,327       | 11,328       | 11,333       | 11,338       | 11,341       | 11,354       |
| <b>90</b>     | 11,393       | 11,393       | 11,393       | 11,394       | 11,394       | 11,394       | 11,396       |
| <b>90,55</b>  | 11,400       | 11,400       | 11,400       | 11,400       | 11,400       | 11,400       | 11,400       |
| <b>95</b>     | 11,458       | 11,456       | 11,455       | 11,451       | 11,447       | 11,445       | 11,435       |
| <b>100</b>    | 11,519       | 11,516       | 11,514       | 11,506       | 11,498       | 11,493       | 11,473       |
| <b>105</b>    | 11,579       | 11,573       | 11,570       | 11,558       | 11,546       | 11,539       | 11,509       |
| <b>110</b>    | 11,635       | 11,629       | 11,624       | 11,608       | 11,592       | 11,583       | 11,543       |
| <b>115</b>    | 11,690       | 11,681       | 11,676       | 11,656       | 11,637       | 11,626       | 11,576       |
| <b>120</b>    | 11,742       | 11,732       | 11,726       | 11,702       | 11,679       | 11,666       | 11,607       |
| <b>125</b>    | 11,793       | 11,781       | 11,774       | 11,747       | 11,721       | 11,705       | 11,638       |
| <b>130</b>    | 11,841       | 11,828       | 11,820       | 11,790       | 11,760       | 11,743       | 11,667       |
| <b>135</b>    | 11,888       | 11,874       | 11,864       | 11,831       | 11,798       | 11,780       | 11,695       |
| <b>140</b>    | 11,934       | 11,918       | 11,908       | 11,871       | 11,835       | 11,815       | 11,722       |
| <b>145</b>    | 11,978       | 11,961       | 11,950       | 11,910       | 11,871       | 11,849       | 11,749       |
| <b>150</b>    | 12,020       | 12,002       | 11,990       | 11,948       | 11,906       | 11,882       | 11,774       |
| <b>153,55</b> | 12,050       | 12,031       | 12,018       | 11,974       | 11,930       | 11,905       | 11,792       |

**Table 8.4 Calculation of the power law wind profiles**

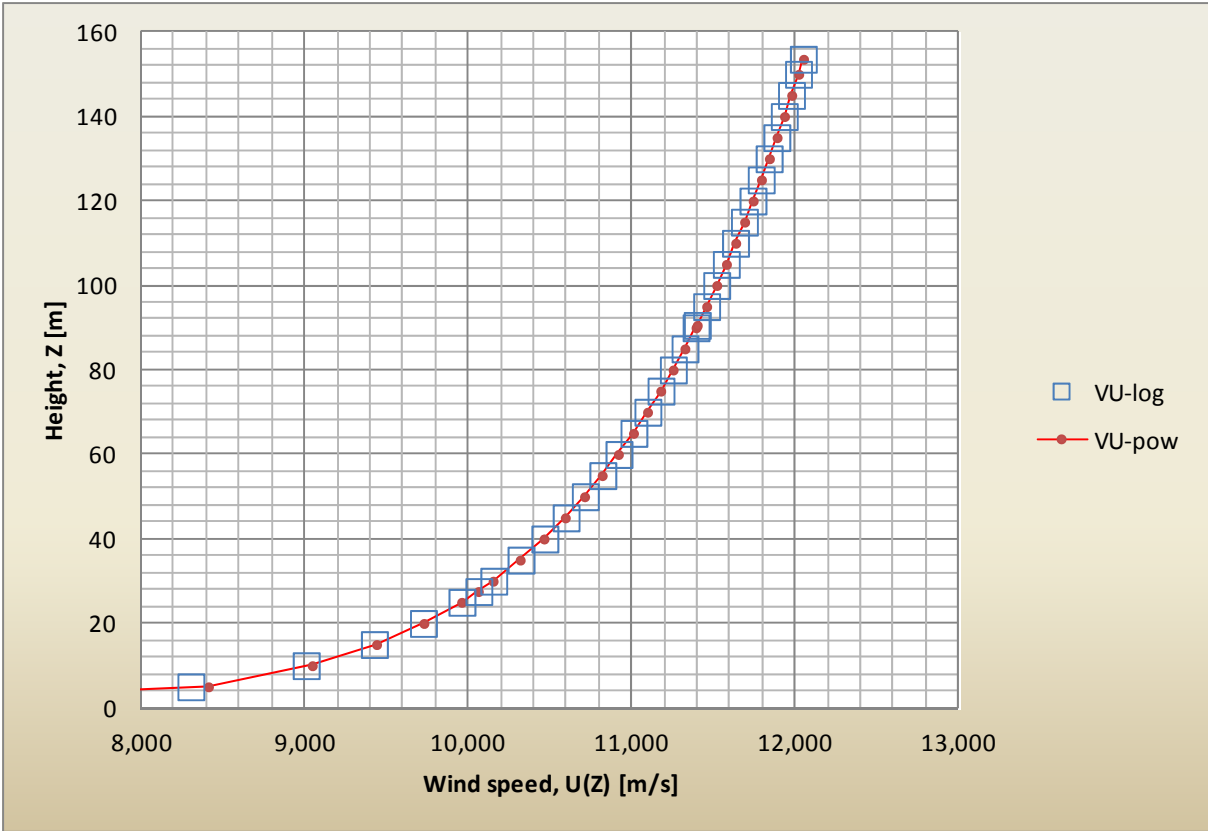


Figure 8.1 Very unstable wind profile –  $\alpha = 0.105$

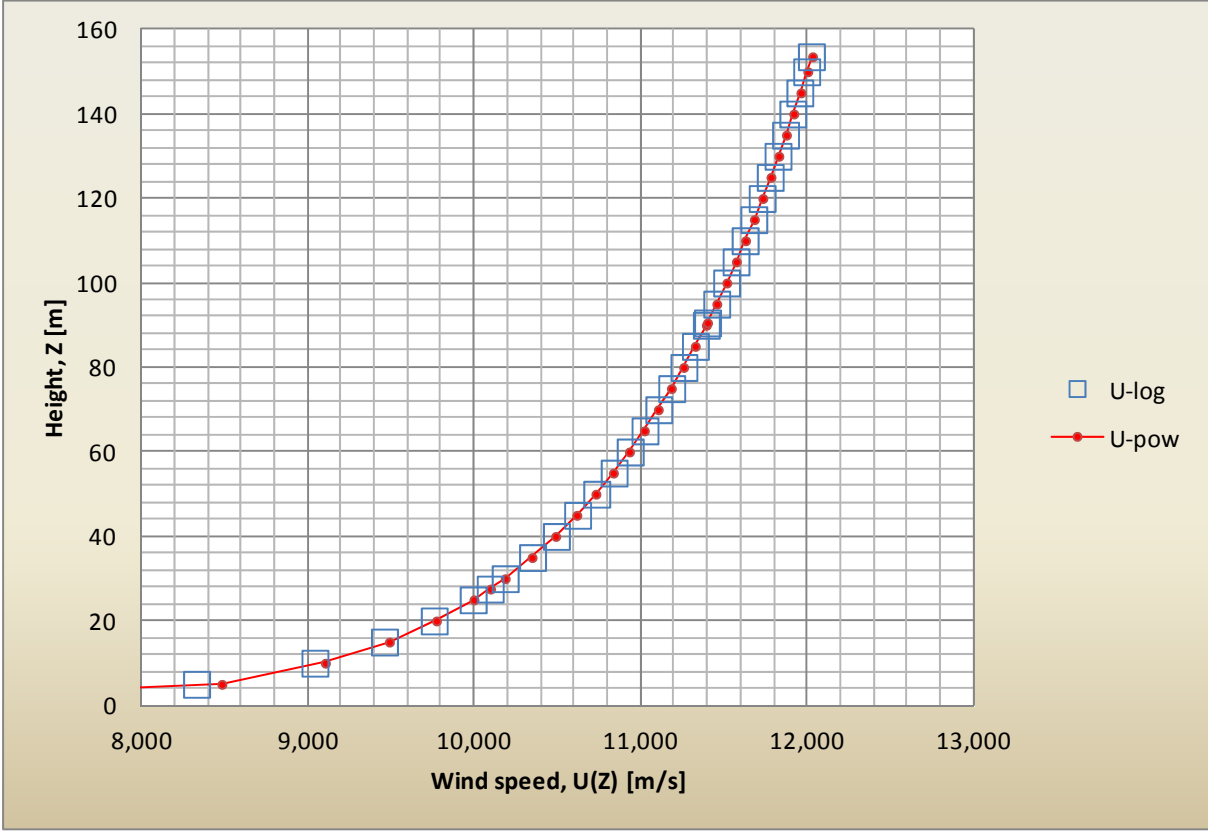


Figure 8.2 Unstable wind profile –  $\alpha = 0.102$

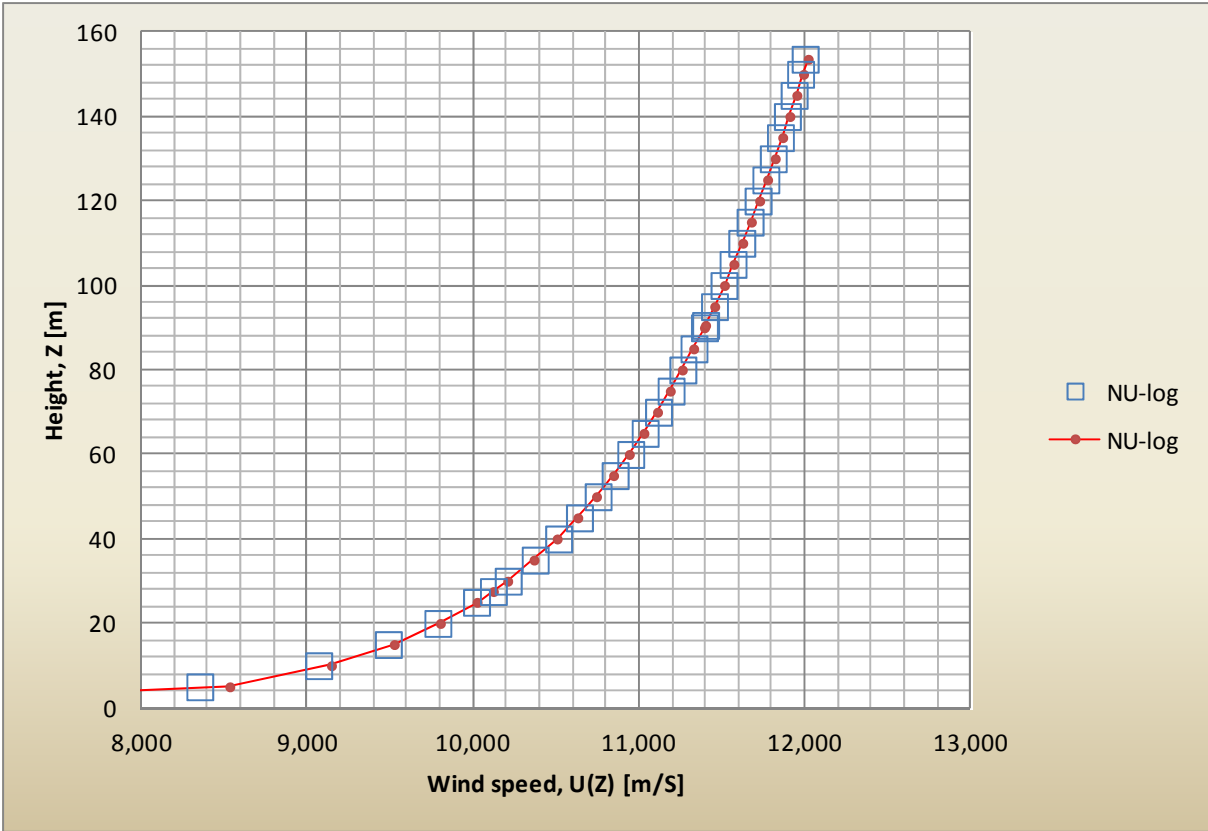


Figure 8.3 Near unstable wind profile –  $\alpha=0.100$

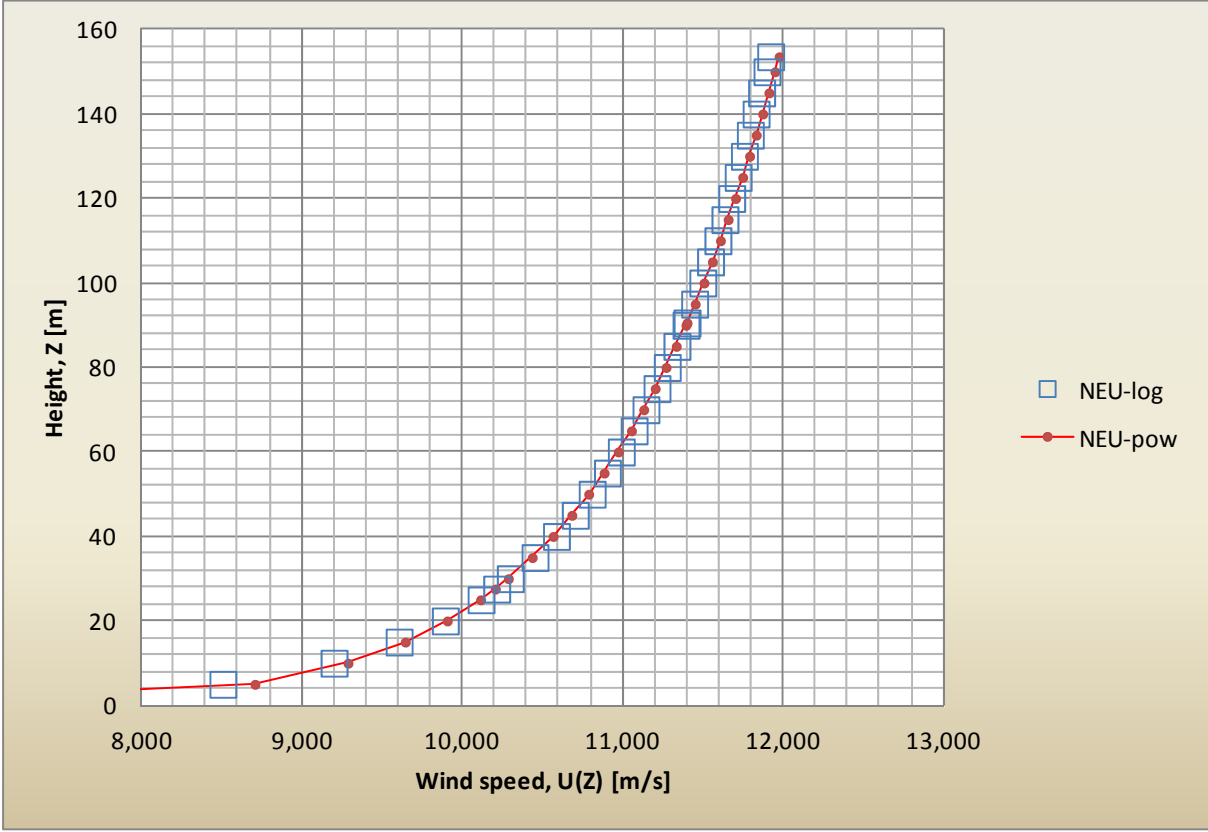


Figure 8.4 Neutral wind profile –  $\alpha=0.093$

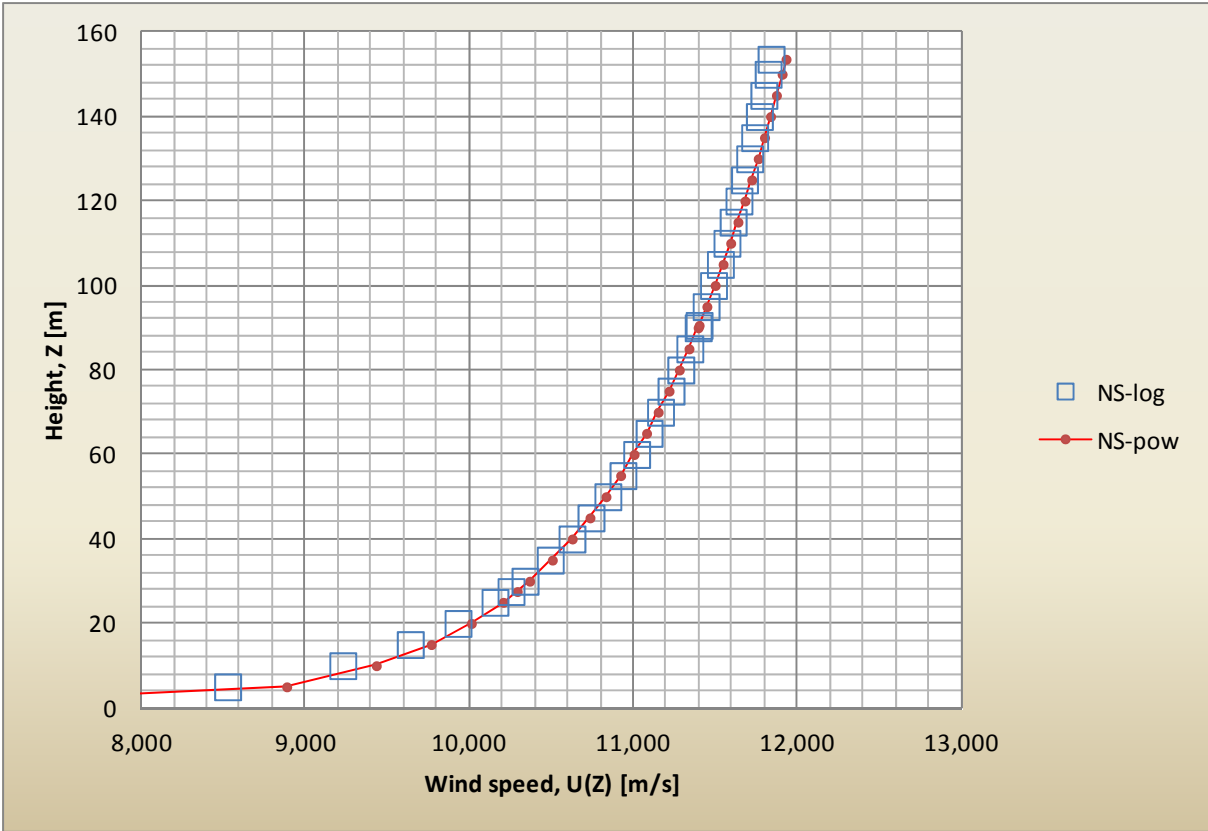


Figure 8.5 Near stable wind profile –  $\alpha=0.086$

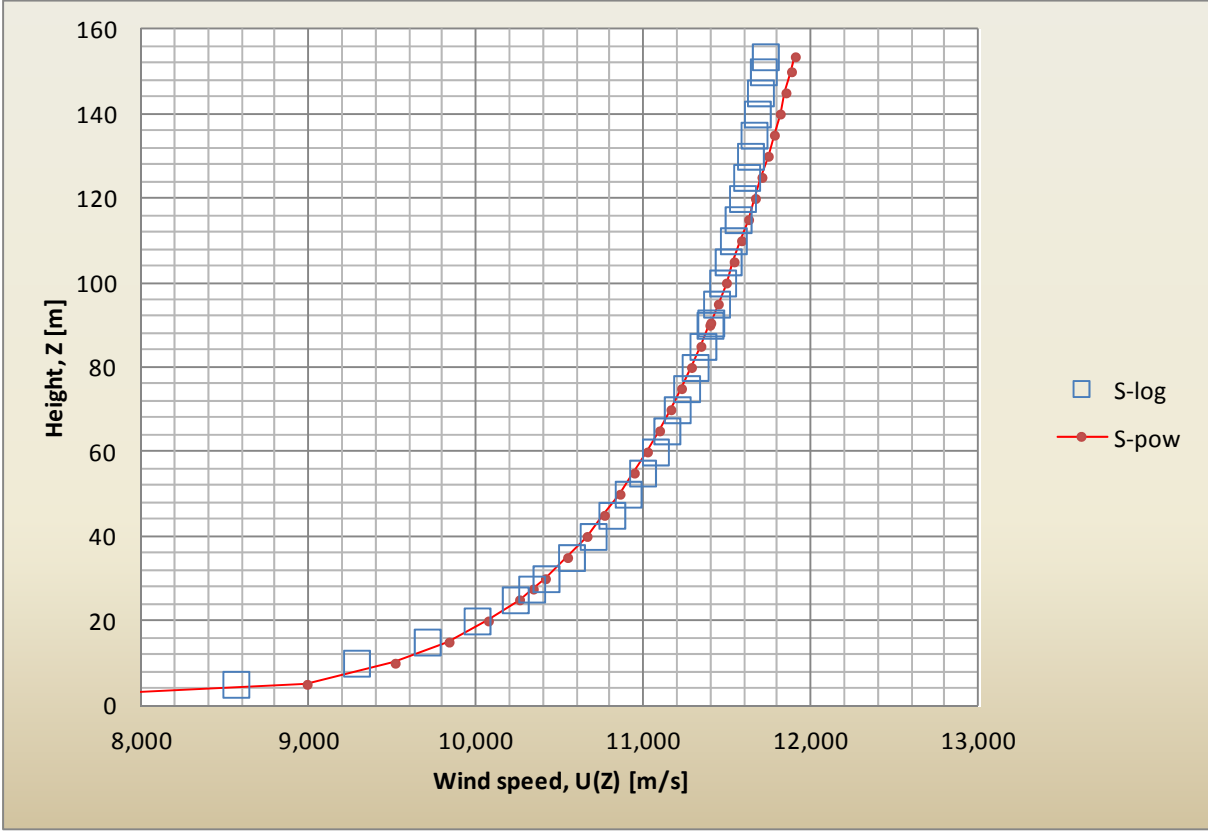


Figure 8.6 Stable wind profile –  $\alpha=0.082$

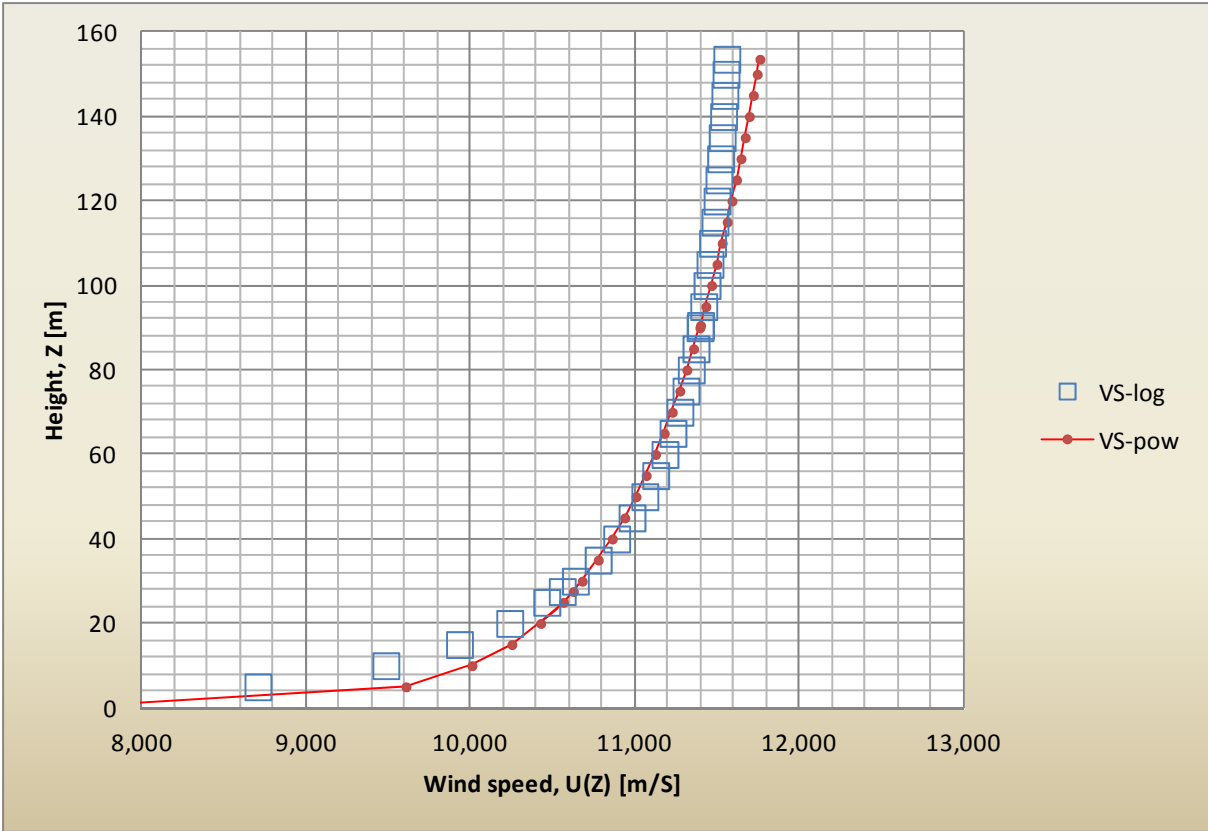


Figure 8.7 Very stable wind profile –  $\alpha= 0.059$

## 8.2 Tables with damage equivalent loads

| Run | RFx | RFy | RFz | RMx  | RMy  | RMz | TTFx | TTFy | TTFz | TTMx | TTMy | TTMz | TBFx | TBFy | TBFz | TBMX | TBMY  | TBMZ |
|-----|-----|-----|-----|------|------|-----|------|------|------|------|------|------|------|------|------|------|-------|------|
| VU1 | 180 | 273 | 338 | 5990 | 6750 | 209 | 205  | 73   | 51   | 736  | 3000 | 3460 | 205  | 84   | 54   | 5610 | 14300 | 3490 |
| VU2 | 172 | 267 | 353 | 5820 | 6510 | 164 | 196  | 54   | 53   | 687  | 3420 | 3640 | 203  | 61   | 56   | 4040 | 13700 | 3680 |
| VU3 | 194 | 272 | 357 | 6000 | 7370 | 252 | 199  | 55   | 52   | 747  | 3540 | 3480 | 204  | 59   | 56   | 4030 | 14000 | 3520 |
| VU4 | 172 | 272 | 310 | 5950 | 6830 | 184 | 196  | 46   | 49   | 642  | 3040 | 3350 | 199  | 50   | 53   | 3450 | 13600 | 3390 |
| VU5 | 174 | 271 | 350 | 6000 | 6650 | 268 | 194  | 64   | 52   | 758  | 3430 | 3780 | 202  | 73   | 56   | 4820 | 13500 | 3820 |
| VU6 | 176 | 271 | 375 | 5920 | 7030 | 202 | 201  | 59   | 48   | 714  | 2900 | 3330 | 208  | 68   | 51   | 4560 | 13800 | 3360 |
| Σ/6 | 178 | 271 | 347 | 5947 | 6857 | 213 | 199  | 58   | 51   | 714  | 3222 | 3507 | 204  | 66   | 54   | 4418 | 13817 | 3543 |

Table 8.5 DEL due to 25 % TI for VU

| Run | RFx | RFy | RFz | RMx  | RMy  | RMz | TTFx | TTFy | TTFz | TTMx | TTMy | TTMz | TBFx | TBFy | TBFz | TBMX | TBMY  | TBMZ |
|-----|-----|-----|-----|------|------|-----|------|------|------|------|------|------|------|------|------|------|-------|------|
| U1  | 189 | 269 | 388 | 5900 | 7060 | 158 | 197  | 63   | 48   | 827  | 3120 | 3410 | 209  | 72   | 51   | 4850 | 14300 | 3440 |
| U2  | 183 | 271 | 321 | 5930 | 7320 | 192 | 197  | 52   | 50   | 654  | 3330 | 3610 | 201  | 59   | 53   | 3890 | 13800 | 3650 |
| U3  | 187 | 271 | 379 | 5970 | 7220 | 169 | 202  | 59   | 50   | 698  | 3240 | 3420 | 211  | 66   | 53   | 4390 | 14200 | 3450 |
| U4  | 172 | 270 | 367 | 5960 | 6870 | 240 | 187  | 51   | 51   | 700  | 3390 | 3390 | 198  | 56   | 54   | 3780 | 13000 | 3430 |
| U5  | 202 | 267 | 355 | 5790 | 7960 | 327 | 197  | 65   | 50   | 706  | 3120 | 3540 | 202  | 74   | 53   | 4920 | 13900 | 3580 |
| U6  | 182 | 269 | 376 | 5910 | 7050 | 174 | 193  | 52   | 50   | 704  | 3140 | 3080 | 206  | 58   | 54   | 3880 | 14100 | 3120 |
| Σ/6 | 186 | 270 | 364 | 5910 | 7247 | 210 | 196  | 57   | 50   | 715  | 3223 | 3408 | 205  | 64   | 53   | 4285 | 13883 | 3445 |

Table 8.6 DEL due to 25 % TI for U

| Run | RFx | RFy | RFz | RMx  | RMy  | RMz | TTFx | TTFy | TTFz | TTMx | TTMy | TTMz | TBFx | TBFy | TBFz | TBMX | TBMY  | TBMZ |
|-----|-----|-----|-----|------|------|-----|------|------|------|------|------|------|------|------|------|------|-------|------|
| NU1 | 192 | 274 | 321 | 5990 | 7210 | 215 | 202  | 82   | 48   | 681  | 3040 | 3370 | 206  | 98   | 51   | 6410 | 14200 | 3410 |
| NU2 | 177 | 271 | 336 | 5920 | 6960 | 243 | 201  | 51   | 50   | 674  | 3090 | 3530 | 201  | 60   | 54   | 3870 | 14200 | 3570 |
| NU3 | 177 | 275 | 362 | 6090 | 7010 | 174 | 192  | 71   | 49   | 765  | 3340 | 3520 | 198  | 82   | 52   | 5460 | 13600 | 3550 |
| NU4 | 183 | 272 | 355 | 6040 | 6850 | 242 | 208  | 91   | 54   | 748  | 3210 | 3660 | 211  | 106  | 57   | 7010 | 14700 | 3700 |
| NU5 | 184 | 274 | 310 | 6040 | 7170 | 261 | 199  | 74   | 49   | 678  | 3090 | 3130 | 207  | 87   | 53   | 5740 | 14300 | 3160 |
| NU6 | 185 | 271 | 333 | 5930 | 7380 | 255 | 197  | 70   | 53   | 764  | 3230 | 3600 | 203  | 80   | 56   | 5410 | 14100 | 3640 |
| Σ/6 | 183 | 273 | 336 | 6002 | 7097 | 232 | 200  | 73   | 50   | 718  | 3167 | 3468 | 204  | 86   | 54   | 5650 | 14183 | 3505 |

Table 8.7 DEL due to 25 % TI for NU

| Run  | RFx | RFy | RFz | RMx  | RMy  | RMz | TTFx | TTFy | TTFz | TTMx | TTMy | TTMz | TBFx | TBFy | TBFz | TBMX | TBMY  | TBMZ |
|------|-----|-----|-----|------|------|-----|------|------|------|------|------|------|------|------|------|------|-------|------|
| NEU1 | 188 | 269 | 333 | 5910 | 7010 | 225 | 210  | 54   | 51   | 683  | 3160 | 3580 | 219  | 63   | 55   | 4140 | 14900 | 3620 |
| NEU2 | 173 | 273 | 349 | 5990 | 6750 | 155 | 192  | 70   | 50   | 654  | 3200 | 3690 | 195  | 80   | 54   | 5320 | 13300 | 3730 |
| NEU3 | 181 | 274 | 353 | 6030 | 6870 | 189 | 184  | 70   | 46   | 733  | 3200 | 3350 | 188  | 79   | 49   | 5280 | 13000 | 3400 |
| NEU4 | 183 | 272 | 319 | 5950 | 7080 | 206 | 220  | 57   | 52   | 679  | 3020 | 3280 | 220  | 68   | 56   | 4420 | 15300 | 3320 |
| NEU5 | 197 | 271 | 349 | 5930 | 7660 | 173 | 206  | 62   | 53   | 679  | 3300 | 3470 | 205  | 69   | 57   | 4700 | 14600 | 3500 |
| NEU6 | 186 | 270 | 383 | 5900 | 7030 | 151 | 184  | 70   | 48   | 803  | 3250 | 3090 | 190  | 83   | 51   | 5470 | 13200 | 3120 |
| Σ/6  | 185 | 272 | 348 | 5952 | 7067 | 183 | 199  | 64   | 50   | 705  | 3188 | 3410 | 203  | 74   | 53   | 4888 | 14050 | 3448 |

Table 8.8 DEL due to 25 % TI for NEU



| Run | RFx | RFy | RFz | RMx  | RMy  | RMz | TTFx | TTFy | TTFz | TTMx | TTMy | TTMz | TBFx | TBFy | TBFz | TBMX | TBMY  | TBMZ |
|-----|-----|-----|-----|------|------|-----|------|------|------|------|------|------|------|------|------|------|-------|------|
| NS1 | 179 | 272 | 319 | 5960 | 6860 | 277 | 198  | 91   | 47   | 710  | 3270 | 3320 | 206  | 108  | 50   | 7180 | 13900 | 3350 |
| NS2 | 188 | 271 | 370 | 6010 | 7100 | 212 | 195  | 70   | 50   | 694  | 3090 | 3290 | 206  | 81   | 54   | 5400 | 13800 | 3330 |
| NS3 | 181 | 270 | 403 | 5940 | 6940 | 161 | 211  | 57   | 52   | 820  | 3130 | 3340 | 214  | 64   | 56   | 4300 | 14800 | 3380 |
| NS4 | 177 | 267 | 346 | 5820 | 7090 | 212 | 181  | 63   | 48   | 676  | 3390 | 3660 | 189  | 73   | 51   | 4800 | 12800 | 3700 |
| NS5 | 189 | 276 | 384 | 6160 | 7310 | 249 | 209  | 81   | 47   | 758  | 3330 | 3120 | 211  | 93   | 50   | 6200 | 14700 | 3160 |
| NS6 | 185 | 271 | 353 | 6010 | 6850 | 155 | 195  | 78   | 50   | 768  | 3170 | 3550 | 197  | 91   | 53   | 6010 | 13300 | 3590 |
| Σ/6 | 183 | 271 | 363 | 5983 | 7025 | 211 | 198  | 73   | 49   | 738  | 3230 | 3380 | 204  | 85   | 52   | 5648 | 13883 | 3418 |

**Table 8.9 DEL due to 25 % TI for NS**

| Run | RFx | RFy | RFz | RMx  | RMy  | RMz | TTFx | TTFy | TTFz | TTMx | TTMy | TTMz | TBFx | TBFy | TBFz | TBMX | TBMY  | TBMZ |
|-----|-----|-----|-----|------|------|-----|------|------|------|------|------|------|------|------|------|------|-------|------|
| S1  | 180 | 269 | 318 | 5790 | 7190 | 228 | 174  | 66   | 51   | 679  | 3030 | 3310 | 178  | 75   | 54   | 5060 | 12100 | 3340 |
| S2  | 183 | 277 | 374 | 6160 | 6910 | 175 | 206  | 50   | 50   | 744  | 3120 | 3420 | 209  | 59   | 53   | 3870 | 14700 | 3460 |
| S3  | 193 | 271 | 373 | 5960 | 7200 | 252 | 212  | 66   | 51   | 775  | 3150 | 3610 | 216  | 78   | 55   | 5090 | 14900 | 3650 |
| S4  | 171 | 273 | 325 | 6000 | 6550 | 149 | 190  | 80   | 50   | 657  | 3120 | 3480 | 195  | 93   | 53   | 6170 | 13700 | 3520 |
| S5  | 190 | 273 | 351 | 6060 | 7240 | 209 | 201  | 55   | 54   | 680  | 3310 | 3730 | 199  | 64   | 57   | 4270 | 14100 | 3760 |
| S6  | 177 | 272 | 380 | 5940 | 6960 | 193 | 190  | 56   | 48   | 746  | 3340 | 3340 | 192  | 65   | 52   | 4280 | 13500 | 3380 |
| Σ/6 | 182 | 273 | 354 | 5985 | 7008 | 201 | 196  | 62   | 50   | 714  | 3178 | 3482 | 198  | 72   | 54   | 4790 | 13833 | 3518 |

**Table 8.10 DEL due to 25 % TI for S**

| Run | RFx | RFy | RFz | RMx  | RMy  | RMz | TTFx | TTFy | TTFz | TTMx | TTMy | TTMz | TBFx | TBFy | TBFz | TBMX | TBMY  | TBMZ |
|-----|-----|-----|-----|------|------|-----|------|------|------|------|------|------|------|------|------|------|-------|------|
| VS1 | 200 | 269 | 383 | 5850 | 7330 | 159 | 201  | 52   | 49   | 774  | 3450 | 3350 | 210  | 59   | 53   | 3880 | 14100 | 3390 |
| VS2 | 197 | 269 | 352 | 5930 | 7460 | 215 | 182  | 61   | 49   | 664  | 3050 | 3310 | 187  | 70   | 52   | 4730 | 13100 | 3350 |
| VS3 | 179 | 270 | 382 | 5890 | 6940 | 142 | 196  | 86   | 51   | 763  | 3200 | 3510 | 211  | 99   | 54   | 6600 | 14000 | 3540 |
| VS4 | 186 | 269 | 352 | 5890 | 7090 | 190 | 205  | 66   | 50   | 695  | 3200 | 3380 | 214  | 76   | 53   | 5020 | 14500 | 3420 |
| VS5 | 187 | 275 | 342 | 6090 | 6980 | 214 | 200  | 75   | 49   | 685  | 3210 | 3500 | 205  | 85   | 53   | 5720 | 14200 | 3540 |
| VS6 | 187 | 269 | 351 | 5860 | 7010 | 183 | 199  | 76   | 48   | 727  | 3020 | 3160 | 202  | 89   | 52   | 5890 | 13800 | 3200 |
| Σ/6 | 189 | 270 | 360 | 5918 | 7135 | 184 | 197  | 69   | 49   | 718  | 3188 | 3368 | 205  | 80   | 53   | 5307 | 13950 | 3407 |

**Table 8.11 DEL due to 25 % TI for VS**

| Run        | RFx        | RFy        | RFz        | RMx         | RMy         | RMz        | TTFx       | TTFy      | TTFz      | TTMx       | TTMy        | TTMz        | TBFx       | TBFy      | TBFz      | TBMX        | TBMY        | TBMZ        |
|------------|------------|------------|------------|-------------|-------------|------------|------------|-----------|-----------|------------|-------------|-------------|------------|-----------|-----------|-------------|-------------|-------------|
| <b>VU1</b> | 105        | 262        | 281        | 5530        | 4230        | 132        | 120        | 36        | 25        | 411        | 1610        | 1630        | 121        | 42        | 27        | 2790        | 8690        | 1640        |
| <b>VU2</b> | 97         | 261        | 282        | 5500        | 3760        | 118        | 114        | 36        | 27        | 381        | 1660        | 1700        | 112        | 42        | 29        | 2820        | 7950        | 1720        |
| <b>VU3</b> | 95         | 262        | 286        | 5510        | 3810        | 132        | 115        | 32        | 27        | 397        | 1630        | 1700        | 119        | 37        | 29        | 2470        | 8150        | 1720        |
| <b>VU4</b> | 105        | 260        | 299        | 5460        | 4160        | 110        | 123        | 38        | 26        | 406        | 1570        | 1600        | 126        | 44        | 28        | 2940        | 8850        | 1610        |
| <b>VU5</b> | 99         | 262        | 278        | 5530        | 3990        | 127        | 110        | 35        | 27        | 407        | 1620        | 1800        | 109        | 41        | 29        | 2730        | 7650        | 1820        |
| <b>VU6</b> | 99         | 262        | 278        | 5540        | 4090        | 114        | 110        | 38        | 26        | 409        | 1540        | 1640        | 113        | 45        | 28        | 2970        | 7780        | 1650        |
| <b>Σ/6</b> | <b>100</b> | <b>262</b> | <b>284</b> | <b>5512</b> | <b>4007</b> | <b>122</b> | <b>115</b> | <b>36</b> | <b>26</b> | <b>402</b> | <b>1605</b> | <b>1678</b> | <b>117</b> | <b>42</b> | <b>28</b> | <b>2787</b> | <b>8178</b> | <b>1693</b> |

**Table 8.12 DEL due to 11 % TI for VU**

| Run        | RFx        | RFy        | RFz        | RMx         | RMy         | RMz        | TTFx       | TTFy      | TTFz      | TTMx       | TTMy        | TTMz        | TBFx       | TBFy      | TBFz      | TBMX        | TBMY        | TBMZ        |
|------------|------------|------------|------------|-------------|-------------|------------|------------|-----------|-----------|------------|-------------|-------------|------------|-----------|-----------|-------------|-------------|-------------|
| <b>U1</b>  | 107        | 261        | 306        | 5480        | 4440        | 91         | 116        | 39        | 24        | 423        | 1540        | 1620        | 112        | 46        | 26        | 3030        | 8080        | 1640        |
| <b>U2</b>  | 104        | 260        | 282        | 5460        | 4280        | 94         | 120        | 35        | 25        | 362        | 1560        | 1740        | 121        | 41        | 27        | 2690        | 8430        | 1760        |
| <b>U3</b>  | 113        | 261        | 285        | 5500        | 4550        | 150        | 117        | 26        | 26        | 361        | 1560        | 1630        | 120        | 28        | 28        | 1900        | 8210        | 1650        |
| <b>U4</b>  | 99         | 261        | 281        | 5470        | 4170        | 111        | 115        | 21        | 26        | 394        | 1650        | 1620        | 116        | 23        | 28        | 1590        | 8140        | 1640        |
| <b>U5</b>  | 114        | 261        | 282        | 5480        | 4680        | 158        | 127        | 30        | 25        | 408        | 1510        | 1630        | 127        | 35        | 27        | 2320        | 9070        | 1650        |
| <b>U6</b>  | 104        | 261        | 290        | 5480        | 4340        | 118        | 123        | 36        | 26        | 380        | 1560        | 1450        | 125        | 42        | 28        | 2800        | 9000        | 1470        |
| <b>Σ/6</b> | <b>107</b> | <b>261</b> | <b>288</b> | <b>5478</b> | <b>4410</b> | <b>120</b> | <b>120</b> | <b>31</b> | <b>25</b> | <b>388</b> | <b>1563</b> | <b>1615</b> | <b>120</b> | <b>36</b> | <b>27</b> | <b>2388</b> | <b>8488</b> | <b>1635</b> |

**Table 8.13 DEL due to 11 % TI for U**

| Run        | RFx        | RFy        | RFz        | RMx         | RMy         | RMz        | TTFx       | TTFy      | TTFz      | TTMx       | TTMy        | TTMz        | TBFx       | TBFy      | TBFz      | TBMX        | TBMY        | TBMZ        |
|------------|------------|------------|------------|-------------|-------------|------------|------------|-----------|-----------|------------|-------------|-------------|------------|-----------|-----------|-------------|-------------|-------------|
| <b>NU1</b> | 104        | 264        | 279        | 5560        | 4130        | 105        | 127        | 33        | 25        | 399        | 1460        | 1570        | 127        | 39        | 27        | 2590        | 9140        | 1590        |
| <b>NU2</b> | 102        | 261        | 277        | 5490        | 4090        | 95         | 116        | 31        | 26        | 371        | 1460        | 1680        | 116        | 36        | 28        | 2370        | 8300        | 1700        |
| <b>NU3</b> | 100        | 259        | 281        | 5430        | 4020        | 143        | 117        | 51        | 26        | 423        | 1470        | 1650        | 120        | 60        | 28        | 3980        | 8280        | 1670        |
| <b>NU4</b> | 103        | 261        | 279        | 5490        | 4070        | 146        | 115        | 40        | 27        | 398        | 1510        | 1690        | 115        | 47        | 29        | 3150        | 8340        | 1710        |
| <b>NU5</b> | 115        | 262        | 286        | 5500        | 4620        | 121        | 128        | 28        | 25        | 406        | 1540        | 1540        | 128        | 33        | 27        | 2180        | 9150        | 1560        |
| <b>NU6</b> | 105        | 260        | 280        | 5440        | 4260        | 132        | 125        | 35        | 27        | 398        | 1590        | 1650        | 126        | 41        | 29        | 2720        | 9200        | 1670        |
| <b>Σ/6</b> | <b>105</b> | <b>261</b> | <b>280</b> | <b>5485</b> | <b>4198</b> | <b>124</b> | <b>121</b> | <b>36</b> | <b>26</b> | <b>399</b> | <b>1505</b> | <b>1630</b> | <b>122</b> | <b>43</b> | <b>28</b> | <b>2832</b> | <b>8735</b> | <b>1650</b> |

**Table 8.14 DEL due to 11 % TI for NU**

| Run         | RFx        | RFy        | RFz        | RMx         | RMy         | RMz        | TTFx       | TTFy      | TTFz      | TTMx       | TTMy        | TTMz        | TBFx       | TBFy      | TBFz      | TBMX        | TBMY        | TBMZ        |
|-------------|------------|------------|------------|-------------|-------------|------------|------------|-----------|-----------|------------|-------------|-------------|------------|-----------|-----------|-------------|-------------|-------------|
| <b>NEU1</b> | 111        | 260        | 282        | 5460        | 4290        | 156        | 133        | 30        | 28        | 422        | 1520        | 1690        | 136        | 36        | 30        | 2360        | 9600        | 1700        |
| <b>NEU2</b> | 101        | 262        | 283        | 5540        | 4100        | 121        | 120        | 38        | 25        | 364        | 1530        | 1730        | 122        | 45        | 27        | 2950        | 8670        | 1750        |
| <b>NEU3</b> | 108        | 263        | 277        | 5570        | 4300        | 125        | 107        | 28        | 24        | 411        | 1610        | 1590        | 107        | 33        | 26        | 2170        | 7540        | 1610        |
| <b>NEU4</b> | 109        | 261        | 282        | 5470        | 4300        | 171        | 127        | 43        | 26        | 387        | 1450        | 1500        | 128        | 50        | 28        | 3310        | 9080        | 1520        |
| <b>NEU5</b> | 118        | 262        | 280        | 5540        | 4860        | 112        | 122        | 35        | 26        | 366        | 1680        | 1590        | 123        | 40        | 28        | 2710        | 8860        | 1600        |
| <b>NEU6</b> | 103        | 261        | 299        | 5470        | 4010        | 149        | 108        | 32        | 25        | 438        | 1580        | 1540        | 110        | 38        | 26        | 2490        | 7880        | 1550        |
| <b>Σ/6</b>  | <b>108</b> | <b>262</b> | <b>284</b> | <b>5508</b> | <b>4310</b> | <b>139</b> | <b>120</b> | <b>34</b> | <b>25</b> | <b>398</b> | <b>1562</b> | <b>1607</b> | <b>121</b> | <b>40</b> | <b>27</b> | <b>2665</b> | <b>8605</b> | <b>1622</b> |

**Table 8.15 DEL due to 11 % TI for NEU**

| Run | RFx | RFy | RFz | RMx  | RMy  | RMz | TTFx | TTFy | TTFz | TTMx | TTMy | TTMz | TBFx | TBFy | TBFz | TBMX | TBMY | TBMZ |
|-----|-----|-----|-----|------|------|-----|------|------|------|------|------|------|------|------|------|------|------|------|
| NS1 | 102 | 261 | 278 | 5500 | 4060 | 150 | 121  | 62   | 24   | 421  | 1560 | 1530 | 121  | 74   | 26   | 4900 | 8660 | 1550 |
| NS2 | 113 | 262 | 284 | 5520 | 4530 | 101 | 123  | 41   | 27   | 387  | 1520 | 1560 | 125  | 48   | 29   | 3220 | 8830 | 1580 |
| NS3 | 117 | 260 | 278 | 5460 | 4710 | 141 | 116  | 27   | 27   | 405  | 1720 | 1680 | 116  | 31   | 29   | 2090 | 8240 | 1700 |
| NS4 | 104 | 259 | 279 | 5410 | 4190 | 143 | 112  | 27   | 25   | 392  | 1650 | 1740 | 115  | 31   | 27   | 2050 | 8140 | 1760 |
| NS5 | 103 | 263 | 286 | 5550 | 4070 | 149 | 116  | 29   | 24   | 429  | 1670 | 1510 | 117  | 33   | 26   | 2230 | 8400 | 1530 |
| NS6 | 96  | 261 | 277 | 5490 | 3740 | 128 | 113  | 29   | 26   | 406  | 1540 | 1670 | 114  | 32   | 28   | 2150 | 7960 | 1680 |
| Σ/6 | 106 | 261 | 280 | 5488 | 4217 | 135 | 117  | 36   | 25   | 407  | 1610 | 1615 | 118  | 42   | 27   | 2773 | 8372 | 1633 |

**Table 8.16 DEL due to 11 % TI for NS**

| Run | RFx | RFy | RFz | RMx  | RMy  | RMz | TTFx | TTFy | TTFz | TTMx | TTMy | TTMz | TBFx | TBFy | TBFz | TBMX | TBMY | TBMZ |
|-----|-----|-----|-----|------|------|-----|------|------|------|------|------|------|------|------|------|------|------|------|
| S1  | 104 | 260 | 276 | 5440 | 4160 | 105 | 111  | 42   | 24   | 352  | 1450 | 1520 | 110  | 48   | 26   | 3240 | 7870 | 1540 |
| S2  | 105 | 263 | 286 | 5560 | 4150 | 97  | 123  | 43   | 26   | 395  | 1510 | 1620 | 124  | 51   | 27   | 3400 | 8630 | 1630 |
| S3  | 103 | 261 | 284 | 5490 | 4150 | 171 | 124  | 27   | 26   | 423  | 1470 | 1700 | 125  | 31   | 28   | 2070 | 8850 | 1720 |
| S4  | 104 | 260 | 279 | 5480 | 4160 | 95  | 112  | 32   | 26   | 388  | 1590 | 1570 | 113  | 37   | 27   | 2440 | 7830 | 1590 |
| S5  | 103 | 262 | 278 | 5560 | 4150 | 118 | 120  | 26   | 27   | 385  | 1620 | 1780 | 114  | 30   | 29   | 2010 | 8560 | 1800 |
| S6  | 110 | 262 | 286 | 5500 | 4350 | 126 | 117  | 20   | 25   | 410  | 1640 | 1600 | 119  | 22   | 27   | 1450 | 8560 | 1620 |
| Σ/6 | 105 | 261 | 282 | 5505 | 4187 | 119 | 118  | 32   | 26   | 392  | 1547 | 1632 | 118  | 37   | 27   | 2435 | 8383 | 1650 |

**Table 8.17 DEL due to 11 % TI for S**

| Run | RFx | RFy | RFz | RMx  | RMy  | RMz | TTFx | TTFy | TTFz | TTMx | TTMy | TTMz | TBFx | TBFy | TBFz | TBMX | TBMY | TBMZ |
|-----|-----|-----|-----|------|------|-----|------|------|------|------|------|------|------|------|------|------|------|------|
| VS1 | 109 | 261 | 288 | 5470 | 4110 | 147 | 119  | 25   | 26   | 416  | 1720 | 1610 | 118  | 26   | 27   | 1790 | 8340 | 1630 |
| VS2 | 99  | 259 | 274 | 5410 | 4020 | 129 | 107  | 26   | 23   | 378  | 1530 | 1570 | 108  | 30   | 25   | 2000 | 7800 | 1590 |
| VS3 | 103 | 260 | 284 | 5440 | 4040 | 105 | 116  | 29   | 25   | 408  | 1540 | 1620 | 119  | 33   | 27   | 2210 | 8170 | 1640 |
| VS4 | 105 | 260 | 280 | 5460 | 4140 | 152 | 125  | 50   | 26   | 417  | 1560 | 1590 | 128  | 60   | 28   | 3950 | 8980 | 1610 |
| VS5 | 104 | 263 | 280 | 5560 | 4050 | 144 | 118  | 50   | 24   | 414  | 1560 | 1660 | 118  | 60   | 26   | 3940 | 8370 | 1680 |
| VS6 | 102 | 261 | 278 | 5470 | 3920 | 116 | 117  | 34   | 25   | 383  | 1440 | 1470 | 118  | 40   | 27   | 2640 | 8260 | 1490 |
| Σ/6 | 104 | 261 | 281 | 5468 | 4047 | 132 | 117  | 35   | 25   | 403  | 1558 | 1587 | 118  | 41   | 27   | 2755 | 8320 | 1607 |

**Table 8.18 DEL due to 11 % TI for VS**

### 8.3 Graphical presentation of damage equivalent loads

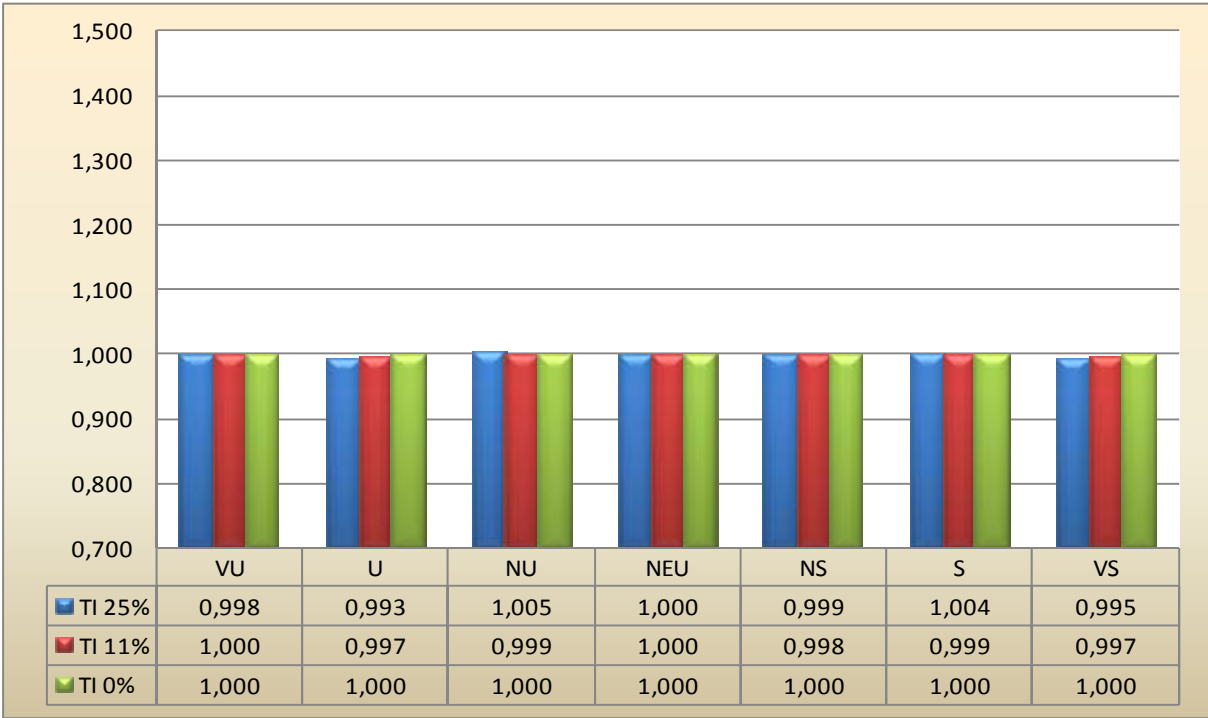


Figure 8.8 RFy – DEL due to force in y-direction at blade root.

Note: Seven wind profiles and three different turbulence intensities are illustrated. DEL is normalized with the neutral wind profile.

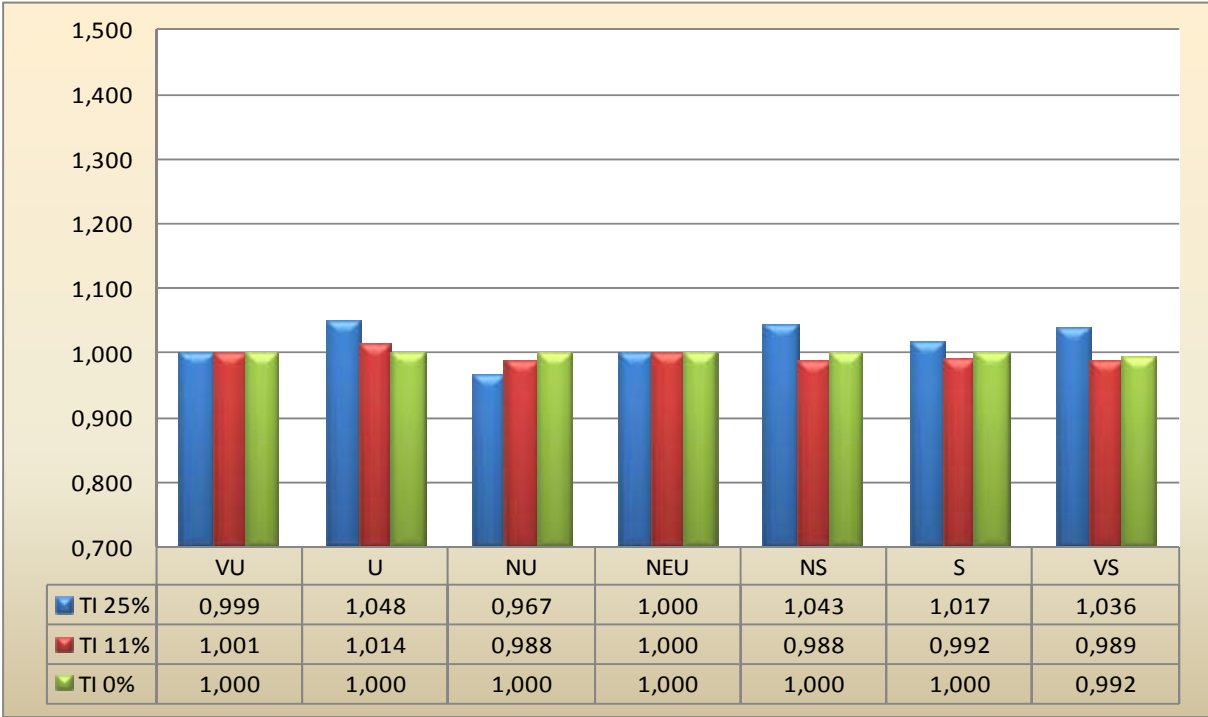
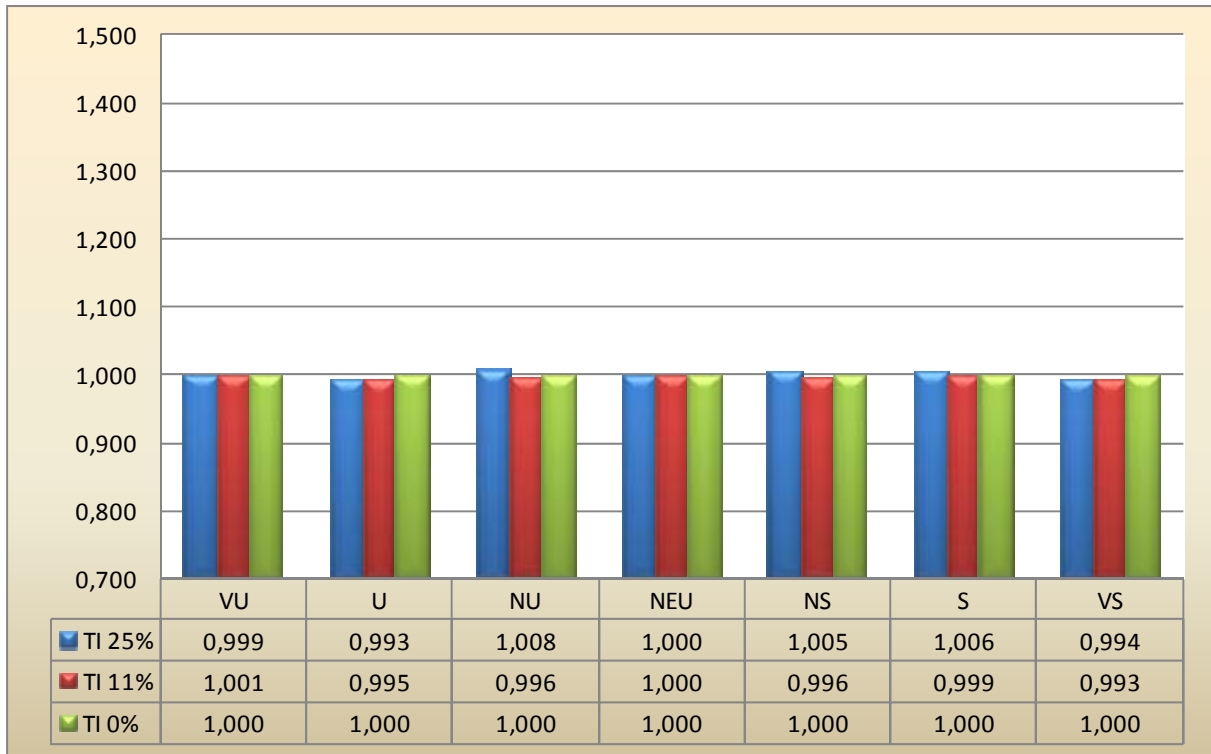


Figure 8.9 RFz – DEL due to force in z-direction at blade root.

Note: Seven wind profiles and three different turbulence intensities are illustrated. DEL is normalized with the neutral wind profile.



**Figure 8.10** RMx – DEL due to bending moment in x-direction at blade root.

Note: Seven wind profiles and three different turbulence intensities are illustrated. DEL is normalized with the neutral wind profile.

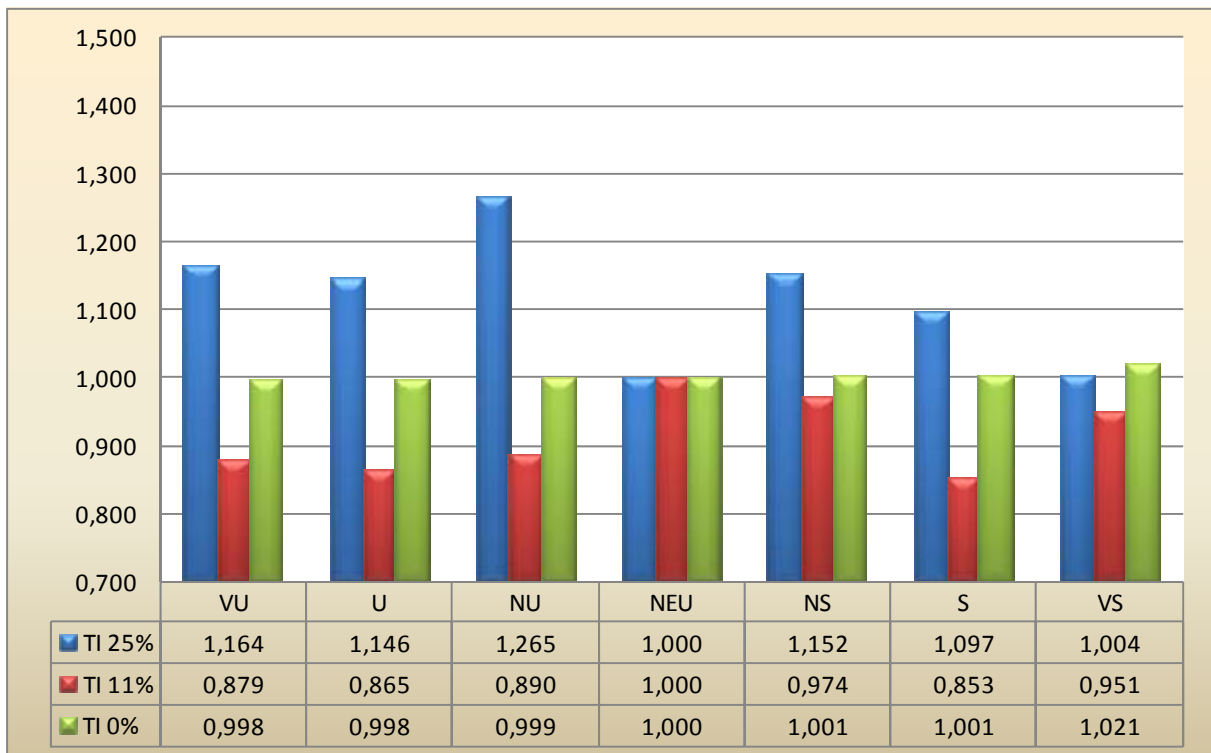


**Figure 8.11** RMz – DEL due to bending moment in z-direction at blade root.

Note: Seven wind profiles and three different turbulence intensities are illustrated. DEL is normalized with the neutral wind profile.

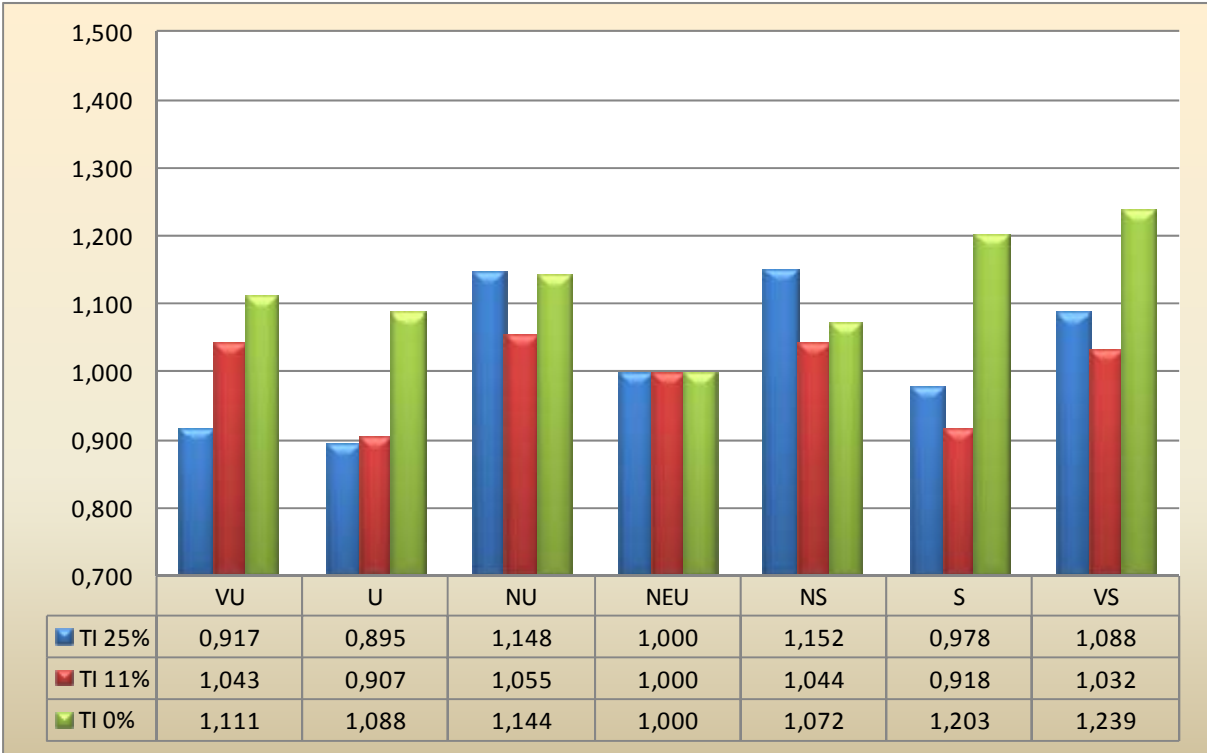


**Figure 8.12 TTFy - DEL due to force in y-direction at tower top.**

Note: Seven wind profiles and three different turbulence intensities are illustrated. DEL is normalized with the neutral wind profile.

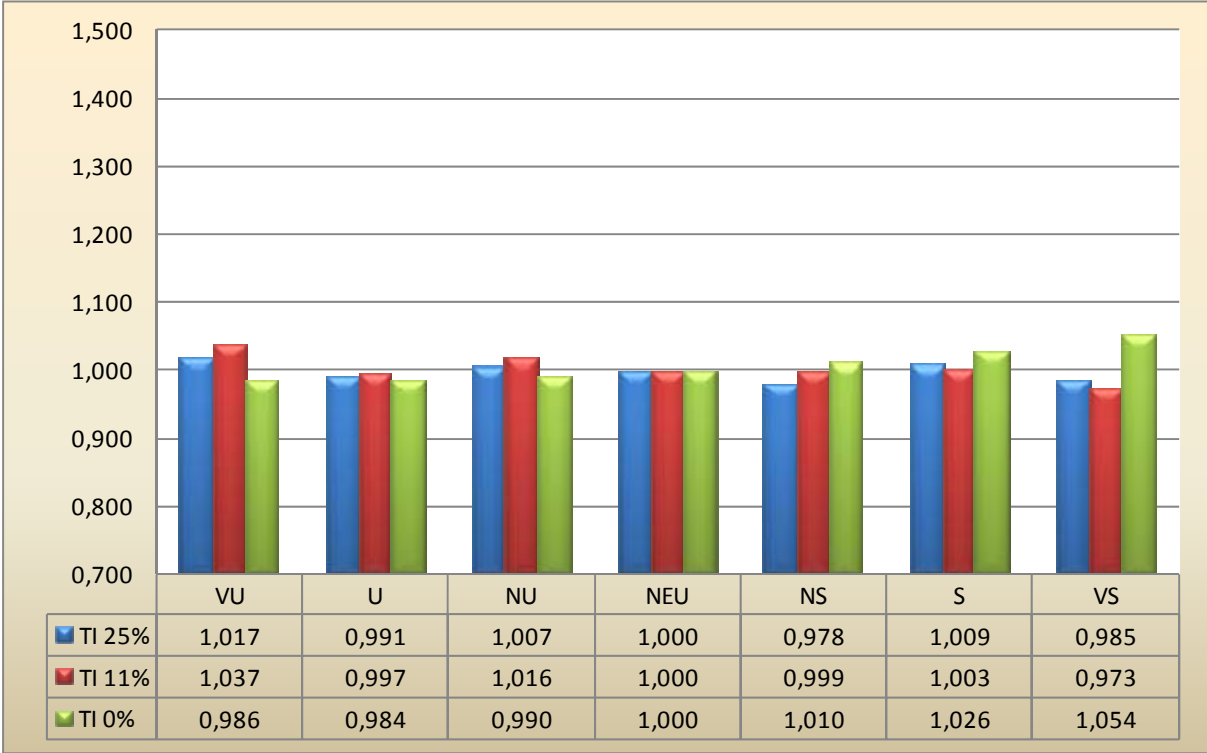


**Figure 8.13 TTFz - DEL due to force in z-direction at tower top.**

Note: Seven wind profiles and three different turbulence intensities are illustrated. DEL is normalized with the neutral wind profile.

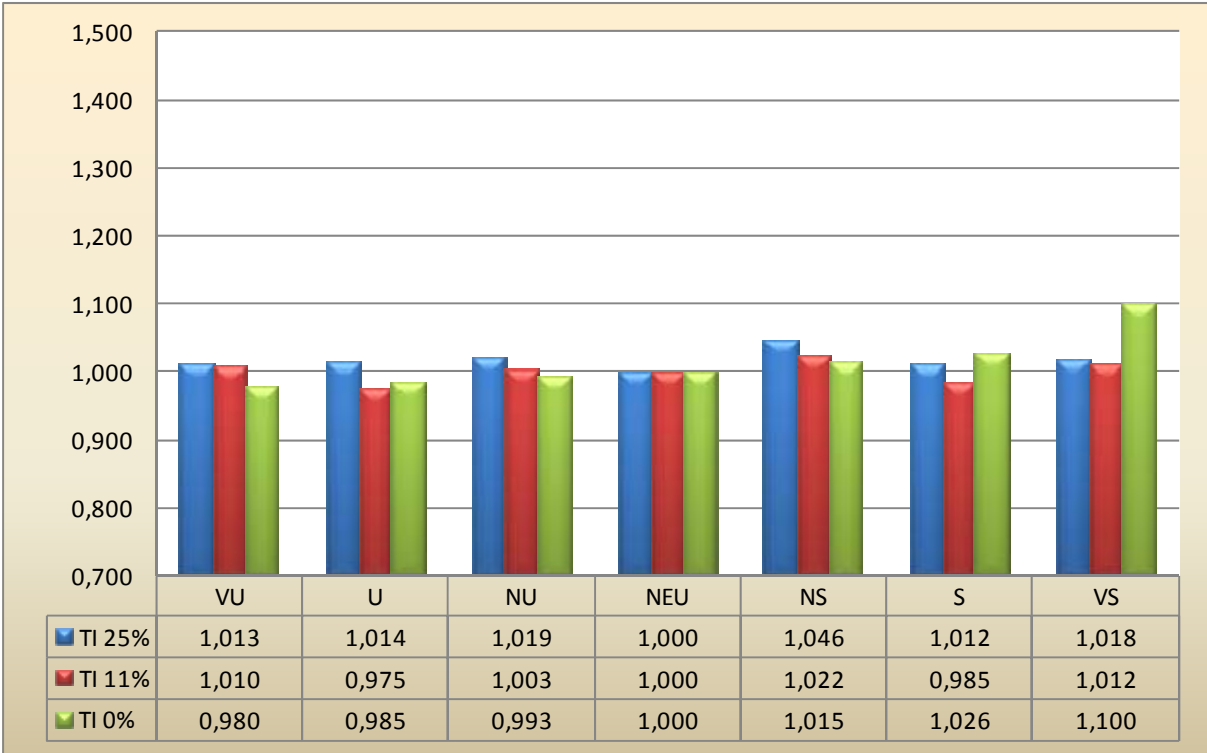


**Figure 8.14** TTMx - DEL due to bending moment in x-direction at tower top.

Note: Seven wind profiles and three different turbulence intensities are illustrated. DEL is normalized with the neutral wind profile.

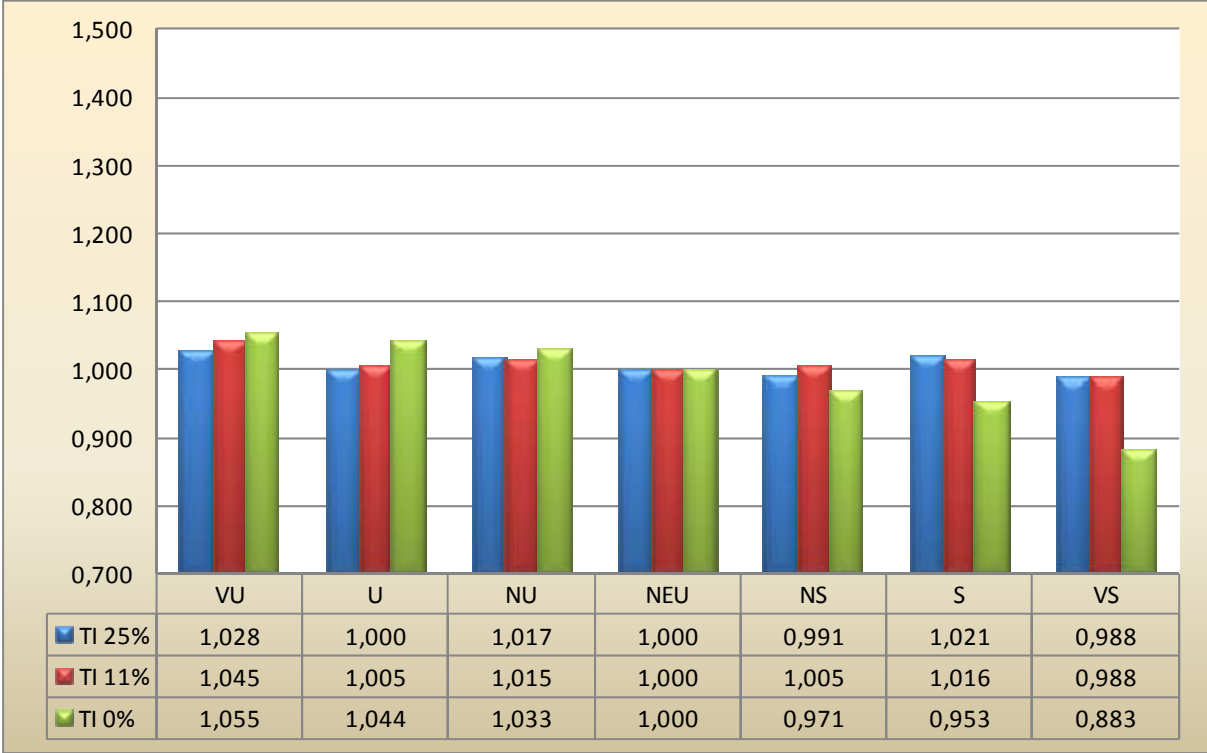


**Figure 8.15** TTMz - DEL due to bending moment in z-direction at tower top.

Note: Seven wind profiles and three different turbulence intensities are illustrated. DEL is normalized with the neutral wind profile.

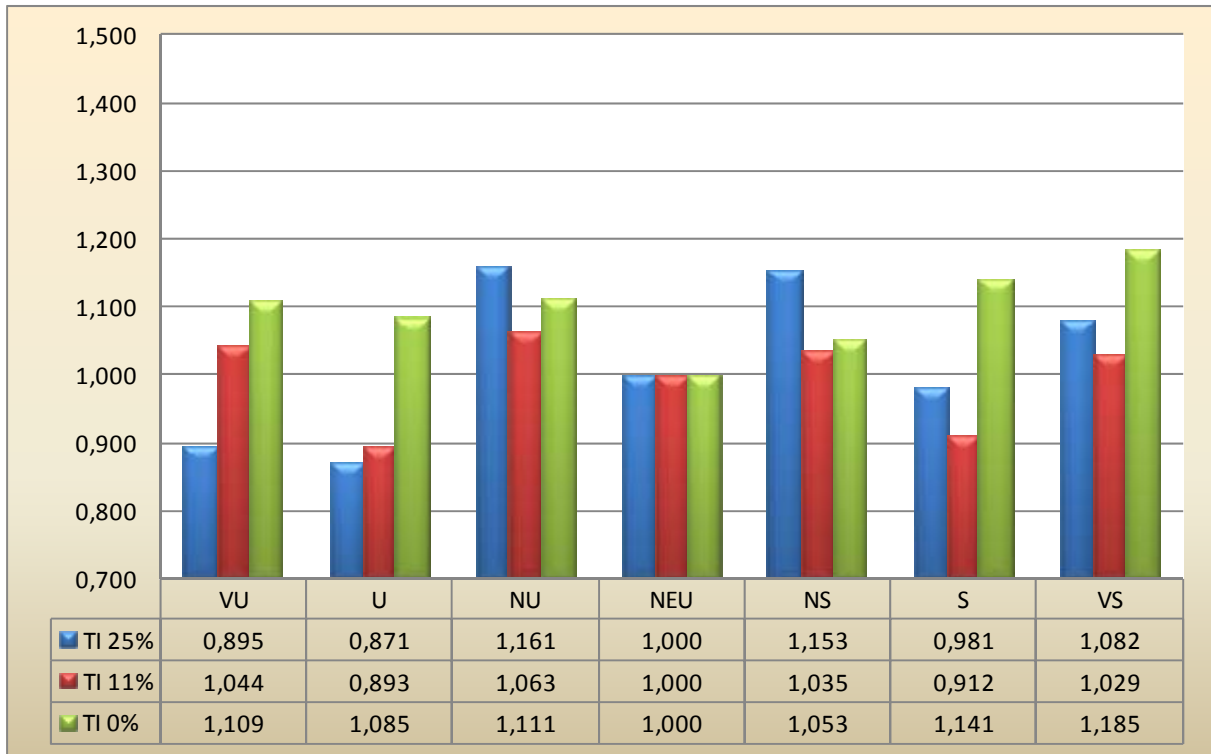


**Figure 8.16 TBFy - DEL due to force in y-direction at tower bottom.**

Note: Seven wind profiles and three different turbulence intensities are illustrated. DEL is normalized with the neutral wind profile.

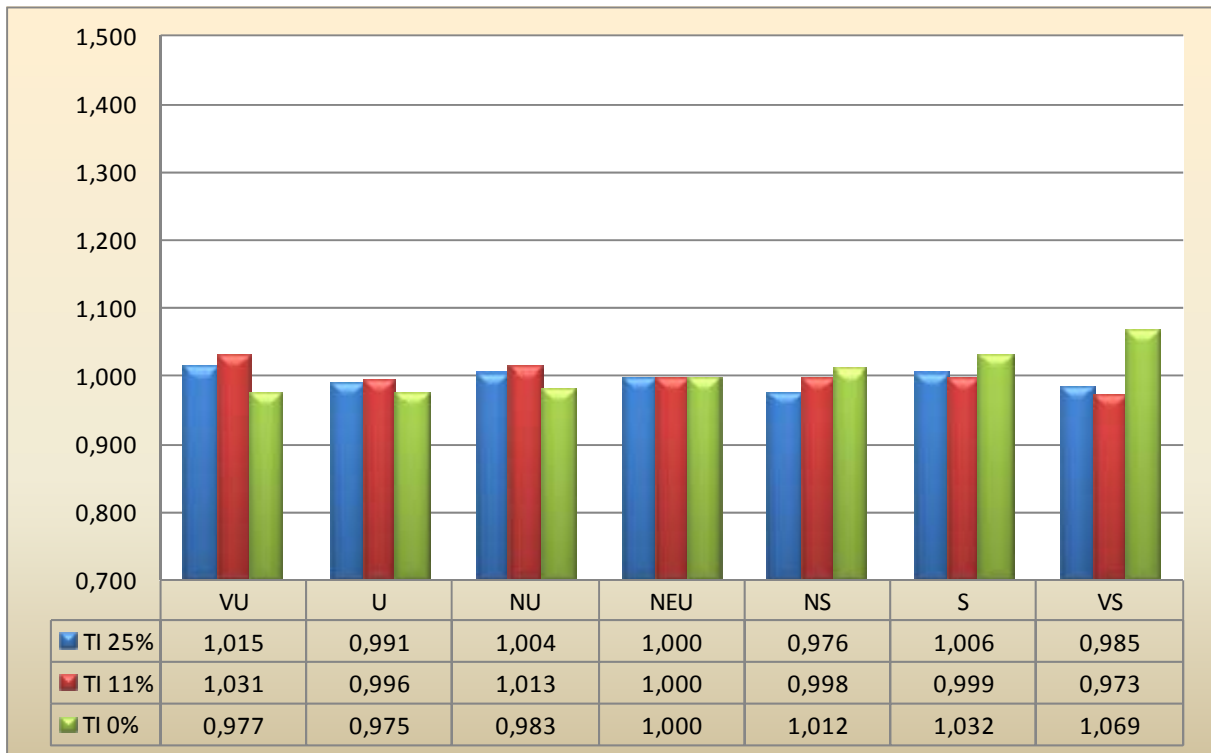


**Figure 8.17 TBFz - DEL due to force in z-direction at tower bottom.**

Note: Seven wind profiles and three different turbulence intensities are illustrated. DEL is normalized with the neutral wind profile.



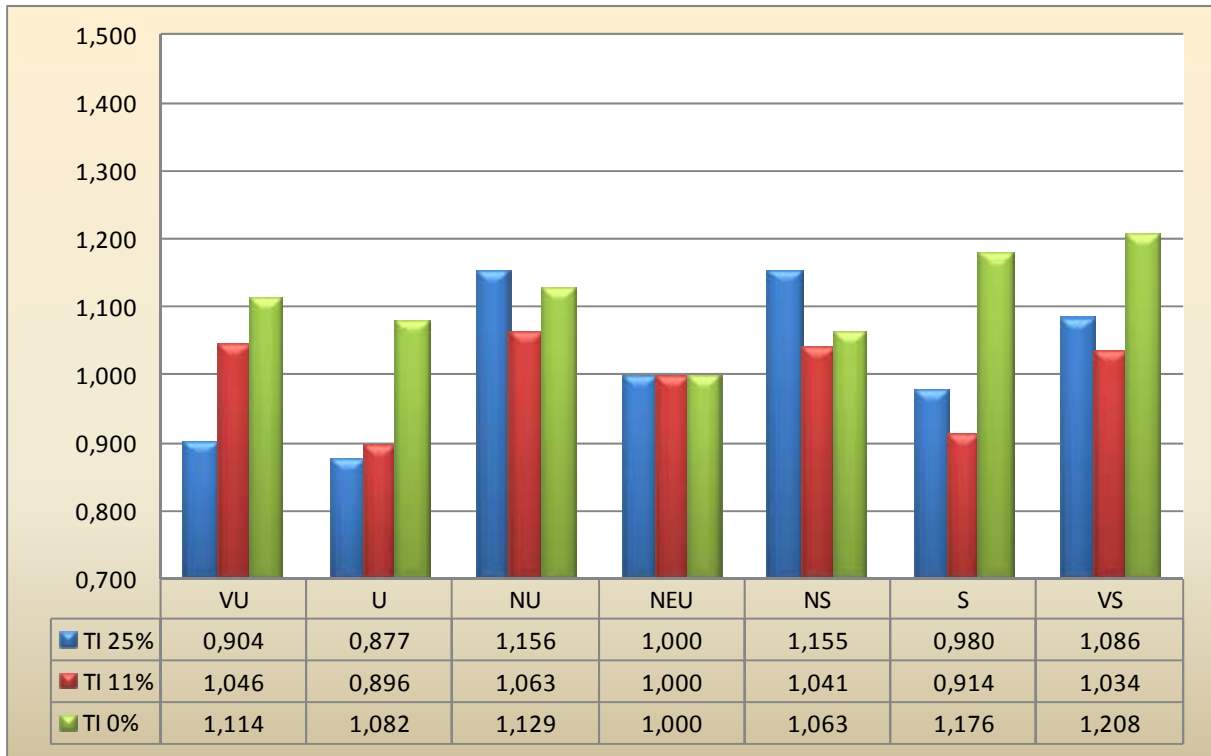


**Figure 8.18 TBM<sub>x</sub> - DEL due to bending moment in x-direction at tower bottom.**

Note: Seven wind profiles and three different turbulence intensities are illustrated. DEL is normalized with the neutral wind profile.

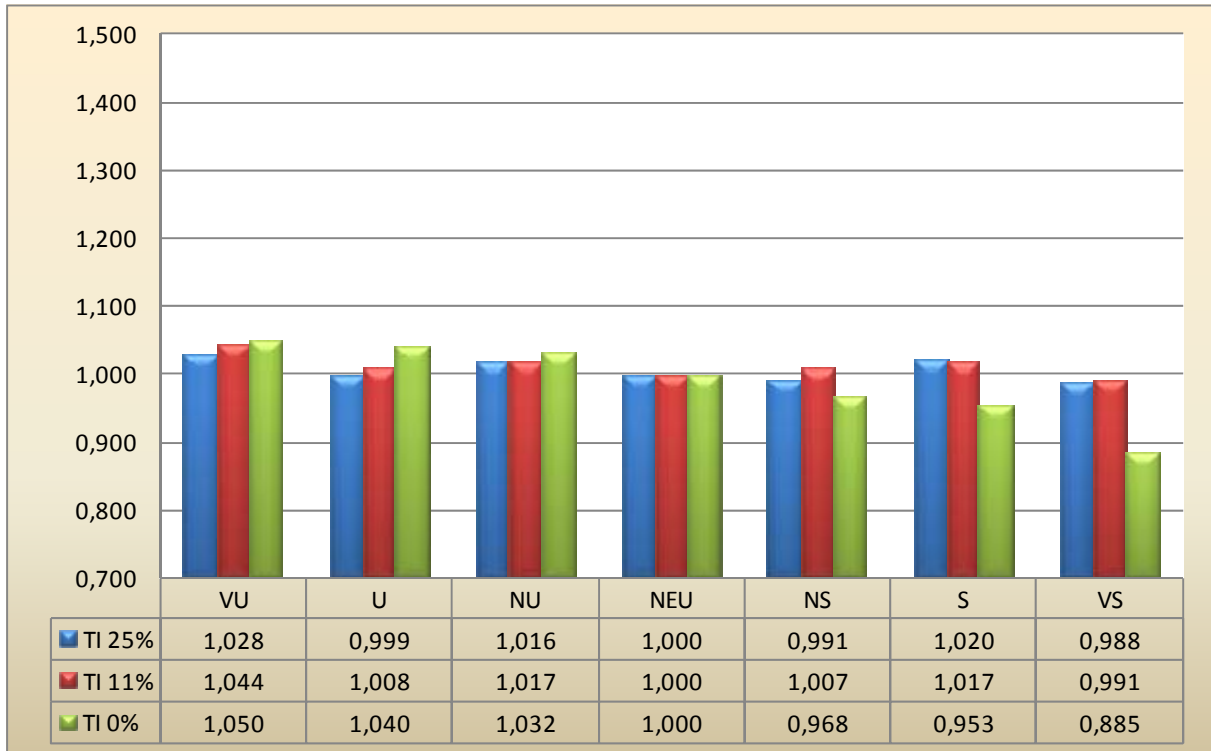


**Figure 8.19 TBM<sub>z</sub> - DEL due to bending moment in z-direction at tower bottom.**

Note: Seven wind profiles and three different turbulence intensities are illustrated. DEL is normalized with the neutral wind profile.

**8.4 Bin widths**

| <b>Loads</b> | <b>Bin width</b> | <b>Loads</b> | <b>Bin width</b> |
|--------------|------------------|--------------|------------------|
| <b>RFx</b>   | 8                | <b>TTMx</b>  | 84               |
| <b>RFy</b>   | 9                | <b>TTMy</b>  | 302              |
| <b>RFz</b>   | 15               | <b>TTMz</b>  | 345              |
| <b>RMx</b>   | 208              | <b>TBFx</b>  | 18               |
| <b>RMy</b>   | 295              | <b>TBFy</b>  | 6                |
| <b>RMz</b>   | 10               | <b>TBFz</b>  | 4                |
| <b>TTFx</b>  | 18               | <b>TBMx</b>  | 378              |
| <b>TTFy</b>  | 5                | <b>TBMy</b>  | 1166             |
| <b>TTFz</b>  | 4                | <b>TBMz</b>  | 348              |

**Table 8.19 Bin widths found by dividing the largest neutral load range by 50**

## 8.5 Turbsim input file

TurbSim Input File. Valid for TurbSim v1.50, 25-Sep-2009. Input File for Certification Test.

-----Runtime Options-----

```

578825      RandSeed1      - First random seed (-2147483648 to 2147483647)
321216      RandSeed2      - Second random seed (-2147483648 to 2147483647) for intrinsic pRNG, or an alternative pRNG:
"RanLux" or "RNSNLW"
False      WrBHHTP        - Output hub-height turbulence parameters in GenPro-binary form? (Generates RootName.bin)
True       WrFHHTP        - Output hub-height turbulence parameters in formatted form? (Generates RootName.dat)
False      WrADHH        - Output hub-height time-series data in AeroDyn form? (Generates RootName.hh)
True       WrADFF        - Output full-field time-series data in TurbSim/AeroDyn form? (Generates RootName.bts)
False      WrBLFF        - Output full-field time-series data in BLADED/AeroDyn form? (Generates RootName.wnd)
False      WrADTWR        - Output tower time-series data? (Generates RootName.twr)
False      WrFMTFF        - Output full-field time-series data in formatted (readable) form? (Generates RootName.u,
RootName.v, RootName.w)
True       WrACT         - Output coherent turbulence time steps in AeroDyn form? (Generates RootName.cts)
True       Clockwise     - Clockwise rotation looking downwind? (used only for full-field binary files - not
necessary for AeroDyn)

0          ScaleIEC      - Scale IEC turbulence models to exact target standard deviation? [0=no additional scaling;
1=use hub scale uniformly; 2=use individual scales]

```

-----Turbine/Model Specifications-----

```

10         NumGrid_Z      - Vertical grid-point matrix dimension
10         NumGrid_Y      - Horizontal grid-point matrix dimension
0.025     TimeStep        - Time step [seconds]
1050.0    AnalysisTime    - Length of analysis time series [seconds] (program will add time if necessary: AnalysisTime
= MAX(AnalysisTime, UsableTime+GridWidth/MeanHWS) )
850.0     UsableTime      - Usable length of output time series [seconds] (program will add GridWidth/MeanHWS
seconds)
90.55     HubHt          - Hub height [m] (should be > 0.5*GridHeight)
130.00    GridHeight     - Grid height [m]
130.00    GridWidth      - Grid width [m] (should be >= 2*(RotorRadius+ShaftLength))
0         VFlowAng       - Vertical mean flow (up tilt) angle [degrees]
0         HFlowAng       - Horizontal mean flow (skew) angle [degrees]

```

-----Meteorological Boundary Conditions-----

```

"IECKAI"   TurbModel      - Turbulence model ("IECKAI"=Kaimal, "IECVKM"=von Karman, "GP_LLJ", "NWTcup", "SMOOTH",
"WF_UPW", "WF_07D", "WF_14D", or "NONE")
3         IECstandard    - Number of IEC 61400-x standard (x=1,2, or 3 with optional 61400-1 edition number (i.e. "1-
Ed2") )
0.00000001 IECturbc       - IEC turbulence characteristic ("A", "B", "C" or the turbulence intensity in
percent) ("KHTST" option with NWTcup, not used for other models)
NTM       IEC_WindType    - IEC turbulence type ("NTM"=normal, "xETM"=extreme turbulence, "xEWM1"=extreme 1-year wind,
"xEWM50"=extreme 50-year wind, where x=wind turbine class 1, 2, or 3)
default   ETMc           - IEC ETM "c" parameter [m/s] (or "default")
PL        WindProfileType - Wind profile type ("JET"=Low-level jet, "LOG"=Logarithmic, "PL"=Power law, "IEC"=PL on rotor
& LOG elsewhere, or "default")
90.55     RefHt          - Height of the reference wind speed [m]
11.4      URef           - Mean (total) wind speed at the reference height [m/s]
350       ZJetMax        - Jet height [m] (used only for JET wind profile, valid 70-490 m)
0.082     PLExp          - Power law exponent (or "default")

```

```

default t      Z0          - Surface roughness length [m] (or "default")
-----Non-IEC Meteorological Boundary Conditions-----
default t      Latitude    - Site latitude [degrees] (or "default")
0.05          RICH_NO      - Gradient Richardson number
default t      UStar       - Friction or shear velocity [m/s] (or "default")
default t      ZI          - Mixing layer depth [m] (or "default")
default t      PC_UW       - Mean hub u'w' Reynolds stress (or "default" or "none")
default t      PC_UV       - Mean hub u'v' Reynolds stress (or "default" or "none")
default t      PC_VW       - Mean hub v'w' Reynolds stress (or "default" or "none")
default t      IncDec1     - u-component coherence parameters (e.g. "10.0 0.3e-3" in quotes) (or "default")
default t      IncDec2     - v-component coherence parameters (e.g. "10.0 0.3e-3" in quotes) (or "default")
default t      IncDec3     - w-component coherence parameters (e.g. "10.0 0.3e-3" in quotes) (or "default")
default t      CohExp      - Coherence exponent (or "default")
-----Coherent Turbulence Scaling Parameters-----
".\EventData" CTEventPath  - Name of the path where event data files are located
LES           CTEventFile - Type of event files ("random", "les" or "dns")
true         Randomize   - Randomize disturbance scale and location? (true/false)
1.0          DistScal    - Disturbance scale (ratio of dataset height to rotor disk).
0.5          CTLY        - Fractional location of tower centerline from right (looking downwind) to left side of the
dataset.
0.5          CTLZ        - Fractional location of hub height from the bottom of the dataset.
30.0         CTStartTime - Minimum start time for coherent structures in RootName.cts [seconds]

```

```

=====
NOTE: Do not add or remove any lines in this file!
=====

```

## 8.6 Mlife text file

```

----- MLife version 1.0 Input File -----
Binned (+Names, -Chans, -CC, -TSp, +Stats, +SwT, -SwX, -SF, -EE, -Bins, -Bp, -PDF, -PDFp, -PSD, -PSDp, -PSDtxt, -PSDxls, +F,
+FBM, +FBM, +DEL, -CF, -FwDELt, +FwDELx, -FwRfT, +FwRfX, +FpBC, -FpPE, -FpCC, -FpRM, +TbDEL, +Multi).
----- Job Options -----
false EchoInp Echo input to <rootname>.echo as this file is being read.
false StrNames Use channel names following a "$" instead of numbers when specifying channels in this
input file.
false OutData Output modified data array after scaling and calculated channels. (currently unavailable)
"%10.2e" RealFmt Format for outputting floating-point values.
"U" AggRoot Root name for aggregate output files.
----- Input-Data Layout -----
0 TitleLine The row with the file title on it (zero if no title is available).
7 NamesLine The row with the channel names on it (zero if no names are available or are specified
below).
0 UnitsLine The row with the channel units on it (zero if no units are available or are specified
below).
1008 FirstDataLine The first row of data.
22 NumChans The number of channels in each input file.
ChanTitle ChanUnits Scale Offset NumCols rows of data follow. Title and units strings must be 10 characters or
less.
"Description" "s" 1.0 0.0
"WindVxI" "m/s" 1.0 0.0
"WindVyI" "m/s" 1.0 0.0
"WindVzI" "m/s" 1.0 0.0
"RootFxc1" "kN" 1.0 0.0
"RootFyc1" "kN" 1.0 0.0
"RootFzc1" "kN" 1.0 0.0
"RootMxc1" "kNm" 1.0 0.0
"RootMyc1" "kNm" 1.0 0.0
"RootMzc1" "kNm" 1.0 0.0
"YawBrFxp" "kN" 1.0 0.0
"YawBrFyp" "kN" 1.0 0.0
"YawBrFzp" "kN" 1.0 0.0
"YawBrMxp" "kNm" 1.0 0.0
"YawBrMyp" "kNm" 1.0 0.0
"YawBrMzp" "kNm" 1.0 0.0
"BottomFx" "kN" 1.0 0.0
"BottomFy" "kN" 1.0 0.0
"BottomFz" "kN" 1.0 0.0
"BottomMx" "kNm" 1.0 0.0
"BottomMy" "kNm" 1.0 0.0
"BottomMz" "kNm" 1.0 0.0
----- Calculated Channels -----
0 NumCChan The number calculated channels to generate.
1234567890 Seed The integer seed for the random number generator (-2,147,483,648 to 2,147,483,647)
ColTitle Units Equation Put each field in quotes. Titles and units are limited to 10 characters. NumCChan rows
of data follow.
----- Time and Wind Speed -----
1 TimeChan The channel containing time.
2 WSChan The primary wind-speed channel (used for mean wind speed and turbulence intensity, 0 for none)
----- Statistics and Extreme Events -----
false DoStats Generate statistics of all the channels.
true WrStatsTxt Write the stats to a text file?
false WrStatsXLS Write the stats to an Excel file?
0 NumSFChans Number of channels that will have summary statistics generated for them.
1 SFChans List of channels that will have summary statistics generated for them. Must number
NumSFChans.
----- Fatigue -----
18 nFatigueChannels The number of fatigue channels. Next six lines ignored if zero.
0.0 FilTRatio The fraction of the maximum range of each channel used as a cutoff range for the
racetrack filter. Use zero for no filter.
630720000 DesignLife Number of seconds in the design lifetime (20 years = 630720000 seconds).
true BinCycles Bin the rainfall cycles?
0.5 UCMult Multiplier for binning unclosed cycles. (0 discards, 1 counts as a full cycle)
true DoSimpDELS Compute short-term (file-based) damage-equivalent loads?
false Dolife Do lifetime-related calculations?
10 WeibullMeanWS Weibull-average wind speed.
2 WeibullShapeFactor Shape parameter for Weibull distribution. 2 = Rayleigh distribution
WSmin Starting value for the wind-speed bins for the Weibull distribution.
BW WSBinFlag BN = number of bins specified or BW = bin width specified
4 WSBinVal Number of bins or the width of the wind-speed bins for the Weibull distribution.
true WrDELSTxt Write DELs to plain-text files?
false WrDELSXLS Write DELs to an Excel workbook?
false WrLifeTxt Write lifetime results to plain-text files?
false WrLifeXLS Write lifetime results to an Excel workbook?
10 EquivFreq The frequency of the damage equivalent load (Hz)
true DELAsRange true = report DELs as a range value, false = report as a one-sided amplitude
Channel# NSIopes SNSIopelst BinFlag BinWidth/Number TypeLMF LUI t BinWidth not used when BinCycles is false.
nFatigueChannels rows of data follow. LUI t >> LMF
5 1 12 BW 0.7 161 9000
6 1 12 BW 7.1 33 9000
7 1 12 BW 7.0 494 9000
8 1 12 BW 145.5 161 152000
9 1 12 BW 32.8 33 152000
10 1 12 BW 2.4 494 152000
11 1 5 BW 1.6 161 57000
12 1 5 BW 0.2 33 57000
13 1 5 BW 0.3 494 57000
14 1 5 BW 2.6 161 707000
15 1 5 BW 16.9 33 707000
16 1 5 BW 10.5 494 707000
17 1 5 BW 1.6 161 57000
18 1 5 BW 0.3 33 57000
19 1 5 BW 0.3 494 57000
20 1 5 BW 18.8 161 707000
21 1 5 BW 104.7 33 707000
22 1 5 BW 10.7 494 707000
1 NumDELGroups Number of DEL groups. DEL tables are organized according to groups.
Nchannel s ChannelList
18 1 2 3 4 5 6 7 8 9 10 11 12 13 14 15 16 17 18
----- Input Files -----
6 NumFiles The number of input files to read.
"U1.out"
"U2.out"
"U3.out"
"U4.out"
"U5.out"
"U6.out"
==EOF==
DO NOT REMOVE OR CHANGE. MUST COME JUST AFTER LAST LINE OF VALID INPUT.

```